

DUDLEY KNOX LIBRARY
NAVAL POSTGRADUATE SCHOOL
MONTEREY, CALIFORNIA 93943-6002

NAVAL POSTGRADUATE SCHOOL

Monterey, California



THESIS

STRESS ANALYSIS OF THE LHA-1 CLASS
SUPERHEATER HEADER BY FINITE ELEMENT
METHOD

by

Jon W. Kaufmann

June 1987

Thesis Advisor
Co-Advisor

G. Cantin
E.L. Wilson

Approved for public release; distribution is unlimited.

T233174

REPORT DOCUMENTATION PAGE

1a REPORT SECURITY CLASSIFICATION UNCLASSIFIED		1b RESTRICTIVE MARKINGS	
2a SECURITY CLASSIFICATION AUTHORITY		3 DISTRIBUTION/AVAILABILITY OF REPORT Approved for public release; distribution is unlimited	
2b DECLASSIFICATION/DOWNGRADING SCHEDULE		5 MONITORING ORGANIZATION REPORT NUMBER(S)	
4 PERFORMING ORGANIZATION REPORT NUMBER(S)		7a NAME OF MONITORING ORGANIZATION Naval Postgraduate School	
6a NAME OF PERFORMING ORGANIZATION Naval Postgraduate School	6b OFFICE SYMBOL (if applicable) 69	7b ADDRESS (City State and ZIP Code) Monterey, California 93943-5000	
8a NAME OF FUNDING/SPONSORING ORGANIZATION		9 PROCUREMENT INSTRUMENT IDENTIFICATION NUMBER	
8b OFFICE SYMBOL (if applicable)		10 SOURCE OF FUNDING NUMBERS	
8c ADDRESS (City State and ZIP Code)		PROGRAM ELEMENT NO	TASK NO
		PROJECT NO	WORK UNIT ACCESSION NO
11 TITLE (Include Security Classification) STRESS ANALYSIS OF THE LHA-1 CLASS SUPERHEATER HEADER BY FINITE ELEMENT METHOD			
12 PERSONAL AUTHOR(S) KAUFMANN, JON WILLIAM			
13a TYPE OF REPORT Master's Thesis	13b TIME COVERED FROM TO	14 DATE OF REPORT (Year Month Day) 1987 June	15 PAGE COUNT 92
16 SUPPLEMENTARY NOTATION			
17 COSATI CODES		18 SUBJECT TERMS (Continue on reverse if necessary and identify by block number)	
FIELD	GROUP	SUB GROUP	
		Thermal Stress Analysis, Finite Element Method, LHA-1 Class Superheater Header	
19 ABSTRACT (Continue on reverse if necessary and identify by block number) Numerous cracks and leaks in the superheater header tube attachment welds in the LHA-1 class of amphibious assault ships have prompted an investigation by the Naval Sea Systems Command (NAVSEA). This thesis describes the stress analysis of the superheater header tube attachment region using a three dimensional axisymmetric Finite Element model. The SAP 80 structural analysis program was utilized to conduct the analysis. Both pre and post processors were employed to obtain graphical representations of the model as well as the results of the stress analysis. This thesis focuses primarily on thermally induced stresses produced in the header. Some results obtained for a nominal 100 Degree F temperature drop across the thickness of the superheater header wall yielded a maximum hoop stress of 19.01 (Ksi) and a maximum in plane stress of 1.58 (Ksi).			
20 DISTRIBUTION/AVAILABILITY OF ABSTRACT <input checked="" type="checkbox"/> UNCLASSIFIED UNLIMITED <input type="checkbox"/> SAME AS RPT <input type="checkbox"/> DTIC USERS		21 ABSTRACT SECURITY CLASSIFICATION UNCLASSIFIED	
22a NAME OF RESPONSIBLE INDIVIDUAL Professor G. CANTIN		22b TELEPHONE (Include Area Code) (408) 646-2364	22c OFFICE SYMBOL 69C1

Approved for public release; distribution is unlimited.

Stress Analysis of the LHA-1 Class
Superheater Header by Finite Element Method

by

Jon W. Kaufmann
Lieutenant, United States Navy
B.S., State University of New York Maritime College, 1981

Submitted in partial fulfillment of the
requirements for the degree of

MASTER OF SCIENCE IN MECHANICAL ENGINEERING

from the

NAVAL POSTGRADUATE SCHOOL
June 1987

ABSTRACT

Numerous cracks and leaks in the superheater header tube attachment welds in the LHA-1 class of amphibious assault ships have prompted an investigation by the Naval Sea Systems Command (NAVSEA). This thesis describes the stress analysis of the superheater header tube attachment region using a three dimensional axisymmetric Finite Element model. The SAP 80 structural analysis program was utilized to conduct the analysis. Both pre and post processors were employed to obtain graphical representations of the model as well as the results of the stress analysis. This thesis focuses primarily on thermally induced stresses produced in the header. Some results obtained for a nominal 100 Degree F temperature drop across the thickness of the superheater header wall yielded a maximum hoop stress of 19.01 (Ksi) and a maximum in plane stress of 1.58 (Ksi).

TABLE OF CONTENTS

I.	INTRODUCTION	8
II.	DETAILED DESCRIPTION OF THE PROBLEM	10
	A. SUPERHEATER DESCRIPTION	10
	B. GEOMETRIC DESCRIPTION OF THE HEADER/TUBE ATTACHMENT REGION	14
	C. DESCRIPTION OF OBSERVED SERVICE FAILURES	14
III.	GENERAL DESCRIPTION OF SAP-80	27
	A. METHOD OF SOLUTION	27
	B. PRE AND POST PROCESSOR CAPABILITIES	28
	C. FINITE ELEMENT MODEL DEVELOPMENT	29
IV.	SOLUTION OF THE PROBLEM	38
	A. MATERIAL PROPERTIES	38
	B. MODEL LOAD DEVELOPMENT	38
	1. Internal Pressure Load	38
	2. Longitudinal Tube Load	39
	3. Thermal Load	41
	C. ERROR CONSIDERATIONS	42
V.	CONCLUSIONS	61
	A. DISCUSSION OF RESULTS	61
	1. Superheater Header Design	61
	2. Effects of Creep	62
	3. Effects of Vibration	62
	B. OPPORTUNITIES FOR FURTHER RESEARCH	62
APPENDIX A:	TEMPERATURE INSTRUMENTATION DATA FROM THE USS BELLEAU WOOD	64

APPENDIX B: MATERIAL PROPERTY TEST DATA 75

APPENDIX C: HEADERT INPUT FILE 76

APPENDIX D: HEADER INPUT FILE 81

APPENDIX E: EXCERPT FROM ASME BOILER CODE 86

APPENDIX F: PROJECTED BOILER OPERATING CYCLE (CV-60
CLASS) 88

LIST OF REFERENCES 89

INITIAL DISTRIBUTION LIST 90

LIST OF FIGURES

2.1	LHA-1 Class Main Engineroom Layout	11
2.2	Side View of the V2M Marine Boiler	12
2.3	Four Pass Superheater Schematic and Alignment Lug Orientation	13
2.4	Superheater Header Cross Section	16
2.5	Detail of Superheater Header Tube Attachment Weld Joint NOTE: Drawing Is Not To Scale	17
2.6	Plot of Constructed Weld Geometry for Modelling Purposes	18
2.7	Intermediate (left) and Inlet, Outlet (right) Superheater Headers After Removal From USS Tarawa (LHA-1)	19
2.8	USS Tarawa Intermediate Header Prepared for Inspection	20
2.9	Magnetic Particle Indications of Transverse Weld Cracks In No. 2 Boiler Intermediate Header	21
2.10	Magnetic Particle Indications of Ligament Cracks in No. 1 Boiler Inlet/Outlet Header	22
2.11	Magnetic Particle Indication of Crack in Weld in No. 2 Boiler Intermediate Header	23
2.12	Magnetic Particle Test Results (Rows 1 - 25)	24
2.13	Magnetic Particle Test Results (Rows 26 - 49)	25
2.14	Magnetic Particle Test Results (Rows 50 - 67)	26
3.1	Local (s,t) and Global (Y,Z) Coordinate Axes for the "ASOLID" Element Type	31
3.2	Finite Element Model of Header Tube Attachment Region	32
3.3	Model Elements No. 1 through 20 (Tube Wall)	33
3.4	Model Elements No. 21 through 56 (Weld Material)	34
3.5	Model Elements No. 57 through 140 (Header Wall)	35
3.6	Model Elements No. 141 through 200 (Header Wall)	36
3.7	Illustration of the "Element Shrinkage" Option	37
4.1	Orientation of the Internal Pressure Load	44
4.2	Hoop Stress for the Pressure Load Condition (Ksi)	45

4.3	Maximum In Plane Stress for Pressure Load Condition (Ksi)	46
4.4	Minimum In Plane Stress for Pressure Load Condition (Ksi)	47
4.5	Deformed Structure for the Pressure Load Condition	48
4.6	Longitudinal Loading of the Superheater Tube	49
4.7	Hoop Stress for the Longitudinal Load Condition (Ksi)	50
4.8	Maximum In Plane Stress for the Longitudinal Load (Ksi)	51
4.9	Minimum In Plane Stress for the Longitudinal Load (Ksi)	52
4.10	Z Displacements for Longitudinal Load Condition (Inches)	53
4.11	Temperature Boundary Conditions for the Model (Degrees F)	54
4.12	Temperature Field Developed for the Model (Degrees F)	55
4.13	Temperature Field - Local Region of the Weld (Degrees F)	56
4.14	Hoop Stress for Thermal Load Condition (Ksi)	57
4.15	Maximum In Plane Stress for Thermal Load Condition (Ksi)	58
4.16	Minimum In Plane Stress for Thermal Load Condition (Ksi)	59
4.17	Y Displacements for Thermal Load Condition (Inches)	60

I. INTRODUCTION

Over the past five years the United States Navy has experienced an unusually large number of failures of the superheater header tube attachment weld utilized in the Combustion Engineering Co. model V2M marine boiler which is installed aboard the LHA-1 class of amphibious assault ships. The Naval Sea Systems Command (NAVSEA) began an investigation to determine the cause of the failure and any possible solutions to the problem. Part of the investigation included an extensive instrumentation of the No. 2 main boiler installed aboard the USS Belleau Wood (LHA-3) for the purpose of determining thermally induced stress information applicable to an LHA-1 Class header model. The instrumentation included thermocouples, strain gages and dial indicators.

During March 1986 the USS Belleau Wood conducted underway operations at various speed and load conditions while the installed instrumentation coupled with an automated data acquisition system recorded temperature, strain and displacement data for the header. Data for the following plant load conditions was recorded:

- cold lite-off cycle (approx. 4 Hrs.)
- 25 % steady state boiler operation
- 50 % steady state boiler operation
- 75 % steady state boiler operation
- 90 % steady state boiler operation

Data readings were recorded automatically at 15 minute intervals during each of these conditions. Details of the instrumentation location and sample data are included as Appendix A.

Despite the extensive amount of temperature data which was recorded, only a limited amount of data was available in the region of the header which was modelled since there were only three thermocouples installed in the local region of the header tube attachment weld.

A Finite Element model of the header was developed using the SAP 80 structural analysis program. Using the model which was developed, a study was made of the effects of thermal gradients on the stresses experienced in the header. A discussion is also included of some of the factors which introduce some non-linearities into the

problem, such as the consideration of temperature dependent material properties and the effects of creep on the structure at the elevated operating temperatures which are experienced.

II. DETAILED DESCRIPTION OF THE PROBLEM

The V2M marine boilers installed aboard the LHA-1 class of ships are two drum, natural circulation "D" type boilers manufactured by the Combustion Engineering Co. Two boilers, one left hand and one right hand are installed in the main engine rooms as shown in Figure 2.1. Each boiler has an integral superheater and extended surface economizer. The boilers are designed to produce superheated steam at 628 Psi at 904 Degrees F at the superheater outlet under full rated conditions.

A. SUPERHEATER DESCRIPTION

The superheater raises the temperature of the saturated steam leaving the steam drum. Superheating the steam is a means of increasing the efficiency of the boiler as well as preventing erosion of the turbine blades. The superheater is made up of 268 "U" shaped tubes which are inclined from the vertical. The 268 tubes are arranged in 67 rows with each row containing four tubes. The tube elements terminate in two headers at the bottom of the boiler, as shown in Figure 2.2. One header is designated the inlet/outlet header while the other is designated the intermediate header. Diaphragms in the inlet/outlet header and the intermediate header divide the superheater into four passes as shown in Figure 2.3.

Tube elements are contact rolled into holes in the headers. The holes are counterbored and the elements are seal welded to the header in the counterbores. The tubes are 1.5 Inch OD X 0.12 Inch minimum wall thickness, seamless 2.25 Chrome tubing (MIL-T-16286, Class E). The headers themselves are 12.75 Inch OD X 2 Inch minimum wall thickness, 2.25 Chrome pipe (ASME-SA-335, Grade P-22). The headers are flattened on top to widen the area where the tubes are attached. There are 23 elliptical handholes in each header on the side opposite to the tube holes. These holes provide access for inspection and seal welding.

The superheater elements are supported from the headers which have support saddles at each end. The alignment of the tubes is maintained by attachment to the third row of screen tubes on one side and the fourth row of 2 Inch tubes at the entrance to the generating bank. This attachment is made by the use of attachment lugs as illustrated in Figure 2.3.

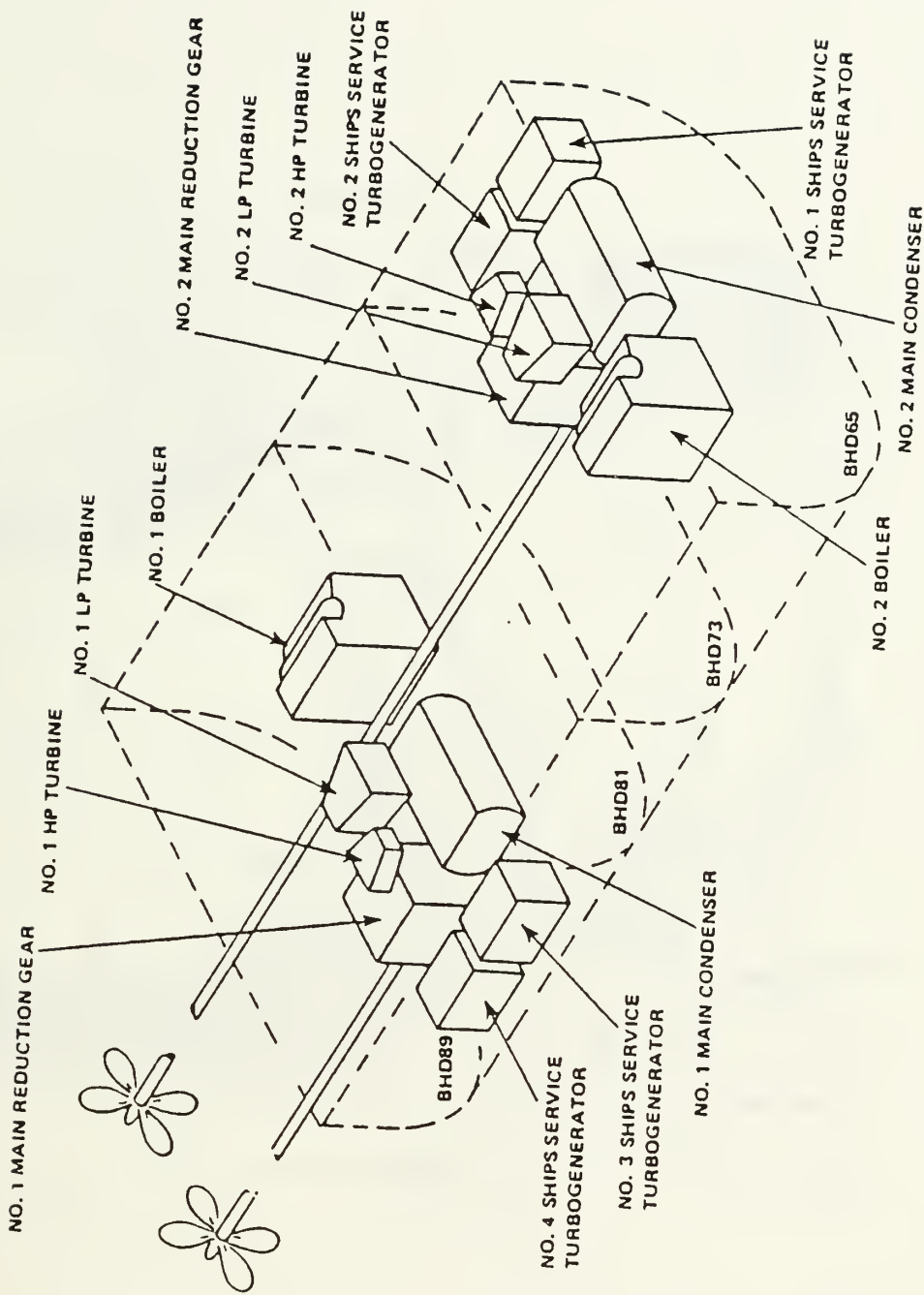


Figure 2.1 LHA-1 Class Main Engine Room Layout.

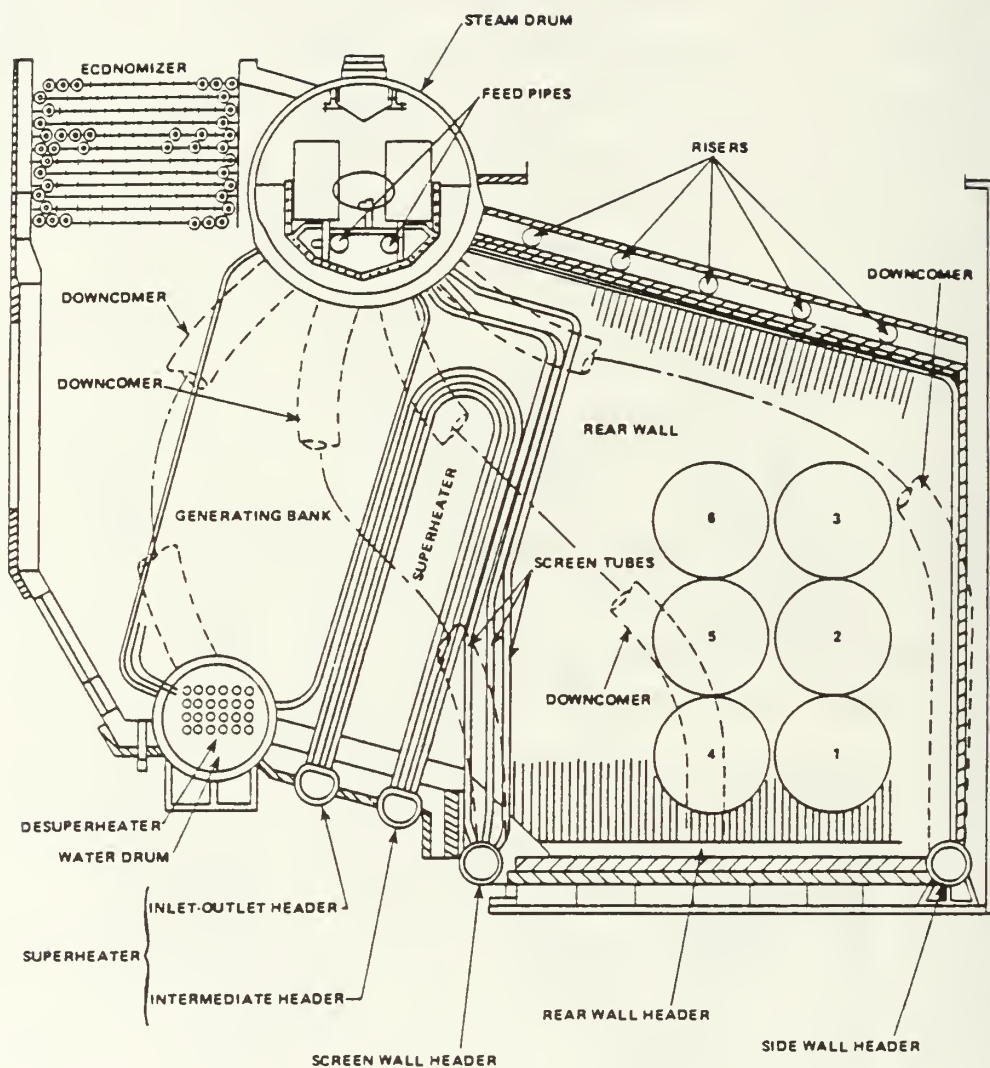
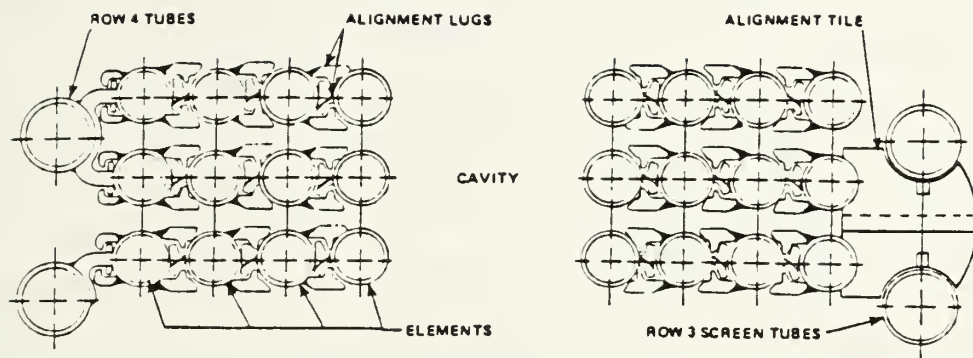


Figure 2.2 Side View of the V2M Marine Boiler.



DETAIL OF ALIGNMENT FITTINGS

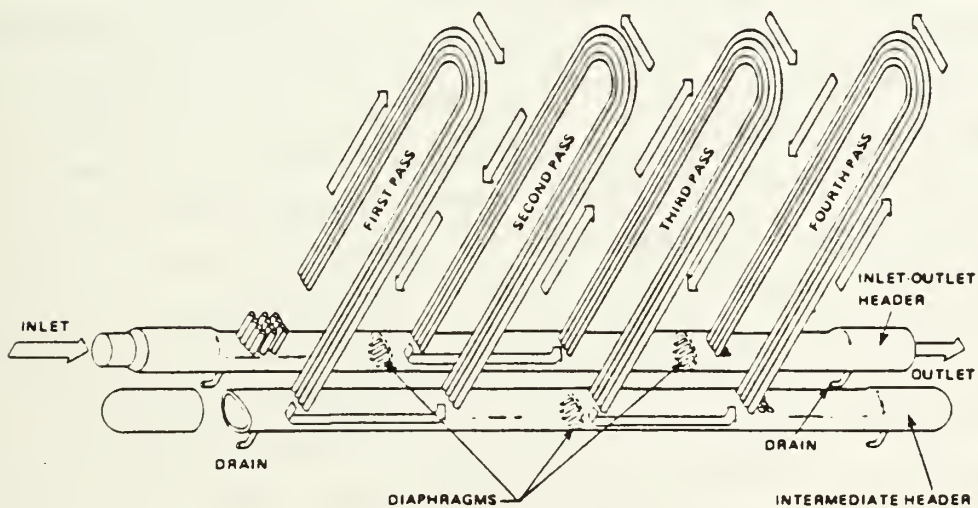


Figure 2.3 Four Pass Superheater Schematic and Alignment Lug Orientation.

B. GEOMETRIC DESCRIPTION OF THE HEADER/TUBE ATTACHMENT REGION

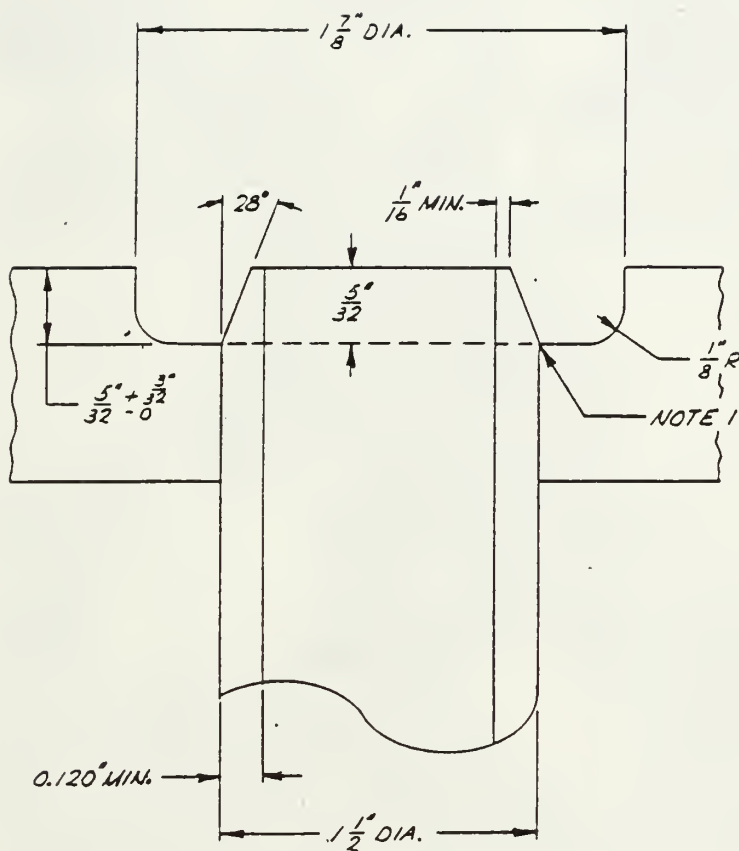
Figure 2.4 illustrates a cross section view of the superheater header which shows the orientation of the tube holes. The counterbore dimensions are indicated on the drawing as well as the arrangement of the tubes with respect to the header. Figure 2.5 offers an expanded view of the header/tube attachment region. As shown, the counterbore has a 1/8 Inch radius of curvature. It should be noted that Figure 2.5 is not to scale and therefore offers a distorted view of the region. Using the dimensions provided in Figure 2.5, Figure 2.6 was then constructed to scale using a scale of 30.449:1. Figure 2.6 was utilized to obtain the coordinates needed to define the geometry of the region for modelling purposes. The shape of the top surface of the weld is restricted not to exceed 1/16 Inches above the surface of the header in [Ref. 1: Page A-18]. As shown in Figure 2.6, a circular arc was chosen to describe the top surface of the weld.

C. DESCRIPTION OF OBSERVED SERVICE FAILURES

The most complete information compiled by NAVSEA concerning failures of the joint in question was obtained after removal of the superheater headers from the USS Tarawa (LHA-1). Figures 2.7, 2.8, 2.9, 2.10 and 2.11 are photographs which were taken after the header was split longitudinally in order to reveal the surface of the welds on the inside of the header. Following removal, magnetic particle tests were performed to detect any cracks which were present in the header. A summary of the results from the magnetic particle tests are illustrated in Figures 2.12, 2.13 and 2.14. The results of the magnetic particle tests showed that there was no particular pattern to the location of the failures. However, as the figures show, the failures seem to be more frequent towards the ends of the header. This fact would tend to discount the hypothesis that the failures were caused by a sagging condition of the header due to the fact that the two saddle supports for the header are located at the inlet and outlet ends of the header. If this hypothesis was correct one would expect to see the failures concentrated in the center region of the header since the stresses produced by sagging would be a maximum in this region. During the examination, it was also discovered that a large percentage of the welds were actually bridged to adjacent welds by excess weld material.

Findings from the USS Tarawa's headers indicated that *all* of the failures appeared to occur in the weld material, and that the most common mode of failure was

a radially oriented crack in the weld material. More detailed metallurgical inspections of the failure surfaces revealed a significant amount of corrosion. The pattern of the corrosion indicated that the failure took place in a progressive manner over a relatively long period of time.



NOTE:

1. TUBE IS POSITIONED SUCH THAT BASE OF TUBE CHAMFER IS FLUSH WITH SQUARE CORNER AT BOTTOM OF COUNTERBORE AS SHOWN

Figure 2.5 Detail of Superheater Header Tube Attachment Weld Joint
NOTE: Drawing Is Not To Scale.

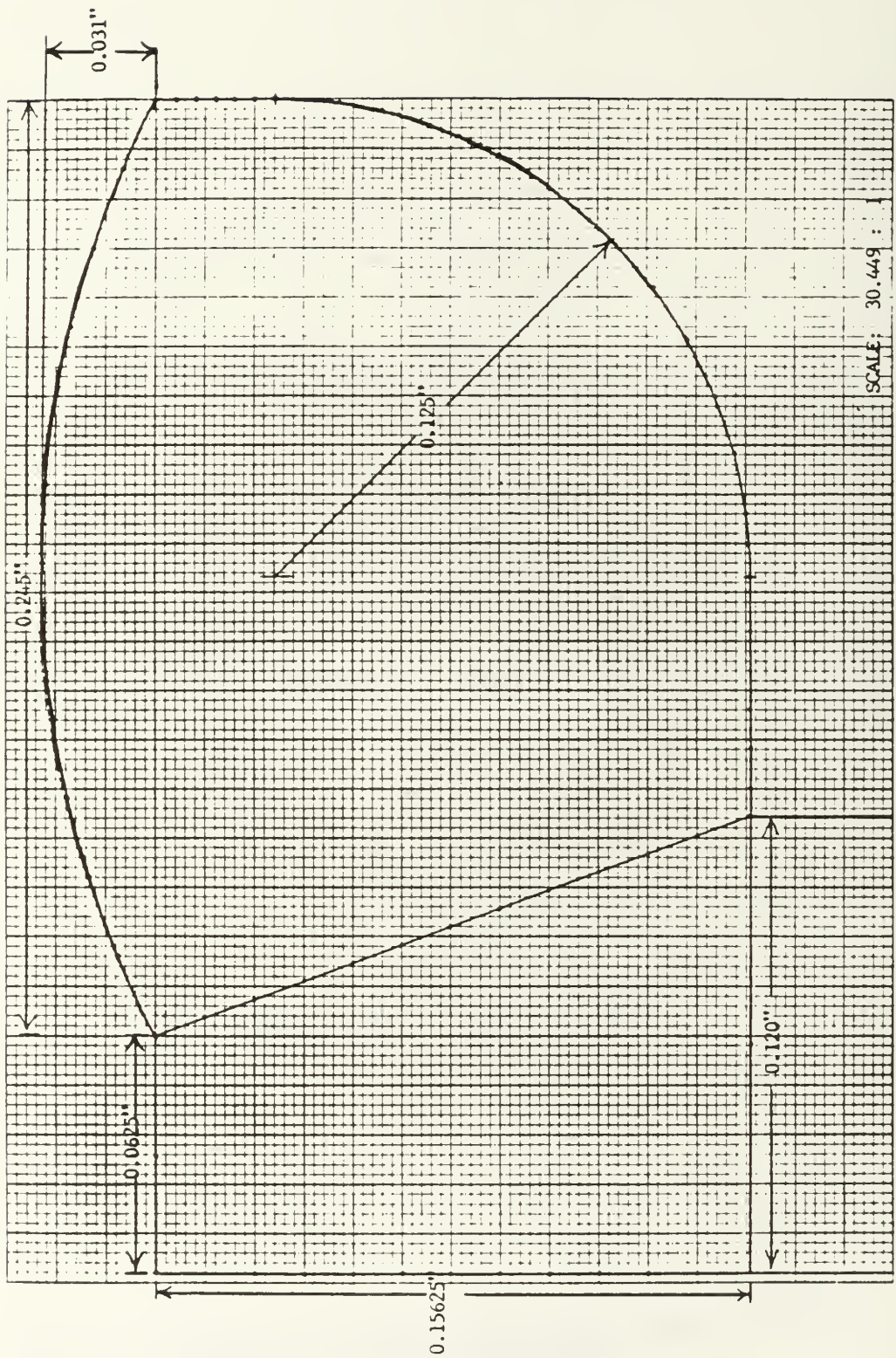


Figure 2.6 Plot of Constructed Weld Geometry for Modelling Purposes.

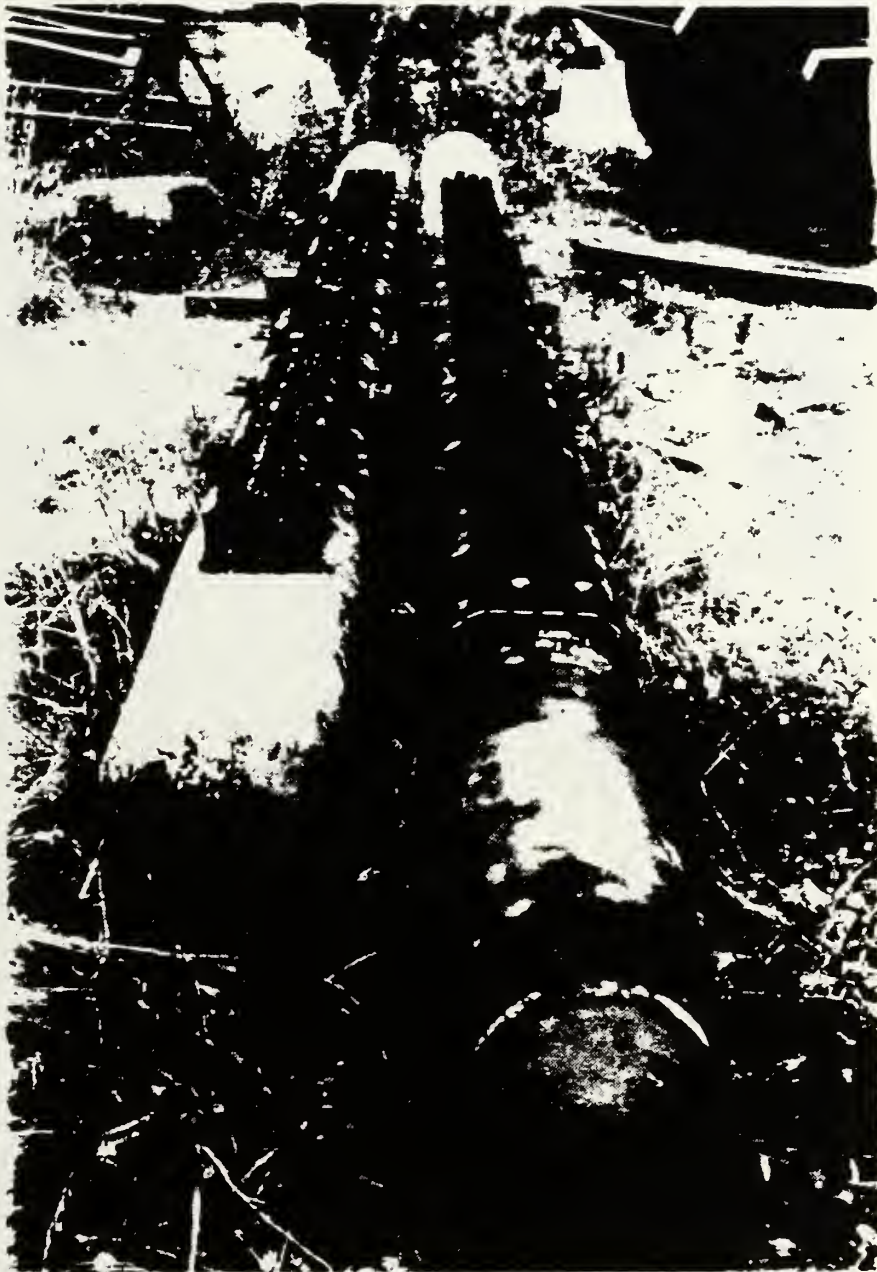


Figure 2.7 Intermediate (left) and Inlet/Outlet (right) Superheater Headers After Removal From USS Tarawa (LHA-1).

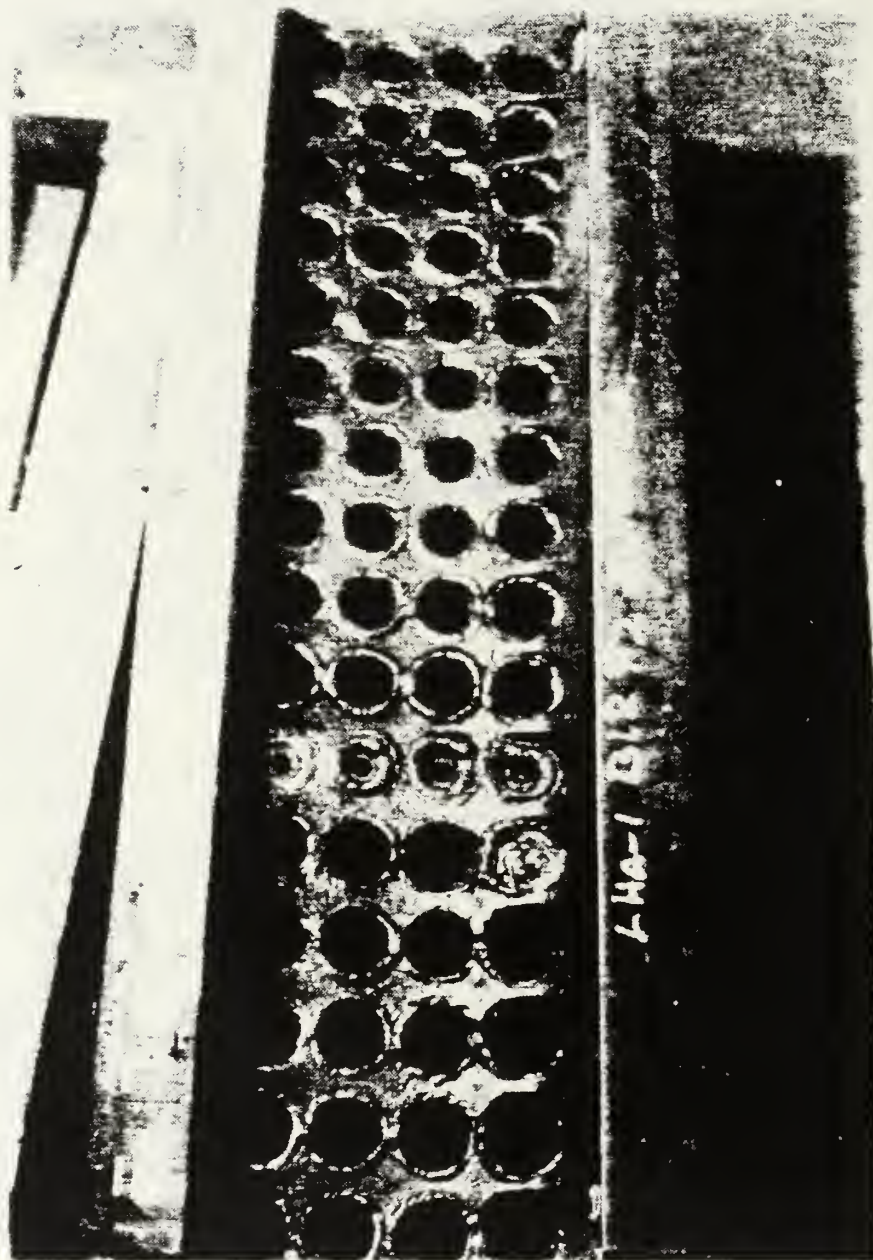


Figure 2.8 USS Tarawa Intermediate Header Prepared for Inspection.



Figure 2.9 Magnetic Particle Indications of Transverse Weld Cracks
In No. 2 Boiler Intermediate Header.

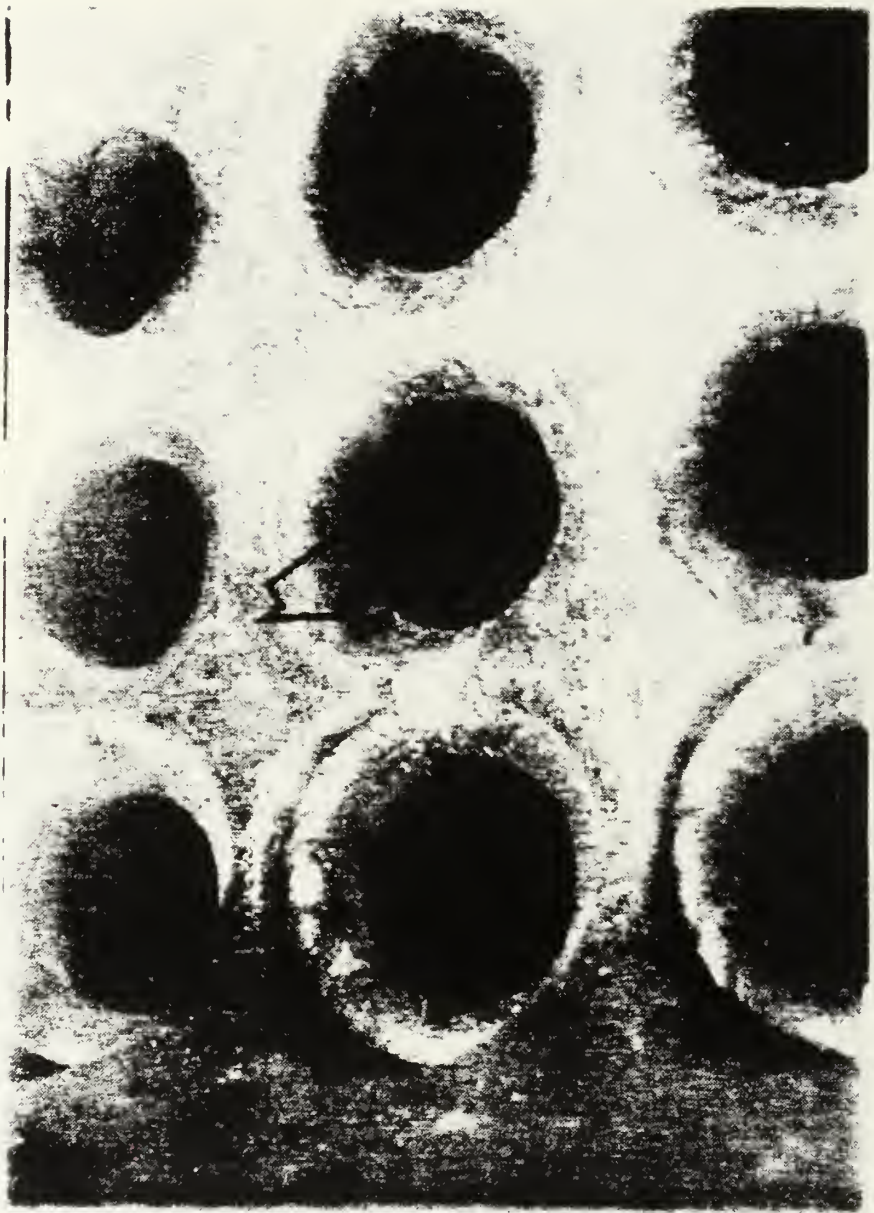


Figure 2.10 Magnetic Particle Indications of Ligament Cracks in No. 1 Boiler Inlet Outlet Header.



Figure 2.11 Magnetic Particle Indication of Crack in Weld in
No. 2 Boiler Intermediate Header.

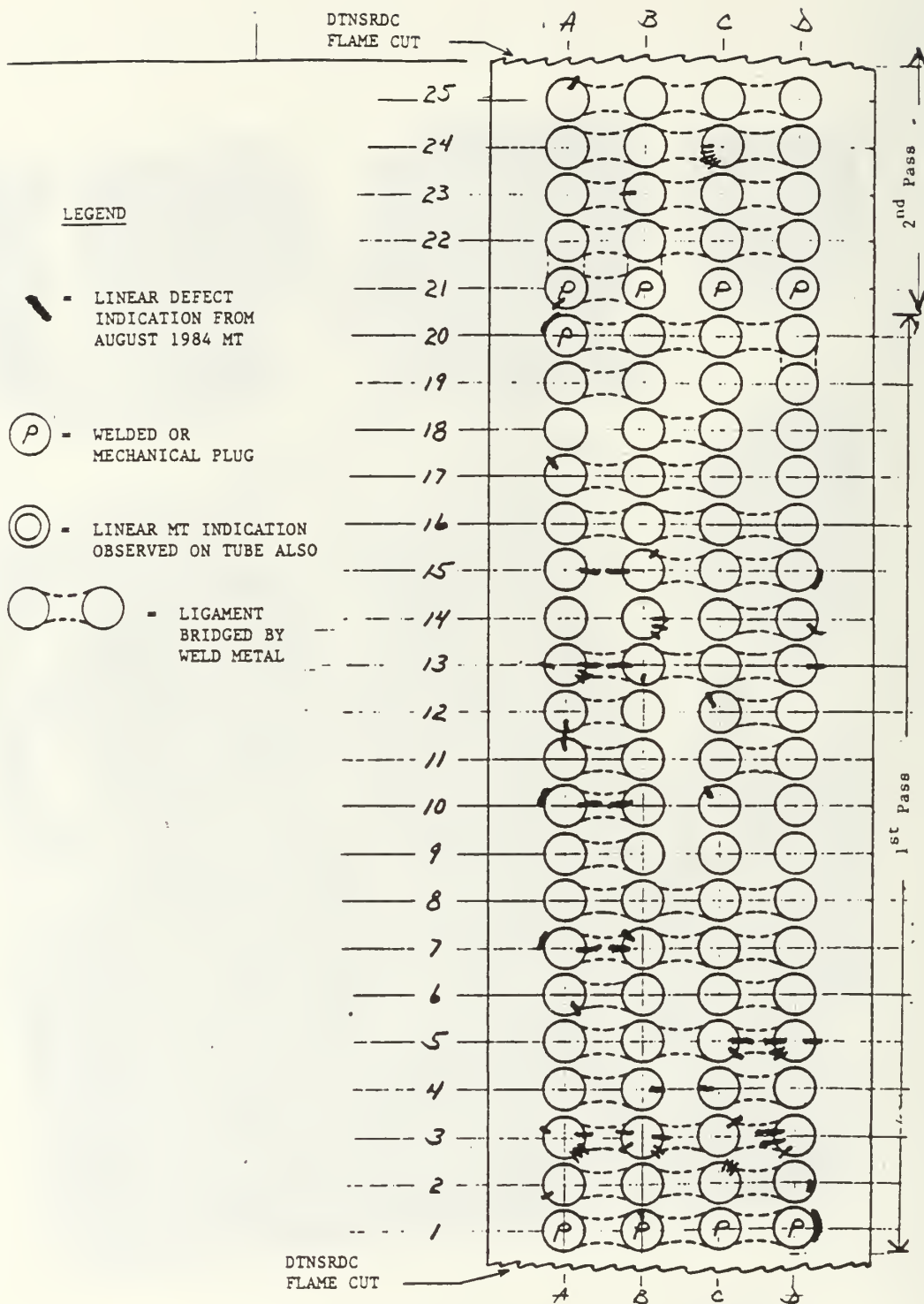


Figure 2.12 Magnetic Particle Test Results (Rows 1 - 25).

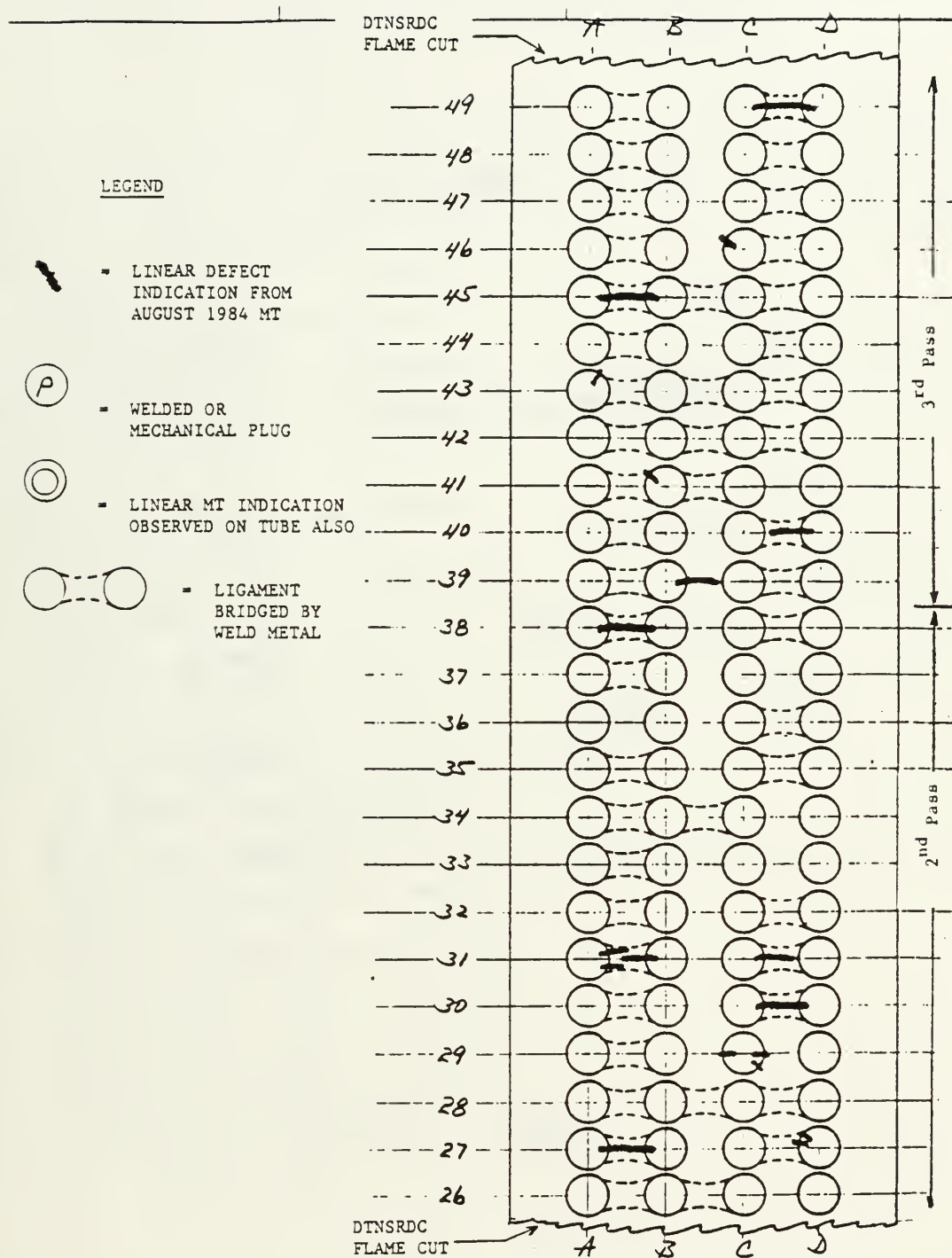


Figure 2.13 Magnetic Particle Test Results (Rows 26 - 49).

III. GENERAL DESCRIPTION OF SAP-80

The SAP-80 structural analysis program is actually a series of computer programs for the static and dynamic Finite Element analysis of structures. The program was developed by Professor Edward L. Wilson of the University of California at Berkeley.

A. METHOD OF SOLUTION

For static analysis of the isoparametric problem, SAP-80 solves the following node point equilibrium equation as developed in [Ref. 2: page 163]:

$$K U = R \quad (\text{eqn 3.1})$$

where:

- K = Union of all the element stiffness matrices
- U = Unknown node displacements
- R = Load matrix which includes concentrated nodal forces, body forces, surface forces and the initial forces.

The stiffness matrix is defined in equation 3.2 :

$$K = \int B^T C B dV \quad (\text{eqn 3.2})$$

where:

- B = Strain - Displacement Transformation Matrix
- C = Constant Material Property Matrix (Stress-Strain Relationship)

The elements of B are functions of the natural coordinates r,s and t being derived from the isoparametric representation of displacements and the inverse of the Jacobian matrix. The integration is carried out in the natural coordinate system of reference, and dV is defined as:

$$dV = \text{Det}(J) dr ds dt \quad (\text{eqn 3.3})$$

where:

- $\text{Det}(J)$ = Determinant of the Jacobian Matrix

The integration is accomplished using Gauss quadrature and the resulting matrix is stored in compacted form.

B. PRE AND POST PROCESSOR CAPABILITIES

Pre and post processing for the SAP-80 system is included in the "SAPLOT" program. SAPLOT is an interactive geometric plotting pre and post processor. The program has options for plotting two and three dimensional views displaying any of the following:

- Undeformed structural geometry
- Static analysis deformed shape
- Steady state analysis deformed shapes
- Mode shapes

The model may be viewed from any arbitrary direction. The user locates any arbitrary point with respect to the Global X, Y, Z coordinate system. This point is called the view control point. The view is set in the direction pointing away from the view control point and towards the SAP-80 Global origin. The actual location of the viewer's eye is assumed to be at infinity. Once the view direction is set, the user can rotate the view by specifying which of the SAP-80 Global axes is to appear vertically upward on the screen.

When displaying the deformed shape of the structure, the user may also plot the undeformed shape with dashed lines. The user can also set the maximum values for displacements in order to accentuate the structural deformation. The deformed shapes

of elements may be plotted with displaced straight lines or with cubic curves. The program also has an option which allows the elements to be shrunk about their centroids, thereby clearly displaying element connectivities and uncovering any overlapped element boundaries. This is called the "element shrinkage" option.

The program has a "window" option which allows the user to display "blowup" images of localized regions within the structure. The program also has the capability to label node points as well as element numbers.

C. FINITE ELEMENT MODEL DEVELOPMENT

After review of the information available concerning the failure of the header tube attachment weld, it was decided to model the region shown in Figure 2.5. The justification for modelling a relatively small area of the header is that *all* of the observed failures occurred in this local region of the structure as indicated earlier in this paper.

SAP-80 provides several elaborate node generation systems which allow for the development of an extensive node mesh. In the model which was developed, three node generation schemes were utilized; Linear generation, Lagrangian generation and Quadrilateral generation. The element chosen for this model was the nine node isoparametric axisymmetric quadrilateral element. [Ref. 3: page 10] discusses the advantages of the nine node quadrilateral element over the eight node quadrilateral element for an analysis of this type. In SAP-80 this type of element is referred to as the "ASOLID" element. Figure 3.1 illustrates the local (r,s) coordinate axes as well as the Global (Y,Z) axes utilized for the axisymmetric (asolid) nine node quadrilateral element which was utilized in the model development. Despite a small increase in the computation time, the addition of the ninth node prevents some possible errors in the solution of the problem. The errors most commonly avoided are ones which arise due to the fact that some of the elements within the mesh may have significantly distorted quadrilateral shapes. The geometry of the structure contains an axis of symmetry, the center line of the superheater tube, which allows the three dimensional structure to be represented by a model which appears to be two dimensional (Y-Z Plane). The axisymmetric element type chosen rotates the structure as represented in the Y-Z Plane through 360 Degrees to form a three dimensional structure. Figure 3.2 shows the model of the header tube attachment region which was developed. The model consists of 1001 node points which form a total of 200 elements.

As shown in Figure 3.3, elements 1 through 20 were developed using the linear generation scheme. Elements 1 through 20 comprise the tube wall of the model. Figure 3.4 illustrates elements 21 through 56 which comprise the weld material of the model. Elements 21 through 56 were developed in such a manner that those elements comprised solely the weld material and no other area of the structure. This was done to allow for the possible input of separate material properties for the weld material. Figure 3.5 illustrates elements 141 through 200 which make up the header wall. Figure 3.6 illustrates elements 57 through 140 which also make up part of the header wall. Figure 3.7 illustrates the usage of the "element shrinkage" option which allows the user to uncover any possible element overlap which would produce erroneous results upon execution of the program.

In SAP-80 every node point of the structural model has six displacement components, three global translations X,Y,Z and three global rotations, RX, RY, and RZ. The directions associated with these six displacement components are known as the degrees of freedom of the node. The boundary conditions are entered by eliminating the appropriate degrees of freedom from the desired node points of the model. In the model that was developed, the right hand side of elements 188 through 200 were assumed to be fixed. To accomplish this both the Y and Z direction degrees of freedom of the appropriate node points were eliminated from the equations to be solved. The boundary between the tube and the header was considered to be a frictional surface. The node points below the weld which are on the boundary between the tube and the header were constrained together in the Y direction but the two surfaces were allowed to move with respect to one another in the Z direction.

The output from the SAP-80 code includes the following:

- Displacements
- Stresses
- Reactions

All of these results are available in either graphical or tabular form. Because of the ability to display a large amount of data in a relatively small space, the results have been presented in graphical form throughout this report. All plotted stress results in this report are in units of Ksi.

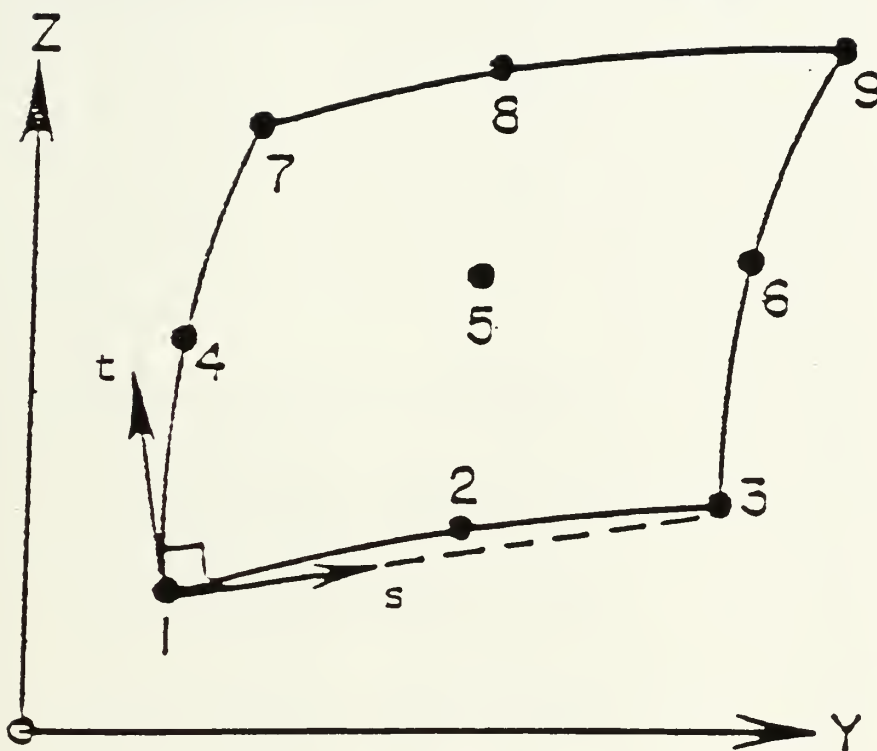


Figure 3.1 Local (s,t) and Global (Y,Z) Coordinate Axes for the "ASOLID" Element Type.

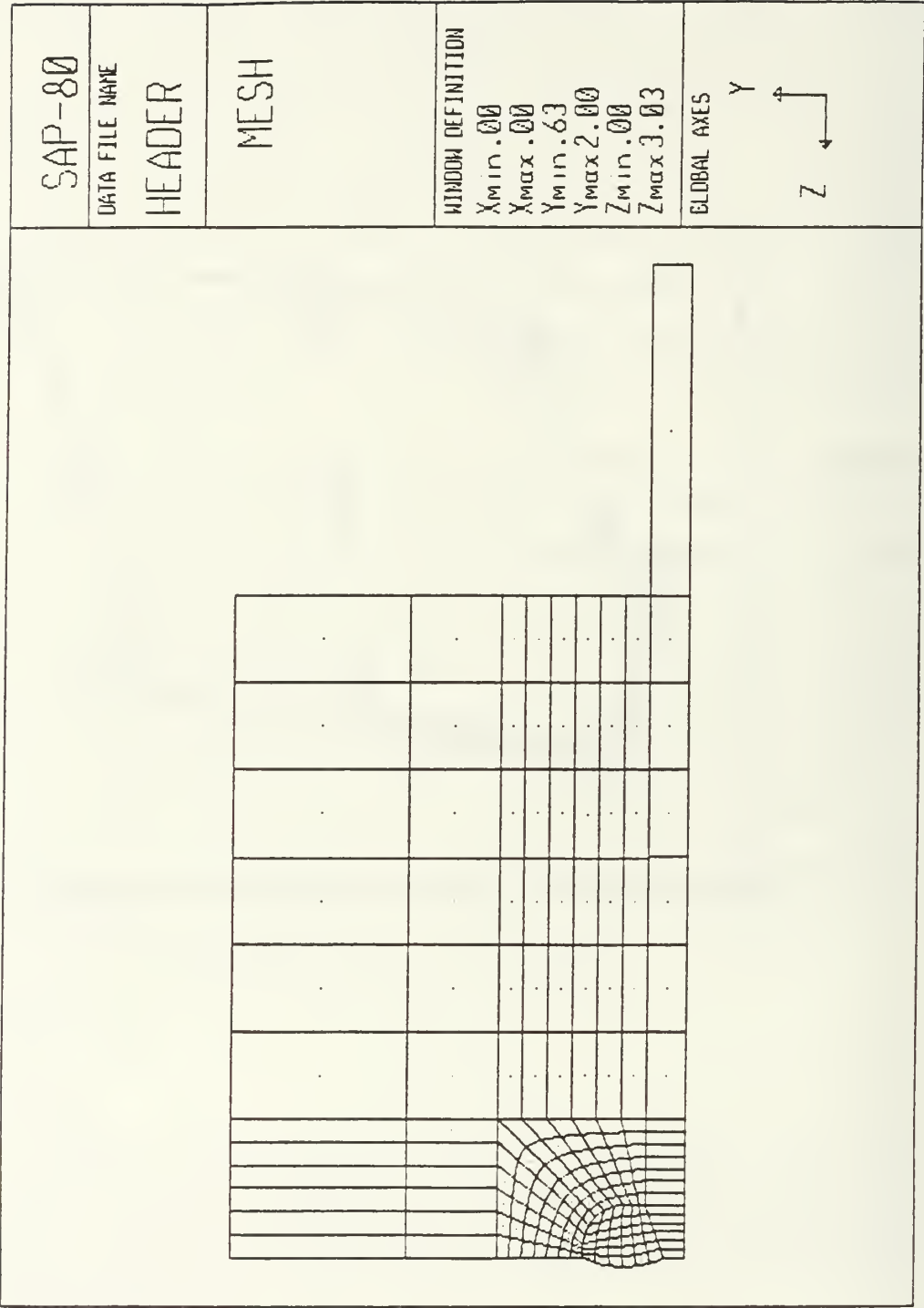


Figure 3.2 Finite Element Model of Header Tube Attachment Region.

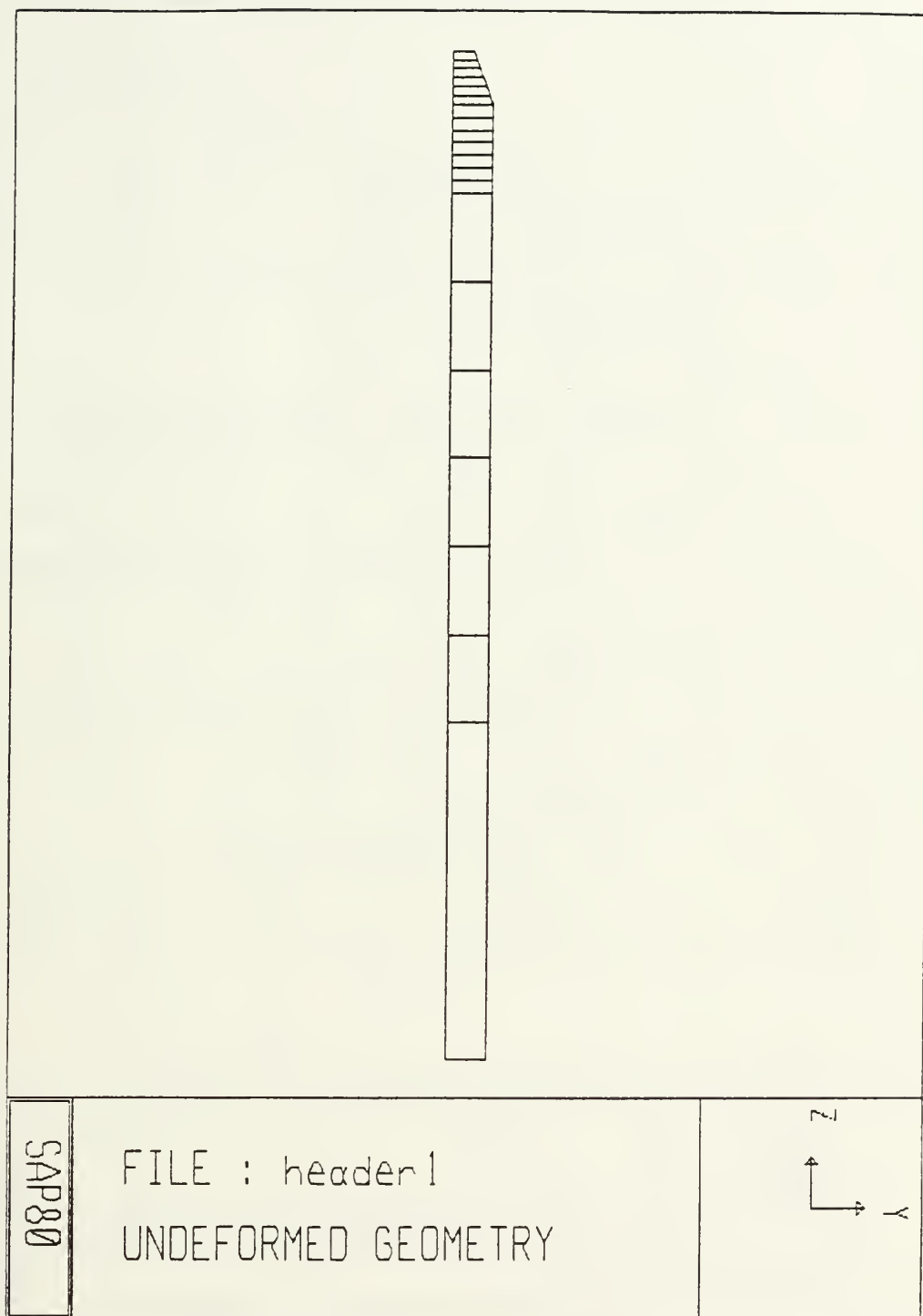


Figure 3.3 Model Elements No. 1 through 20 (Tube Wall).

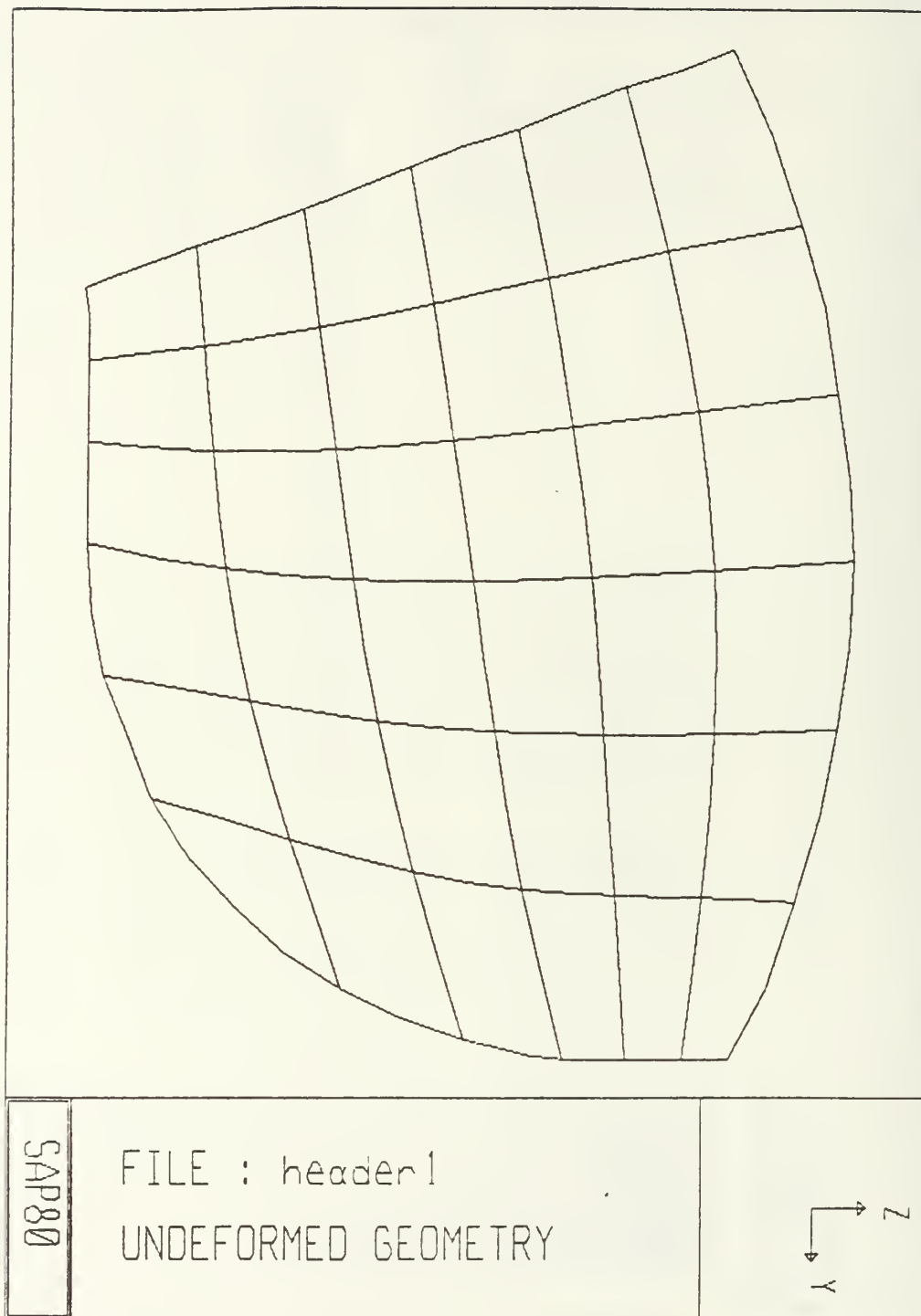


Figure 3.4 Model Elements No. 21 through 56 (Weld Material).

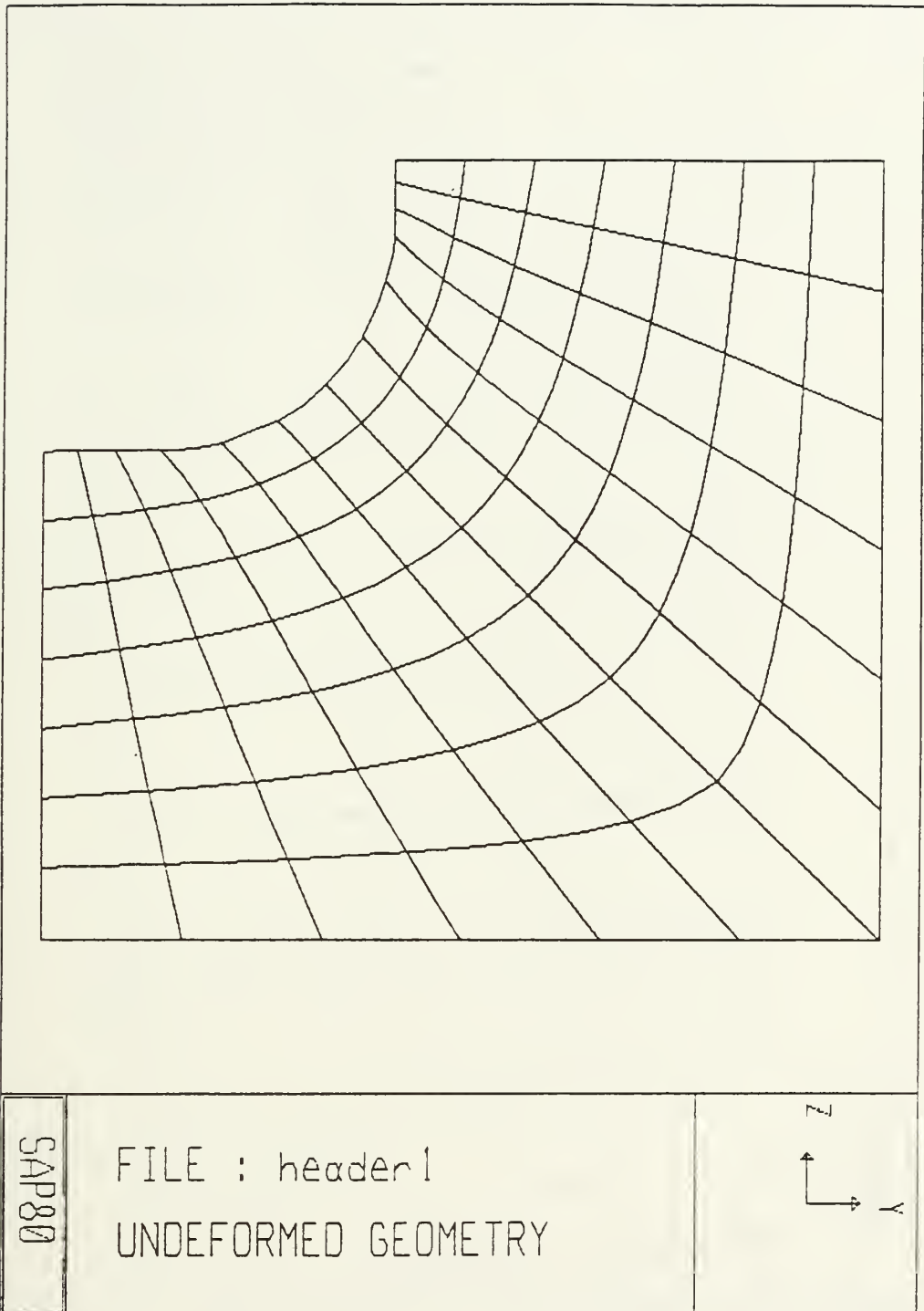


Figure 3.5 Model Elements No. 57 through 140 (Header Wall).

[illegible]

Figure 3.6 Model Elements No. 141 through 200 (Header Wall).

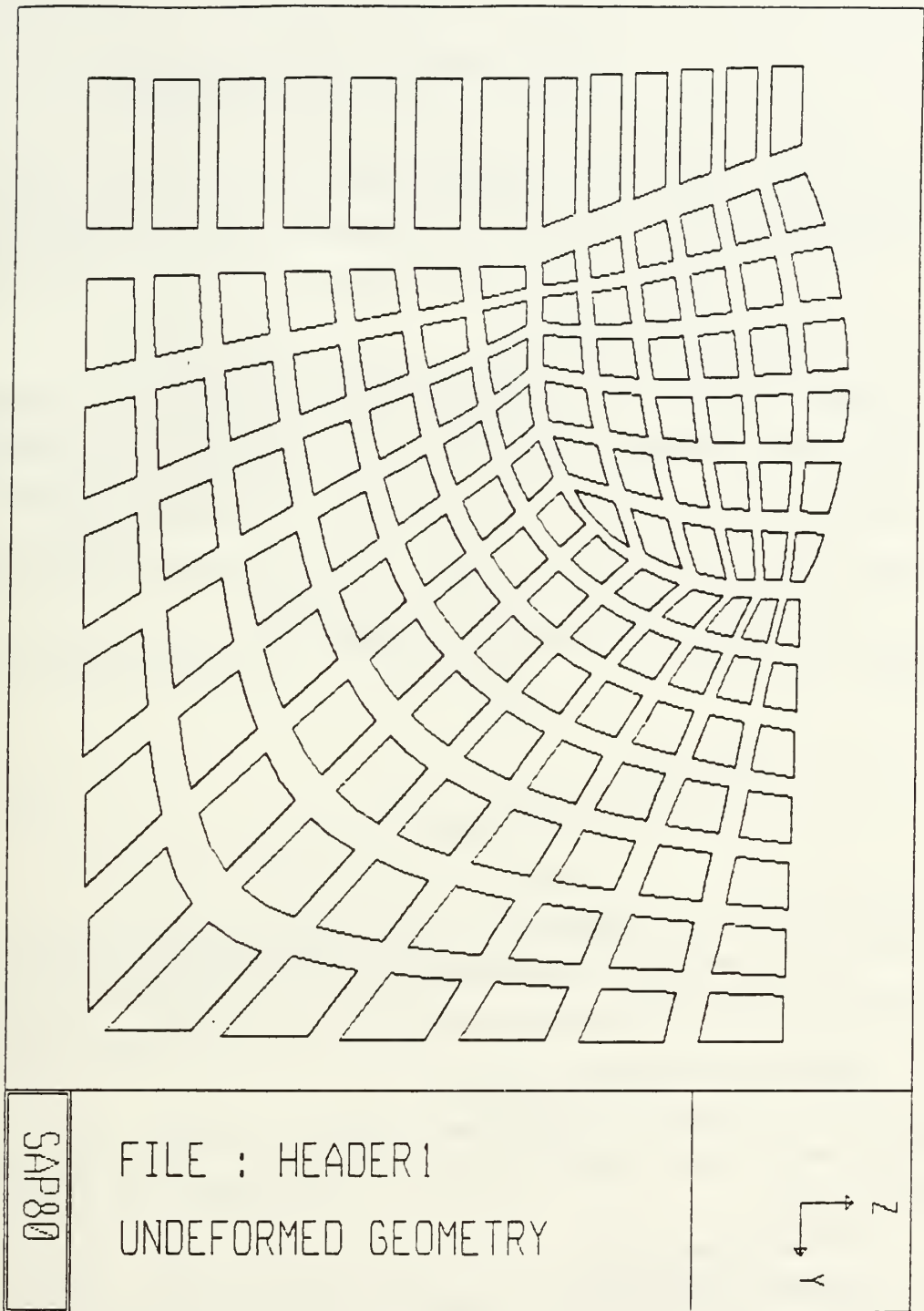


Figure 3.7 Illustration of the "Element Shrinkage" Option.

IV. SOLUTION OF THE PROBLEM

The SAP-80 code was implemented on an IBM PC AT computer at the Naval Postgraduate School. All execution including pre and post processor graphics were accomplished on the same computer.

A. MATERIAL PROPERTIES

The material used for construction of the superheater tubes as well as the header is 2.25 % Chromium 1 % Molybdenum Steel (ASTM Grade 22). The properties of concern include Young's Modulus (E), Poisson's Ratio (ν), the Coefficient of Thermal Expansion (α), the ultimate tensile strength and the yield strength. NAVSEA performed several tensile tests to obtain Yield and Ultimate tensile strength data. The results of the material tests are included as Appendix B.

The values used for the remaining properties were obtained in [Ref. 4: page 4.71], and are as listed below:

- $E = 29.6$ (Kpsi)
- $\alpha = 6.5$ (μ Inch / Inch Degree F)
- $\nu = .30$

It should be noted at this point that all three of these constants are actually functions of temperature and therefore they introduce some non linearities into the problem. The values mentioned above are all evaluated at approximately room temperature.

B. MODEL LOAD DEVELOPMENT

A total of three load conditions were applied to the model. These include an internal pressure load, thermal loading and a longitudinal load applied to the superheater tube.

1. Internal Pressure Load

An internal pressure load was applied to all node points which are located on the inside walls of the tube and header as indicated in Figure 4.2. During normal operation of the boiler the maximum full rating value for internal pressure is 690 Psi. As a "worst case" scenario, an internal pressure of 700 Psi was applied to the model as

described above. The results obtained for the pressure load condition alone are illustrated in Figures 4.2, 4.3, 4.4 and 4.5. In the region of interest, the maximum hoop stress obtained was 0.69 (Ksi). Figure 4.2 illustrates the hoop stresses which were calculated. Figure 4.3 and 4.4 illustrate the principal stresses which were calculated. Figure 4.5 illustrates the deformed structure with the pressure load applied. Using the "window" option all of these stresses have been plotted in the local region of the header tube attachment weld. From these results it is clear that the pressure loading condition has a minimal effect on the stress level of the superheater header structure.

2. Longitudinal Tube Load

The second load developed was a longitudinal load resulting from the internal pressure. If the superheater tube is assumed to be a thin walled cylindrical pressure vessel with an internal pressure, then from [Ref. 5: page 308], the longitudinal stress can be calculated as follows:

$$\sigma_l = \frac{p r}{2 t} \quad (\text{eqn 4.1})$$

where:

- p = internal pressure = 700 (Psi)
- r = inner radius of cylinder = 0.75 (Inches)
- t = thickness of cylinder wall = 0.12 (Inches)

Using these values, the following longitudinal stress is obtained:

$$\sigma_l = 1837.5 \text{ (Psi)} \quad (\text{eqn 4.2})$$

This stress is then converted to a force by multiplying by the cross section area of the tube:

$$\text{Area} = \pi (r_o^2 - r_i^2) \quad (\text{eqn 4.3})$$

$$\text{Area} = .520 \text{ (Inches}^2\text{)} \quad (\text{eqn 4.4})$$

The force F can now be calculated as:

$$F = \sigma_l \times \text{Area} = 955.5 \text{ (Lb}_f\text{)} \quad (\text{eqn 4.5})$$

In order to apply this force to the three dimensional model the force must be calculated per radian. This is calculated as follows:

$$F' = 955.5 (1/2\pi) = 152 \text{ (Lb}_f\text{)} \quad (\text{eqn 4.6})$$

Now utilizing the principle of consistent loading as developed in [Ref. 6: page 164], this load was applied to nodes 85, 86, and 87 as follows:

- $F_{85} = F' (1/6) = 25.3 \text{ (Lb}_f\text{)}$
- $F_{86} = F' (2/3) = 101.3 \text{ (Lb}_f\text{)}$
- $F_{87} = F' (1/6) = 25.3 \text{ (Lb}_f\text{)}$

This loading is illustrated in Figure 4.6

The results for the longitudinal tube load in the region of interest indicated a maximum hoop stress of 0.96 (Ksi). Figures 4.7, 4.8 and 4.9 illustrate the results

obtained for this load condition. Once again the magnitude of the stresses resulting from this load are extremely small when compared to the potential magnitude of the thermal stresses.

3. Thermal Load

The thermal loading of the structure in this case is probably the most important simply because of the relative magnitudes of the other stress compared to the magnitude of the thermal stresses. From the basic thermal stress equation:

$$\sigma_{th} = E \alpha \Delta T \quad (\text{eqn 4.7})$$

and using the values for E and α stated earlier, and a nominal ΔT of 100 Degrees F:

$$\sigma_{th} = 19.24 \text{ (Ksi)} \quad (\text{eqn 4.8})$$

Clearly then, the potential magnitude of the thermal stresses in this problem indicate that the development of a plausible temperature gradient for application to the model is an integral part of the stress analysis of the structure.

In order to develop a realistic temperature gradient in the structure it became apparent that a solution of the heat conduction equation was necessary. To accomplish this an analogy to the stress strain problem was developed. By making the appropriate changes to the SAP-80 code a solution to the steady state heat conduction problem was obtained. The input file for this modified problem was designated HEADERT. The input for this program was the temperature boundary conditions on the model. The data from Appendix A indicates that the maximum temperature difference between the outside and inside walls of the superheater header during operation was approximately 100 Degrees F. From this same data it was clear that the temperature variation during "flex tests" where the load is varied from 90% to 50%

and back to 90% was minimal. It became clear that the only substantial temperature gradients would exist during the start up or shut down of the boiler. The normal practice when securing the boiler is to place a "steam blanket" on the boiler as the boiler is shut down. The normal pressure of the steam used for this process is 150 (Psi). The corresponding saturation temperature for this pressure is approximately 350 Degrees F. During this process the top of the header and the surface of the superheater tube is exposed to the air inside the boiler. Using this information, boundary temperatures were assumed as illustrated in Figure 4.11. The output of the HEADERT program was the steady state temperature at each of the 1001 node points in the model. Figures 4.12 and 4.13 illustrate the temperature field which was created using the boundary conditions mentioned above. The results from the HEADERT program were substituted into the "potential" file of the HEADER program prior to solution of the equations.

Having developed a plausible temperature field for the model the program HEADER was executed. The load "combination" option of the SAP-80 code allows the user to obtain results for any selected combination of the load conditions which are included in the SAP-80 input file. The input file for HEADER contained two load conditions; the thermal loading as well as the longitudinal load applied to the superheater tube. The listing of the HEADERT and HEADER input files are included as Appendices E and F respectively.

The results for the thermal load condition, in the local region of the weld, indicated a maximum hoop stress of 19.01 (Ksi). Figures 4.14 illustrates the calculated hoop stresses in this region. Figures 4.15 and 4.16 illustrate the maximum and minimum principal stresses in the same region of the model. These results clearly show that the magnitude of the thermal stresses greatly overshadows both the internal pressure load and the longitudinal tube load.

C. ERROR CONSIDERATIONS

One of the best indicators of the accuracy of a finite element solution is to examine the results at the boundaries of adjacent elements. With the graphical results that have been presented, a feel for the accuracy can be obtained by looking closely at the stress contours that are plotted. In all of the results that have been obtained in this analysis, the stress contours exhibit extremely good continuity and there are very few places where there seems to be a significant difference in calculated stresses at the boundaries of adjacent elements. Despite the fact that some of the quadrilateral

elements were quite distorted, no mathematical singularities were encountered during solution of the problem. This can most likely be attributed to the use of a sufficiently fine mesh and the nine node quadrilateral element.

Probably the largest source of error is actually introduced in the definition of the problem to be solved. In this analysis several assumptions had to be made in order to arrive at an adequate problem definition. The various assumptions which were made have been discussed as they arose during the problem formulation. The assumptions made during the problem formulation are most likely the largest source of error in the solution of the problem.

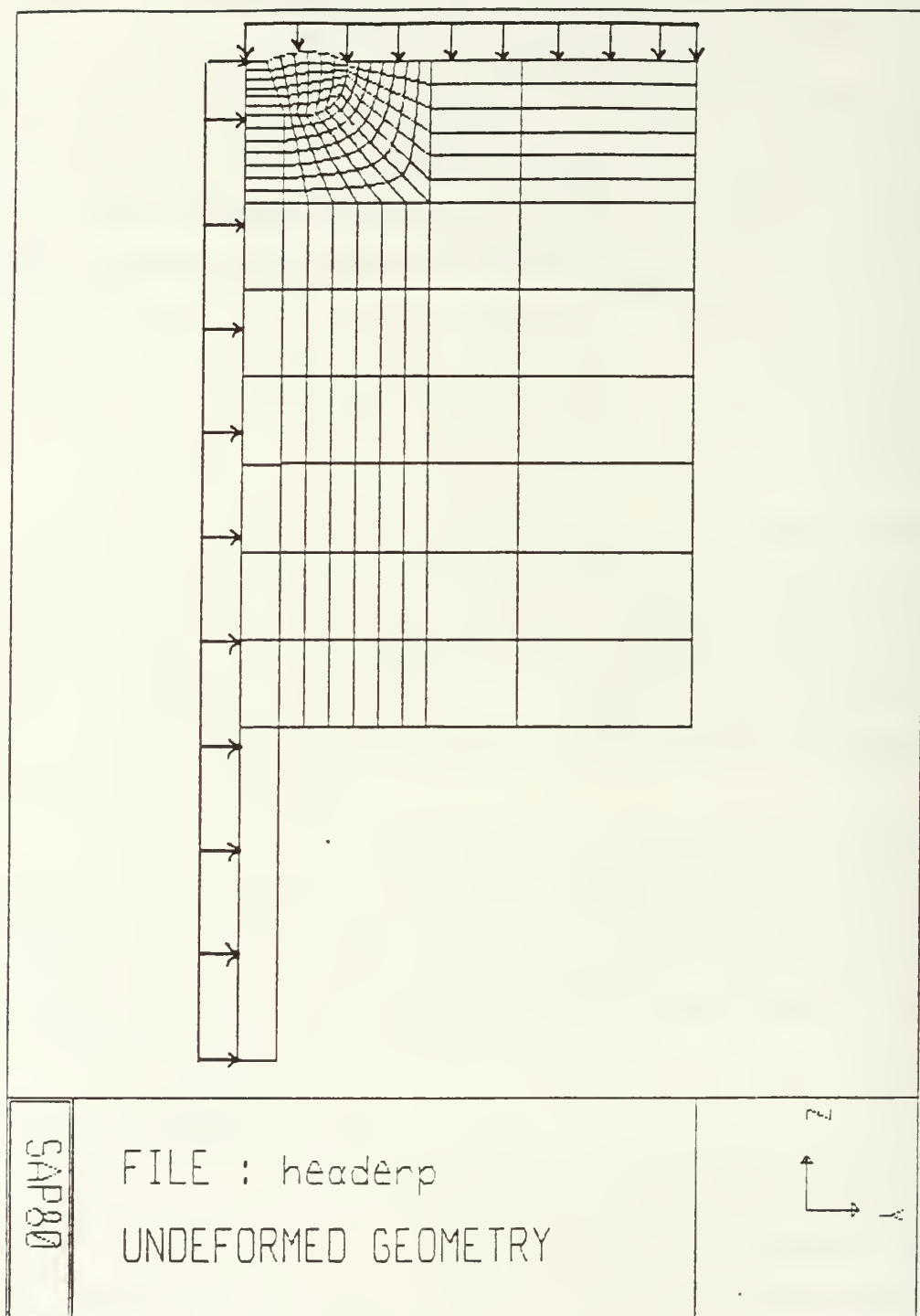


Figure 4.1 Orientation of the Internal Pressure Load.

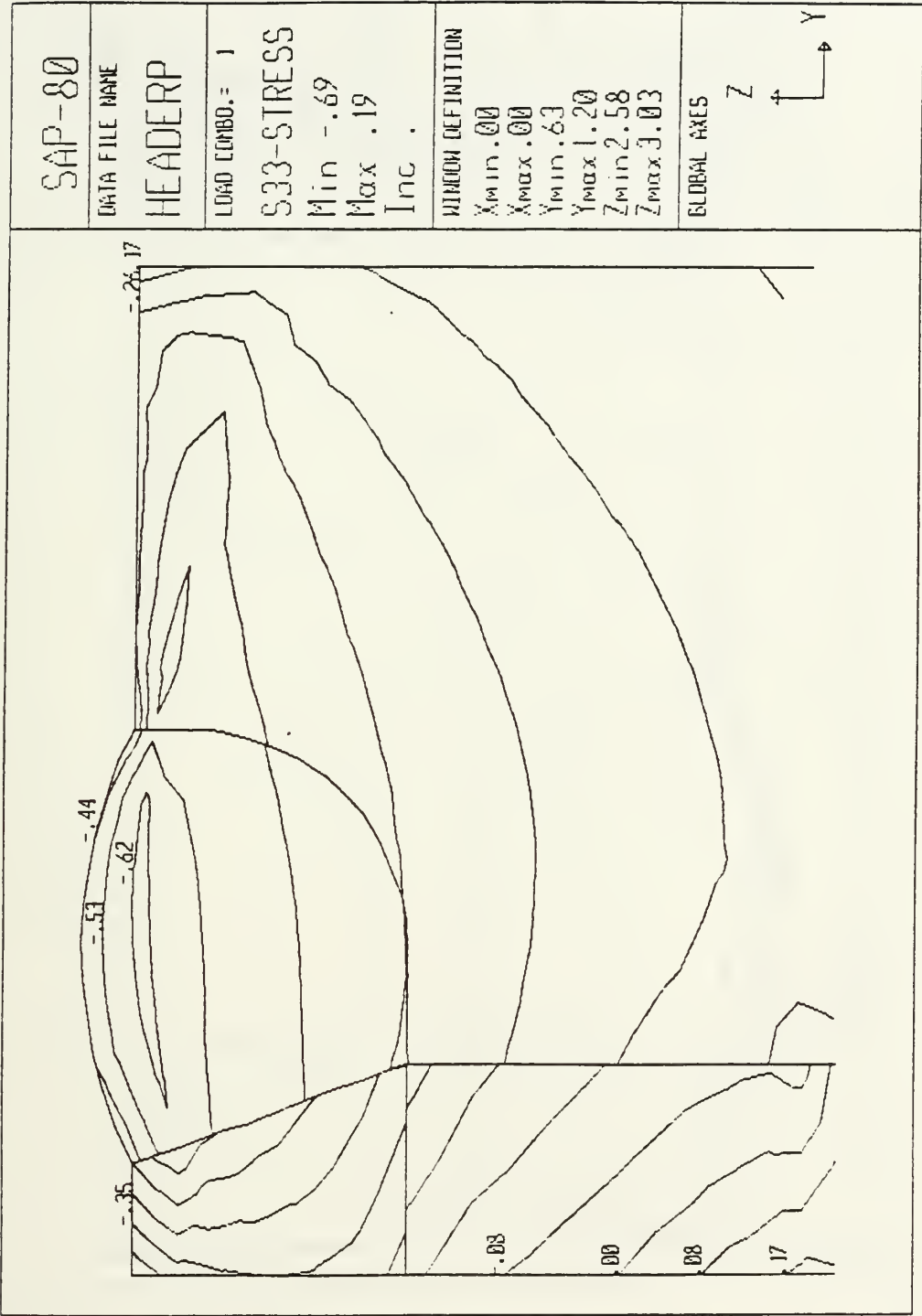


Figure 4.2 Hoop Stress for the Pressure Load Condition (Ksi).

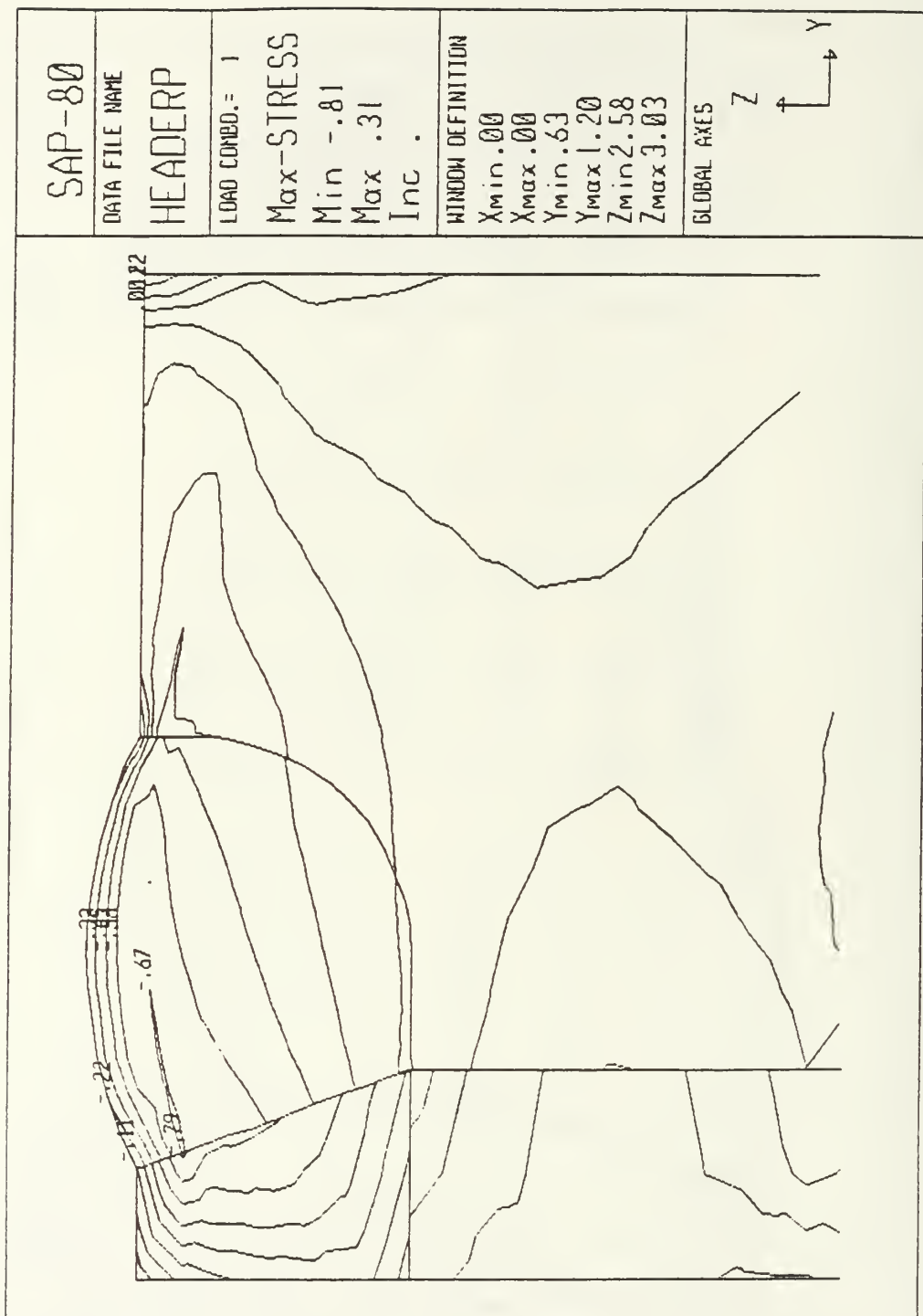


Figure 4.3 Maximum In Plane Stress for Pressure Load Condition (Ksi).

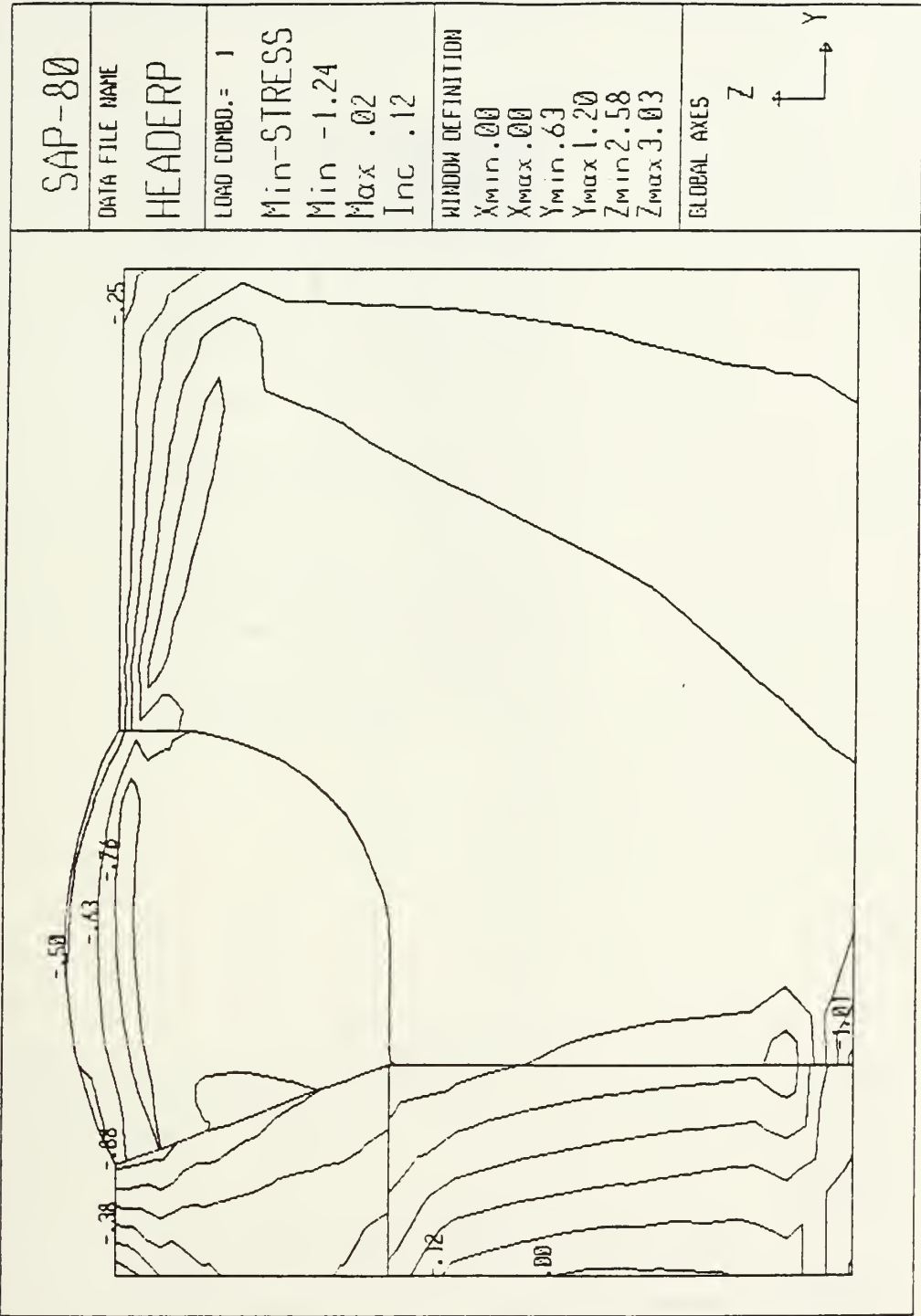


Figure 4.4 Minimum In Plane Stress for Pressure Load Condition (Ksi).

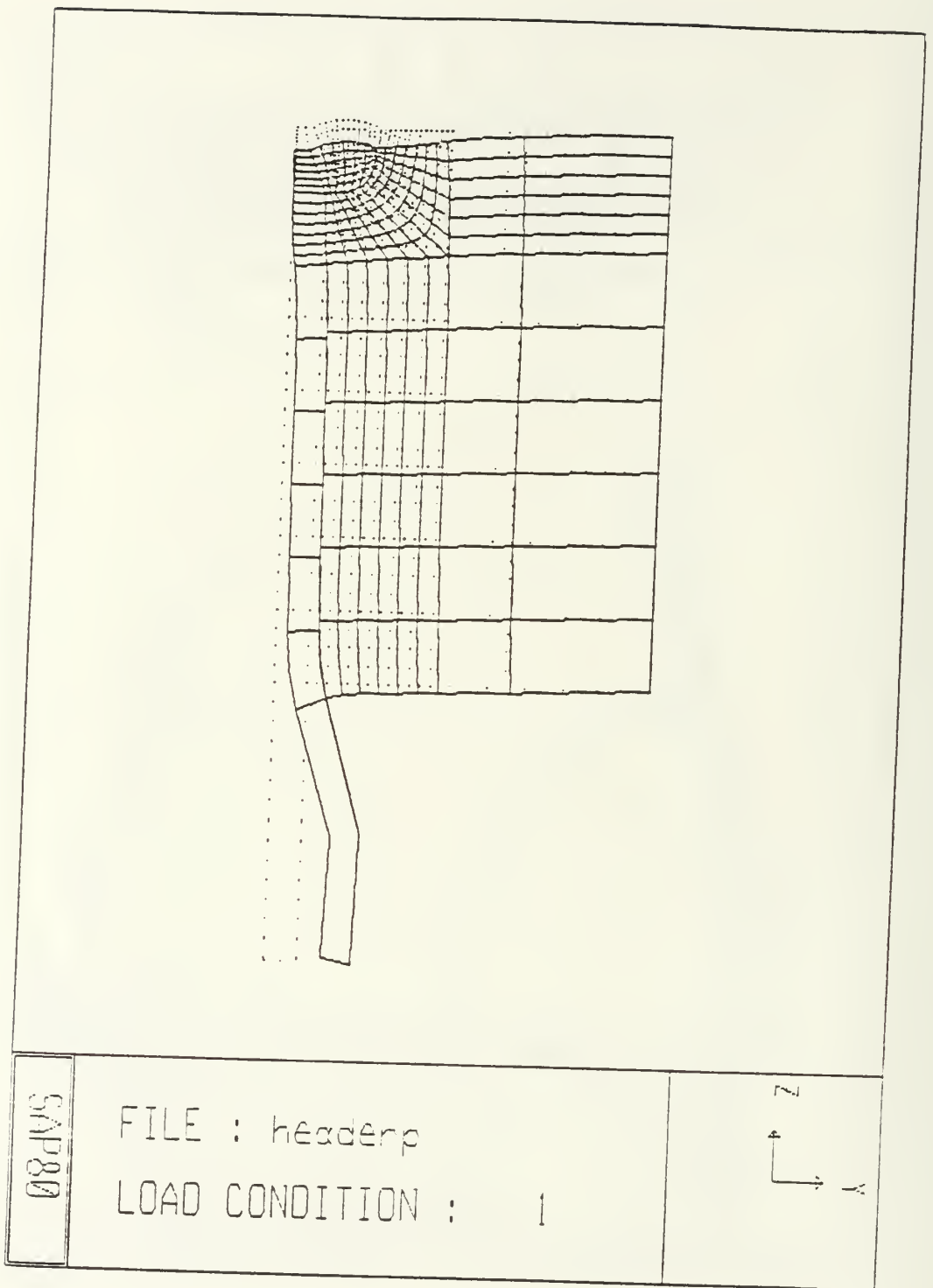


Figure 4.5 Deformed Structure for the Pressure Load Condition.

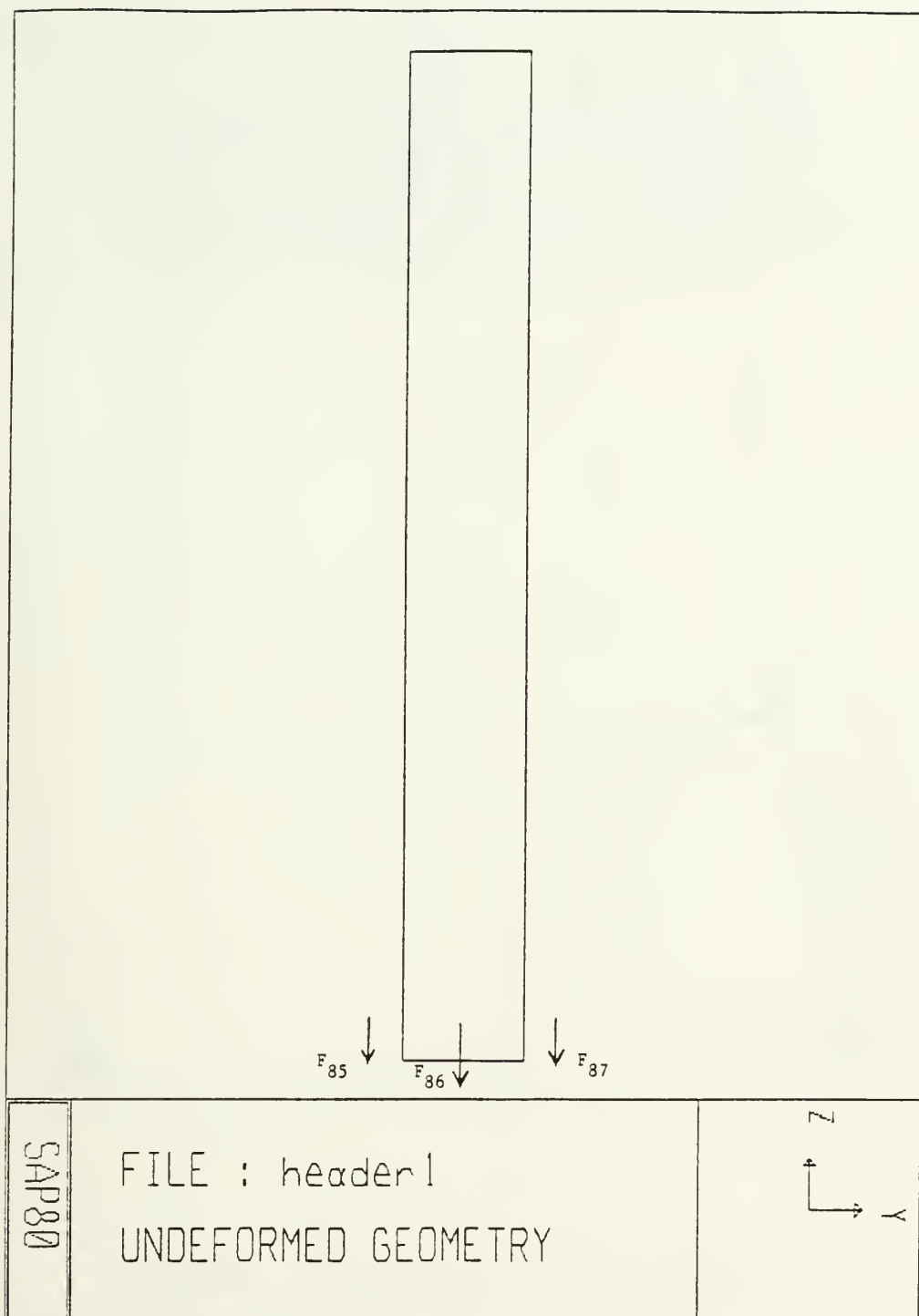


Figure 4.6 Longitudinal Loading of the Superheater Tube.

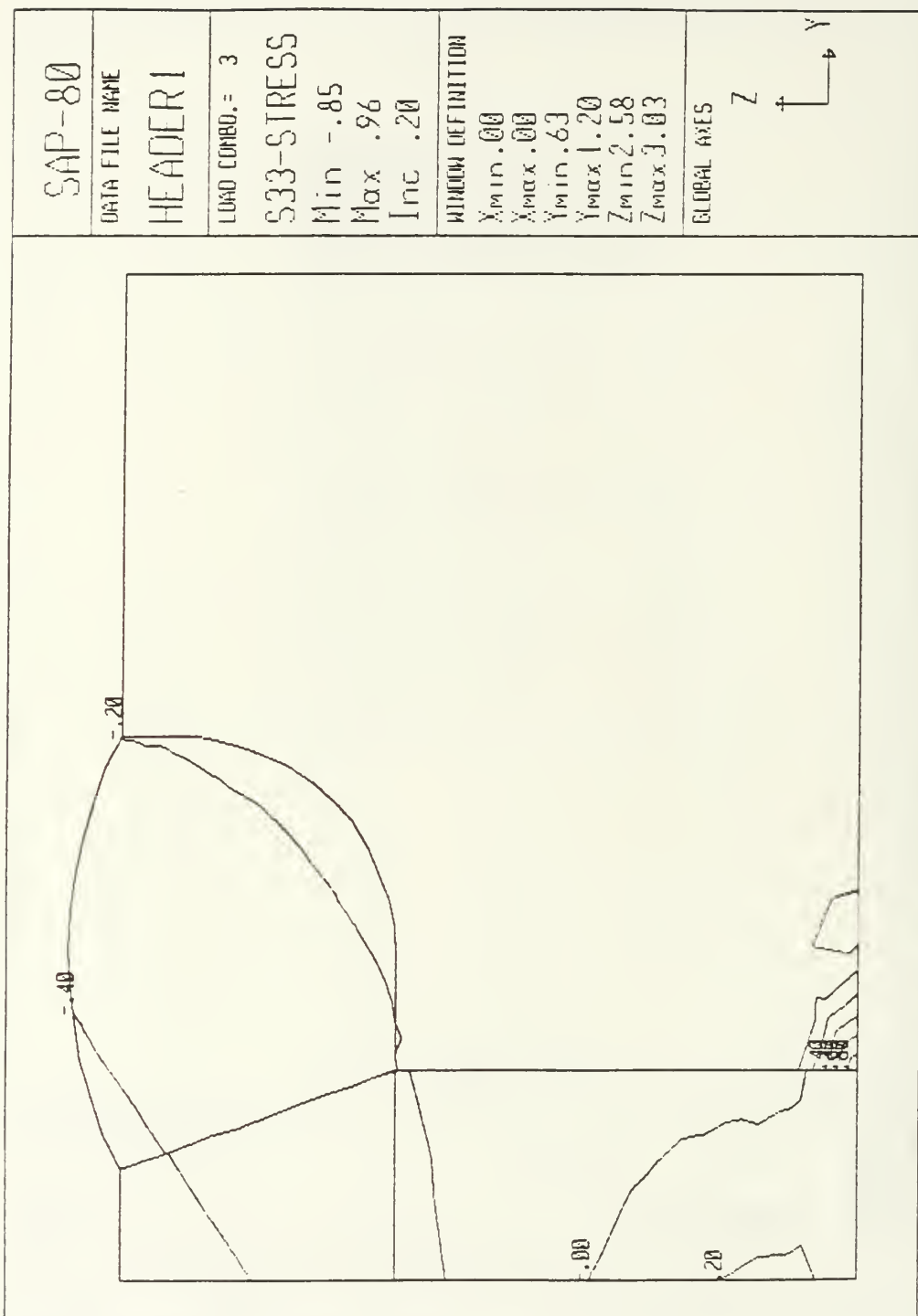


Figure 4.7 Hoop Stress for the Longitudinal Load Condition (Ksi).

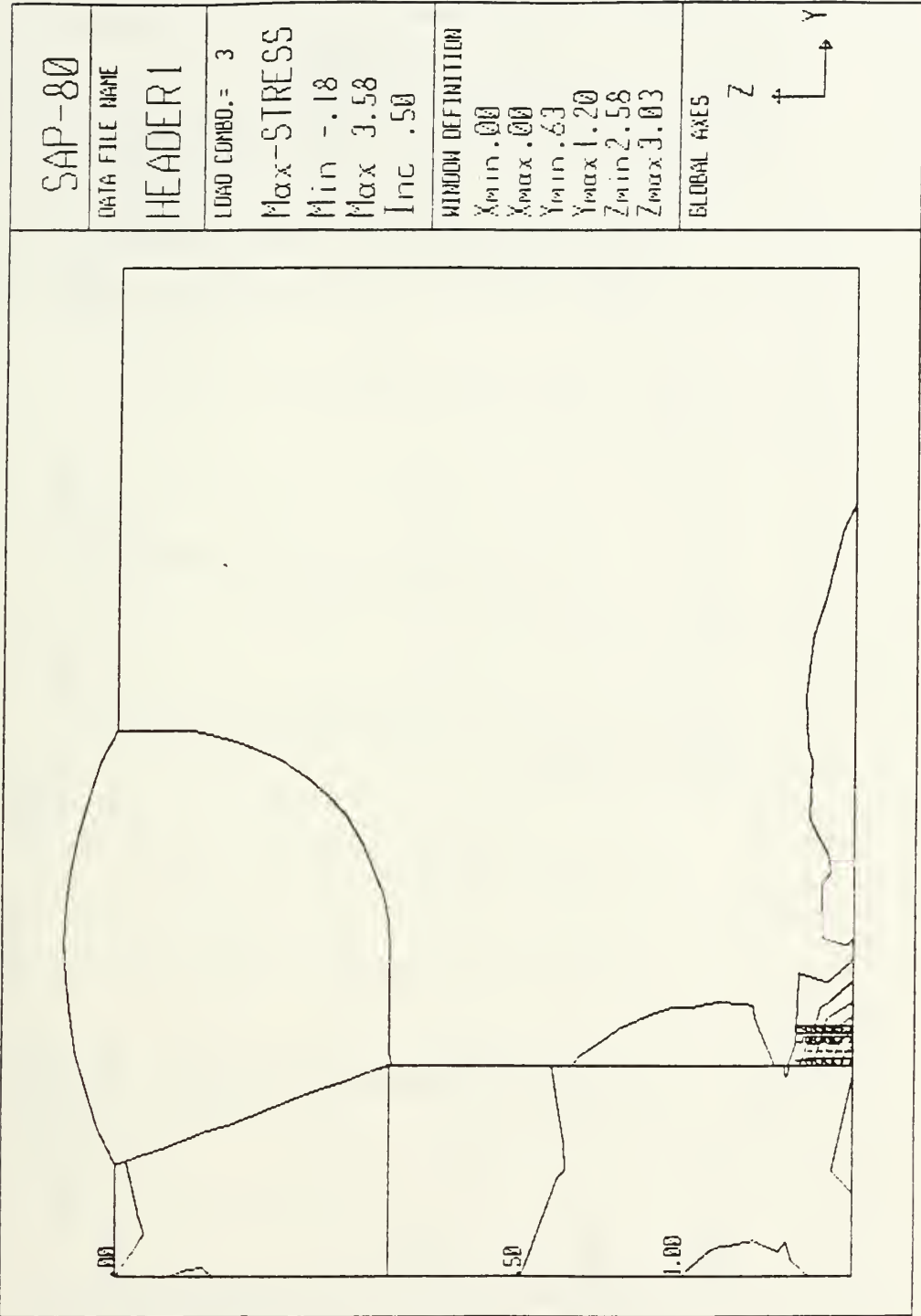


Figure 4.8 Maximum In Plane Stress for the Longitudinal Load (Ksi).

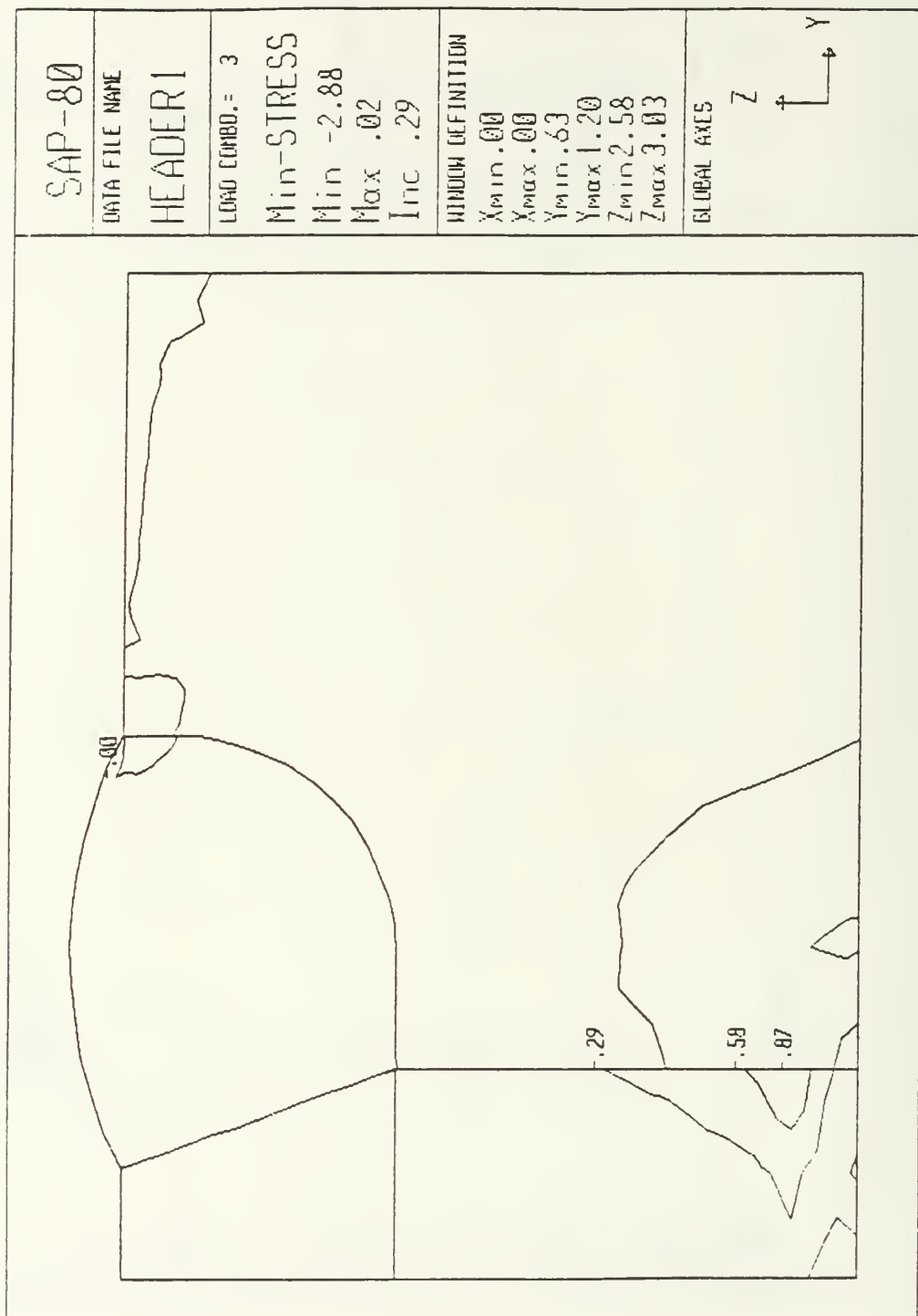


Figure 4.9 Minimum In Plane Stress for the Longitudinal Load (Ksi).

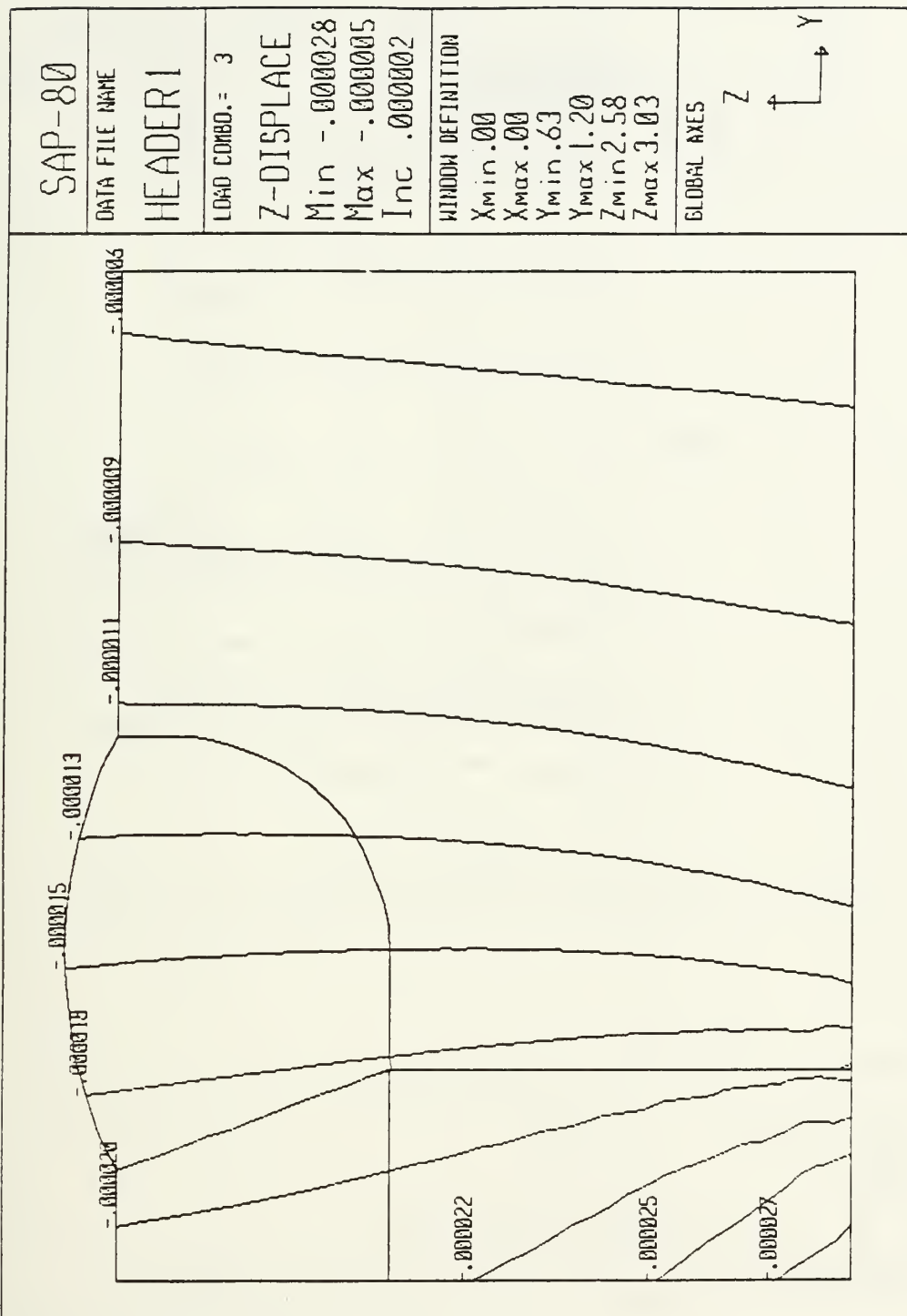


Figure 4.10 Z Displacements for Longitudinal Load Condition (Inches).

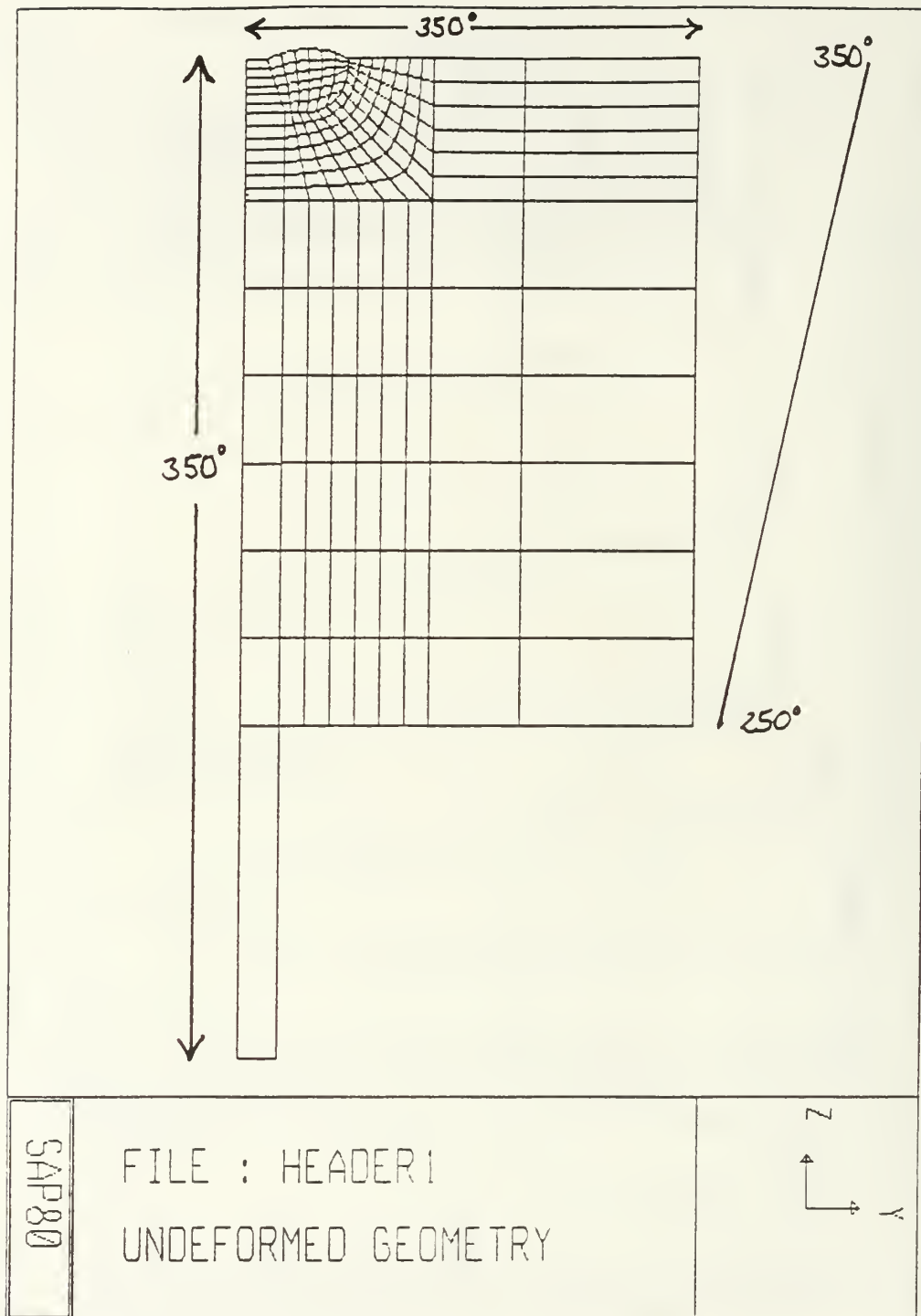


Figure 4.11 Temperature Boundary Conditions for the Model (Degrees F).

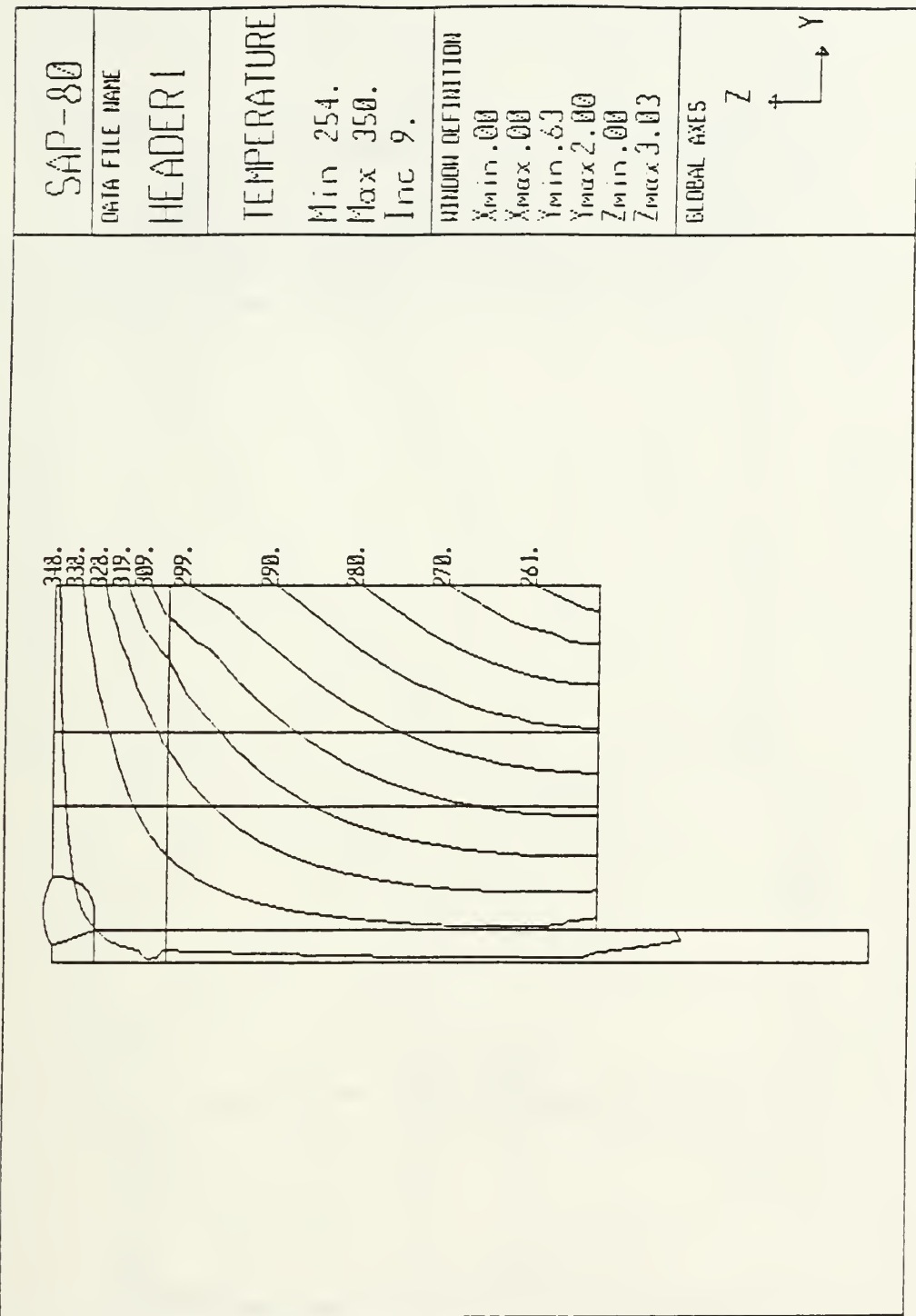


Figure 4.12 Temperature Field Developed for the Model (Degrees F).

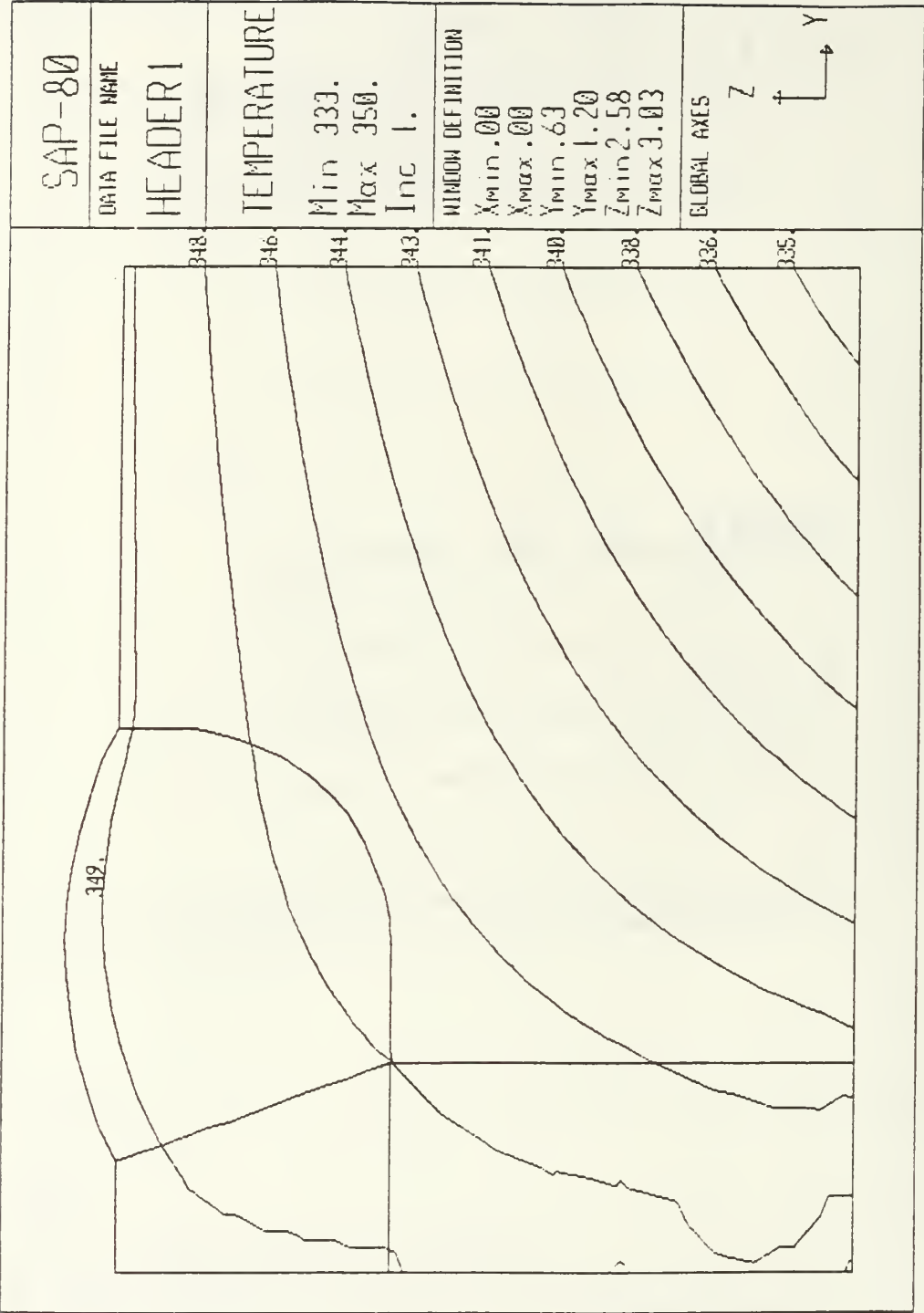


Figure 4.13 Temperature Field - Local Region of the Weld (Degrees F).

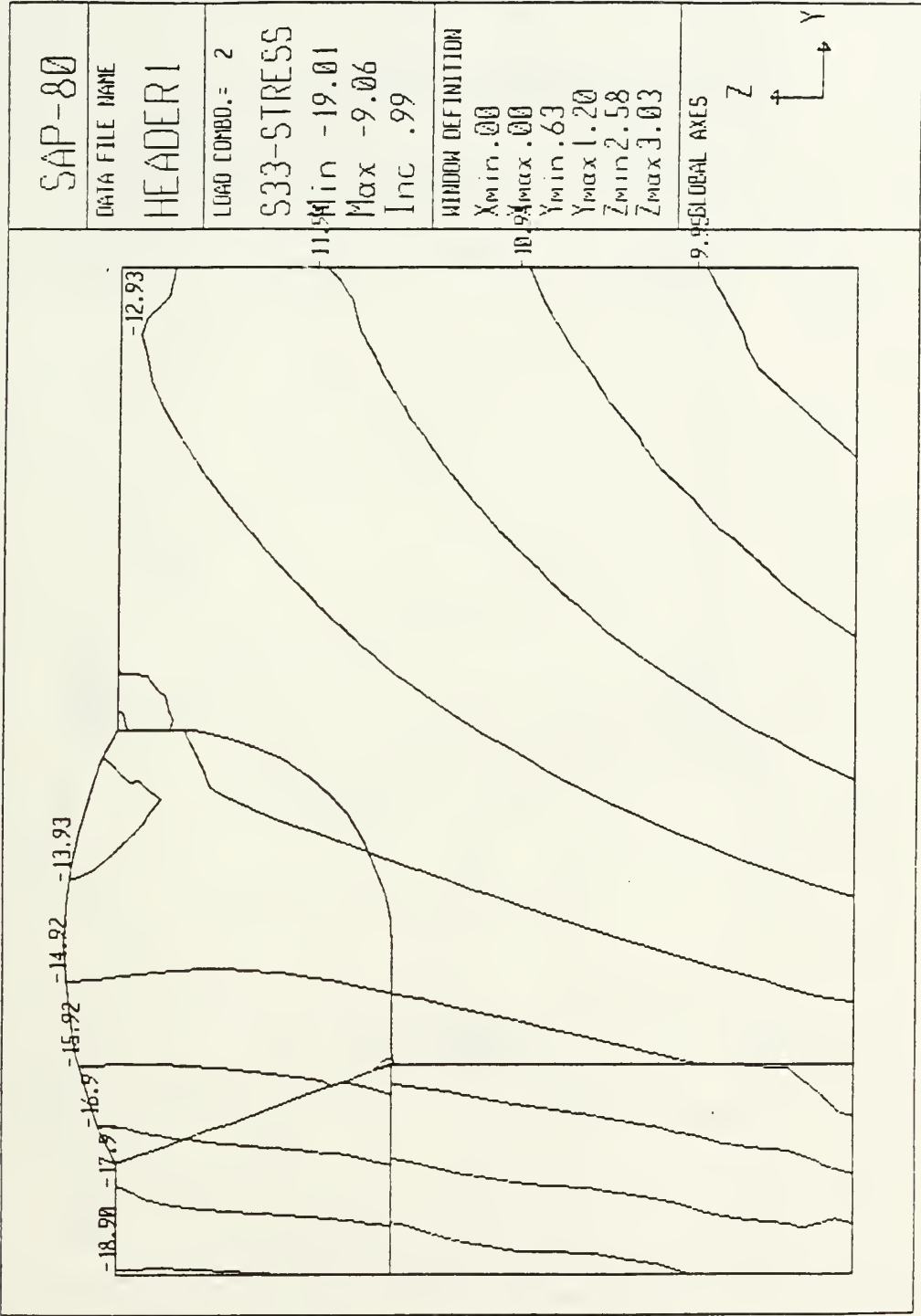


Figure 4.14 Hoop Stress for Thermal Load Condition (Ksi).

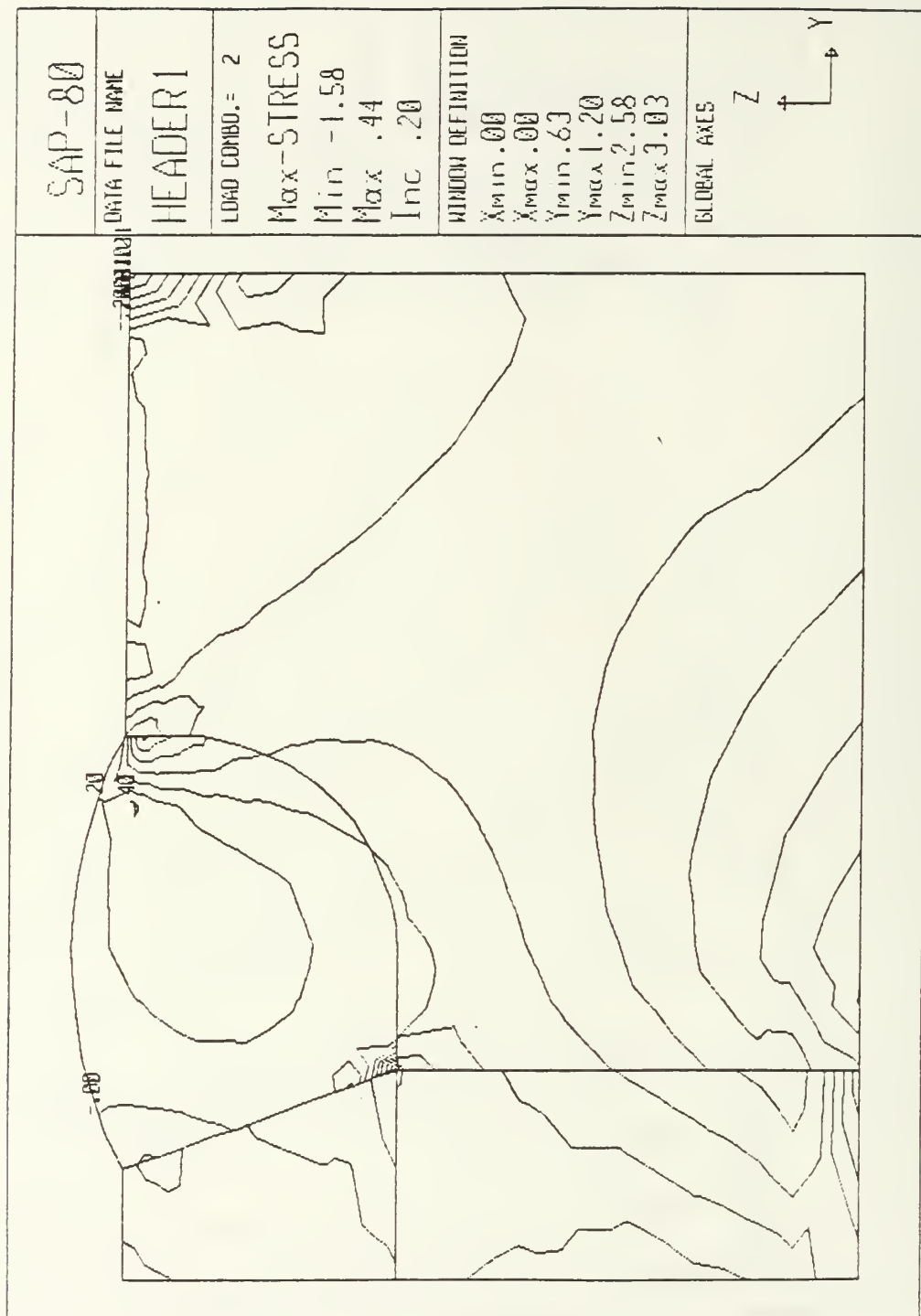


Figure 4.15 Maximum In Plane Stress for Thermal Load Condition (Ksi).

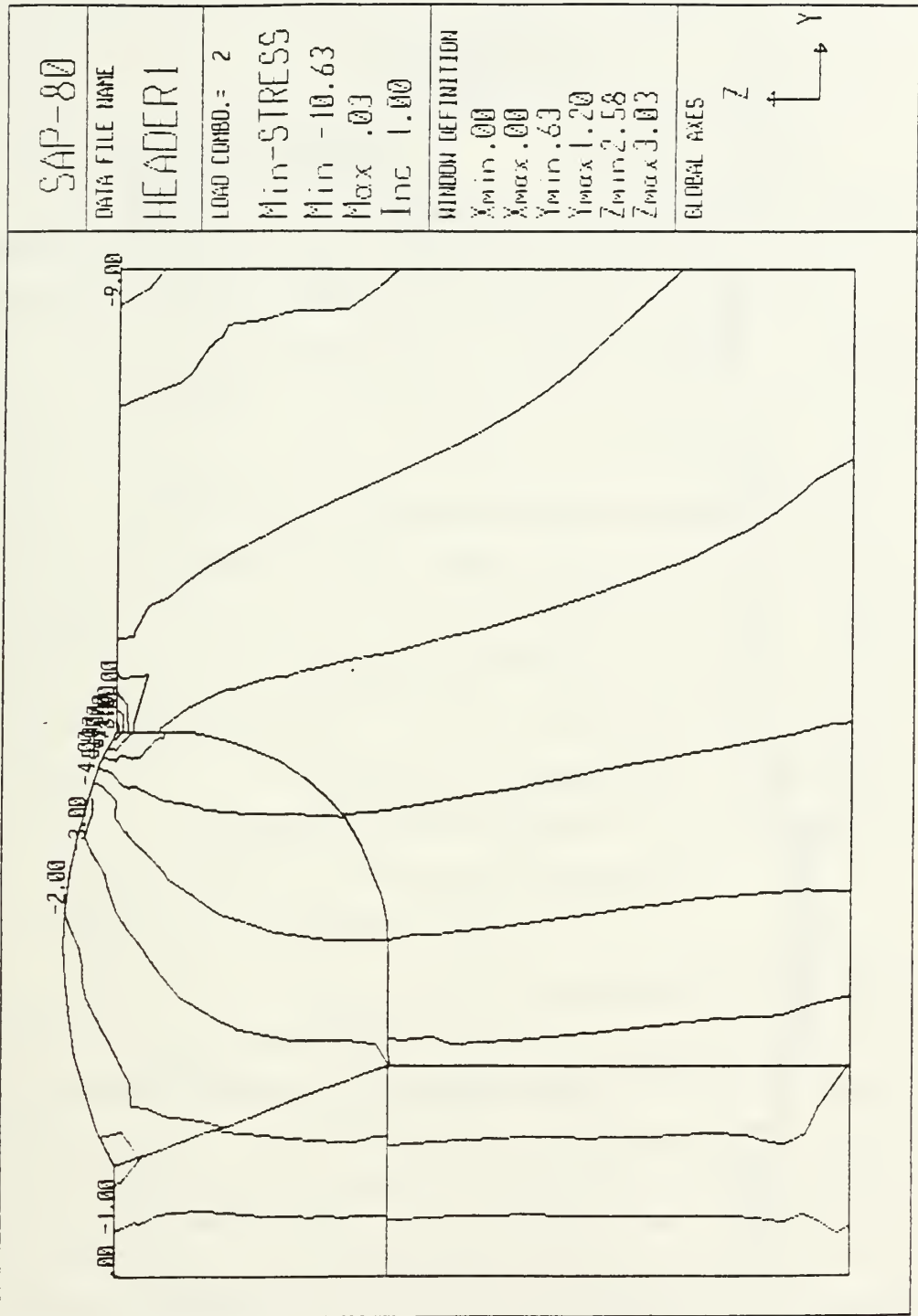


Figure 4.16 Minimum In Plane Stress for Thermal Load Condition (Ksi).

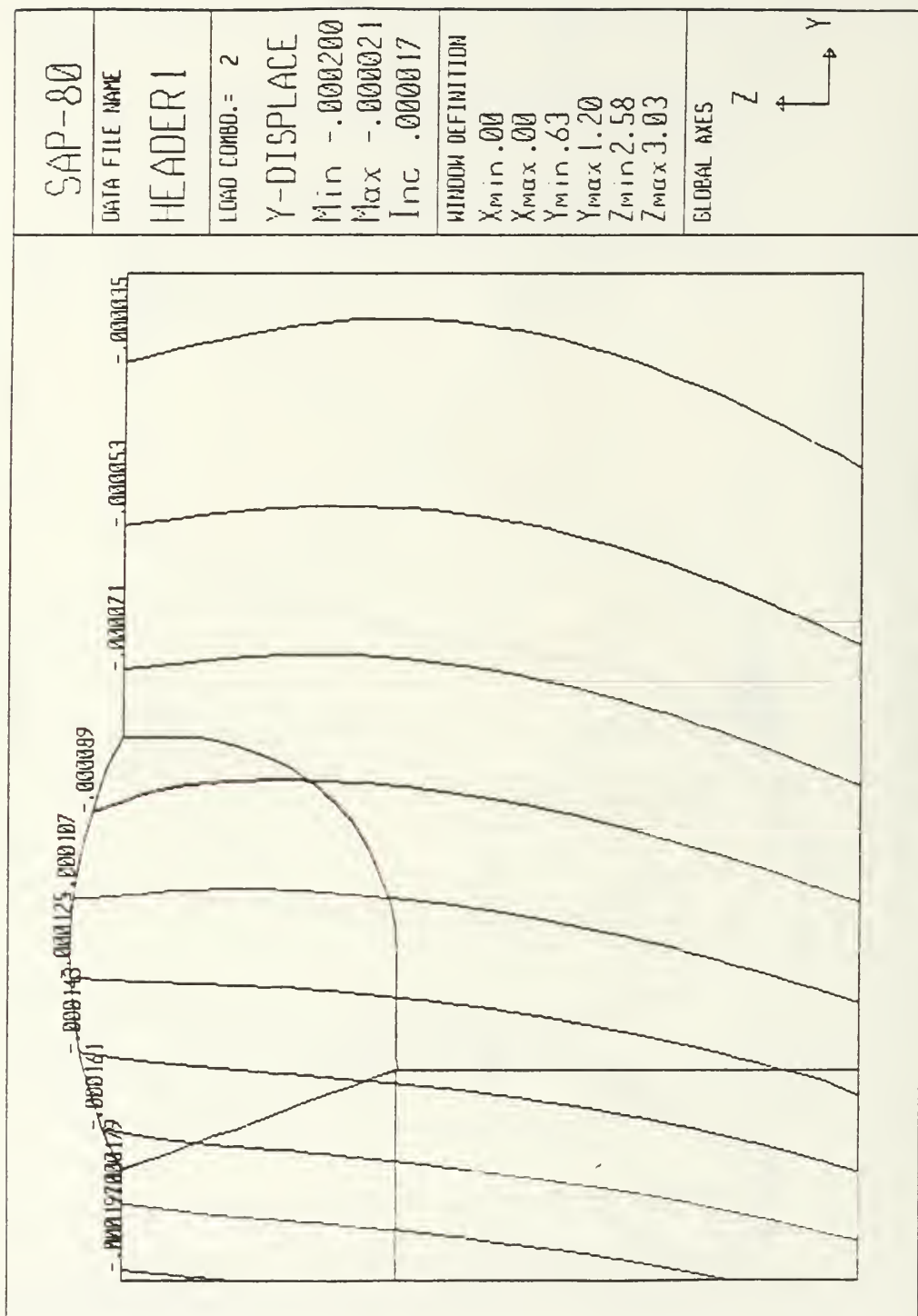


Figure 4.17 Y Displacements for Thermal Load Condition (Inches).

V. CONCLUSIONS

A. DISCUSSION OF RESULTS

As illustrated in the previous chapter, the thermal stresses are by far the most dominant stresses in this problem. The maximum calculated hoop stress of 19.01 (Ksi) does not exceed the yield strength of the material, which is approximately 35 (Ksi), as listed in Appendix B. However, if the possible effects of fatigue are considered, it is very possible that these stresses could significantly contribute to the failure of the superheater header. As indicated in Appendix E, an excerpt from the ASME boiler code, for an operating temperature of 400 Degrees F the maximum allowable stress is 15.0 (Ksi). Appendix F indicates that during a five year operating cycle there would be approximately 300 boiler shutdowns. Approximately 50% of these shutdowns would employ the use of a steam blanket as described earlier. The rest of the shutdowns would be from operating pressure down to ambient pressure. These shutdowns not utilizing a steam blanket would lead to even larger thermal gradients in the header. Although the data in Appendix F is for the CV-60 class of ship, the operating cycle should be similar to the operating cycle of the LHA-1 class. Using this criteria, the results of the stress analysis would definitely indicate that a possible failure condition exists. Some other pertinent considerations are included below.

1. Superheater Header Design

The U.S. Navy employs a similar header cross section in six classes of ships. The only class which has experienced such a large number of failures is the LHA-1 class. The other applications which use a similar cross section differ in one major area. The other applications of this header utilize a "sectionalized" design. In this design instead of having one inlet/outlet header and one intermediate header which run the entire width of the boiler, the header is broken down into four smaller headers, with each of the smaller headers being approximately one fourth the width of the boiler. For the LHA-1 class the steam inlet temperature is approximately 500 Degrees F and the outlet temperature is approximately 850 Degrees F during normal operation. Therefore the superheater header is subjected to a temperature difference of approximately 350 Degrees F from the inlet side to the outlet side. In the case of the "sectionalized" headers, the temperature difference from the inlet to the outlet of each

section is in most cases less than 100 Degrees F. Since it has been demonstrated that the thermal stresses and in particular the temperature gradients which produce them, are the driving force for the stresses experienced in the header, it would seem that the LHA-1 class definitely has the potential for larger thermal stresses to be developed. Also adding to the problem is the fact that the LHA-1 class header has a mass which is approximately four times that of each of the smaller sections. From the consideration of the heat transfer problem, this would lead to a much longer time for the header to reach equilibrium and therefore the header would be subjected to these larger thermal gradients for a longer period of time. From a structural point of view, the sectionalized headers provide more flexibility and thus tend to reduce stresses.

2. Effects of Creep

Although this study has not considered the effects of high temperature creep on the structure, these effects are certainly important in this problem. If the boiler is operated at an elevated temperature for an extended period of time, it is possible that through the creep relaxation process that the header could actually experience extremely small stresses or possibly a zero stress condition during elevated temperature operation. However, after this extended period of elevated temperature operation it would be possible for a "stress reversal" to take place when the boiler is secured. If for example, the header was in compression during elevated temperature operation, upon shut down of the boiler it might be possible for the header to actually go into a state of tension. If it is also considered that this process would occur each time the boiler was secured, this process could lead to a fatigue condition in the header.

3. Effects of Vibration

Despite the fact that the effects of vibration have not been studied in this report it is certainly possible that a frequency analysis of the structure would yield some significant information. Since the V2M boiler is the largest propulsion boiler employed by the U.S. Navy, the superheater tubes are subjected to an extremely large volume of air flowing through and around the superheater structure. It would seem that the potential for some significant stresses to be produced due to vibration exists. The possibility of a resonance situation is one which certainly would justify further investigation of the transient response of this structure.

B. OPPORTUNITIES FOR FURTHER RESEARCH

The model which has been developed in this thesis provides a basis for further studies to be made of the structure in question. With this basic model, the effects of

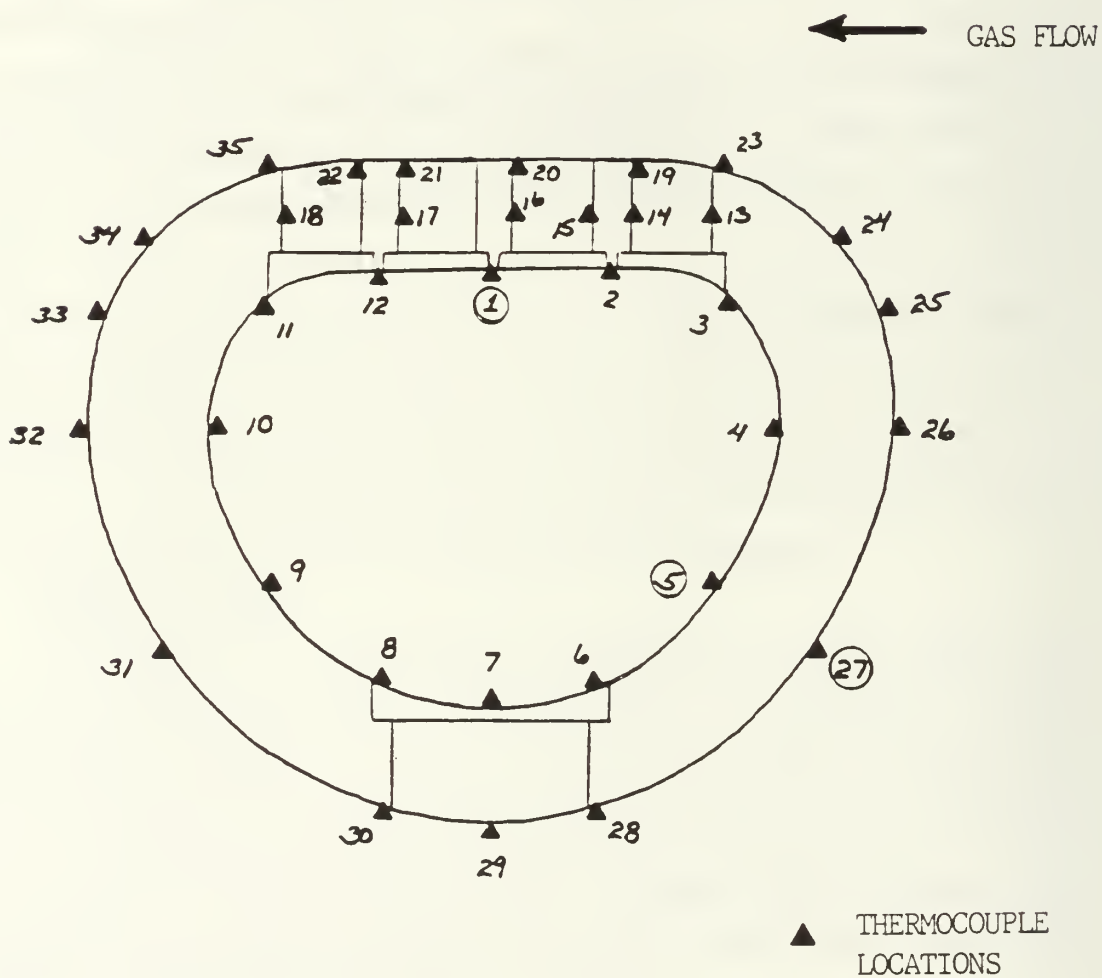
numerous load conditions, boundary conditions and temperature fields can be studied. Some possible avenues for further investigation are listed below:

- Obtain more detailed experimental temperature data in the weld region
- More detailed study of the heat conduction problem
- Inclusion of temperature dependent material properties
- Inclusion of distinct material properties for the weld material
- Consideration of high temperature "creep" effects on the structure
- Transient response of the structure
- Further investigation of appropriate boundary conditions

Due to the complexity of this problem, it is not likely that one report could include all of the possible areas to be investigated. This report has attempted to develop a basic model of the superheater header tube attachment region and to identify and investigate the significant factors affecting the stress level and possible failure of the structure. It is hoped that follow-on studies will be made to further investigate the cause or causes of the numerous failures which have taken place.

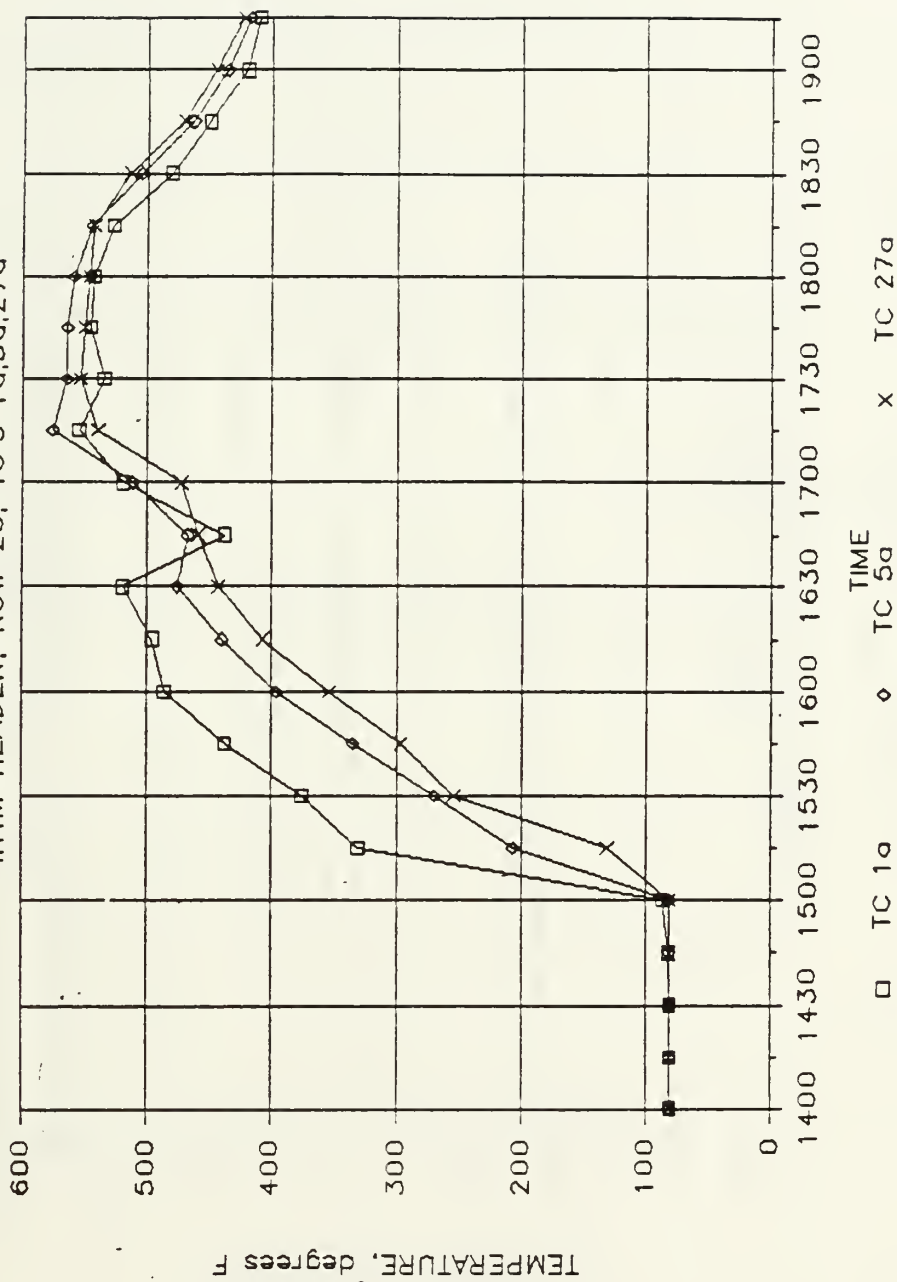
APPENDIX A
TEMPERATURE INSTRUMENTATION DATA FROM THE USS
BELLEAU WOOD

SUPERHEATER HEADER CROSS SECTION



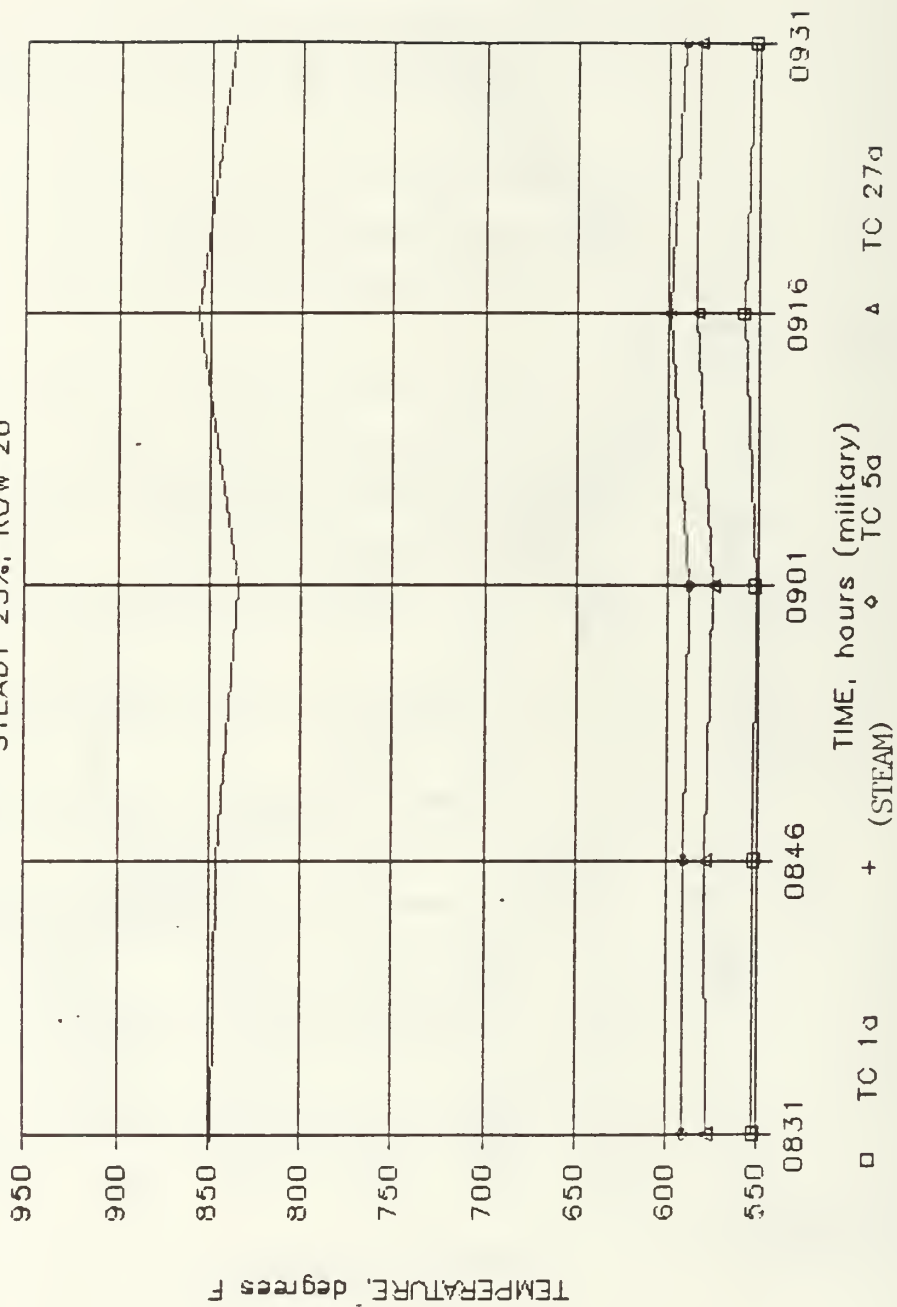
LHA-3 COLD LIGHT-OFF

INTM HEADER, ROW 20, TC'S 1a,5a,27a



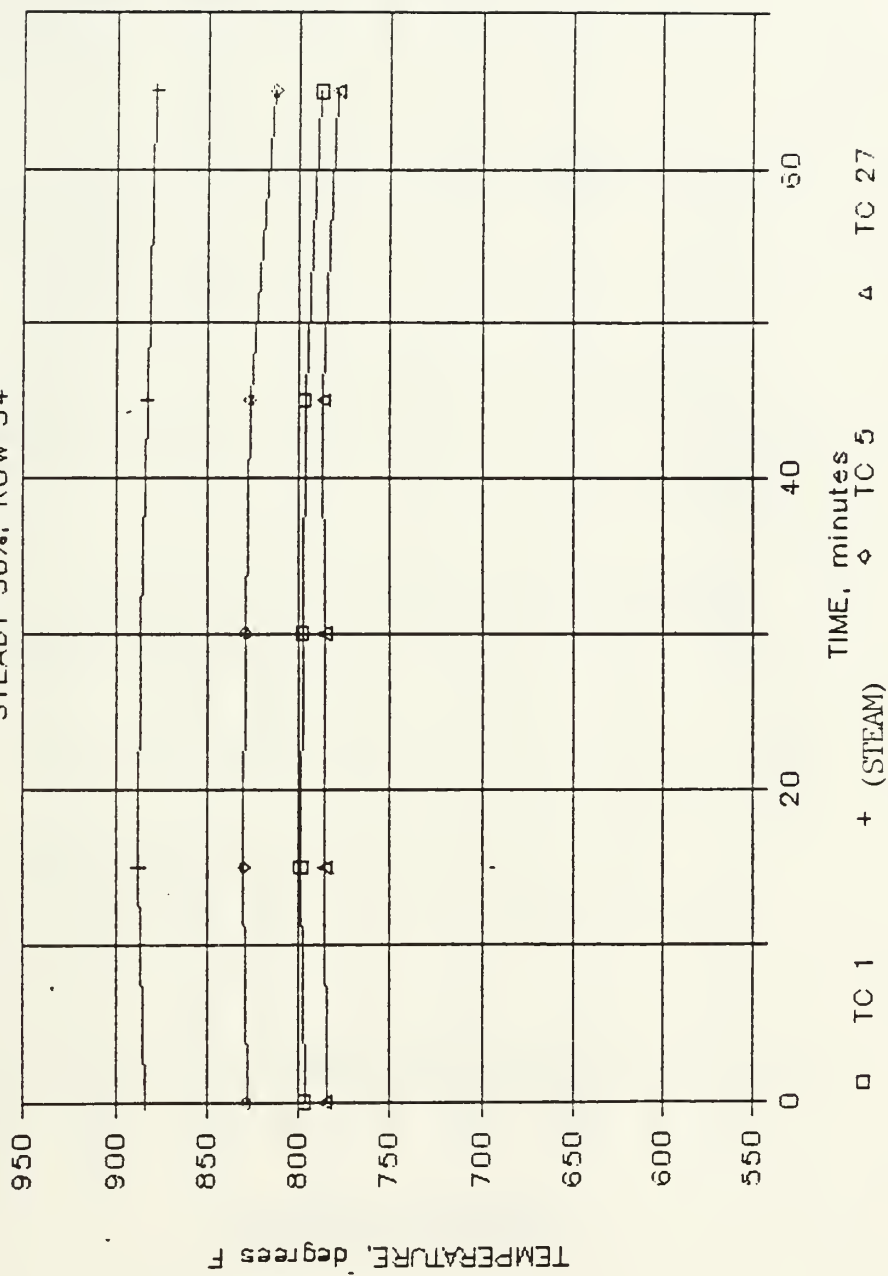
LHA-3 THERMAL DATA

STEADY 25%, ROW 20



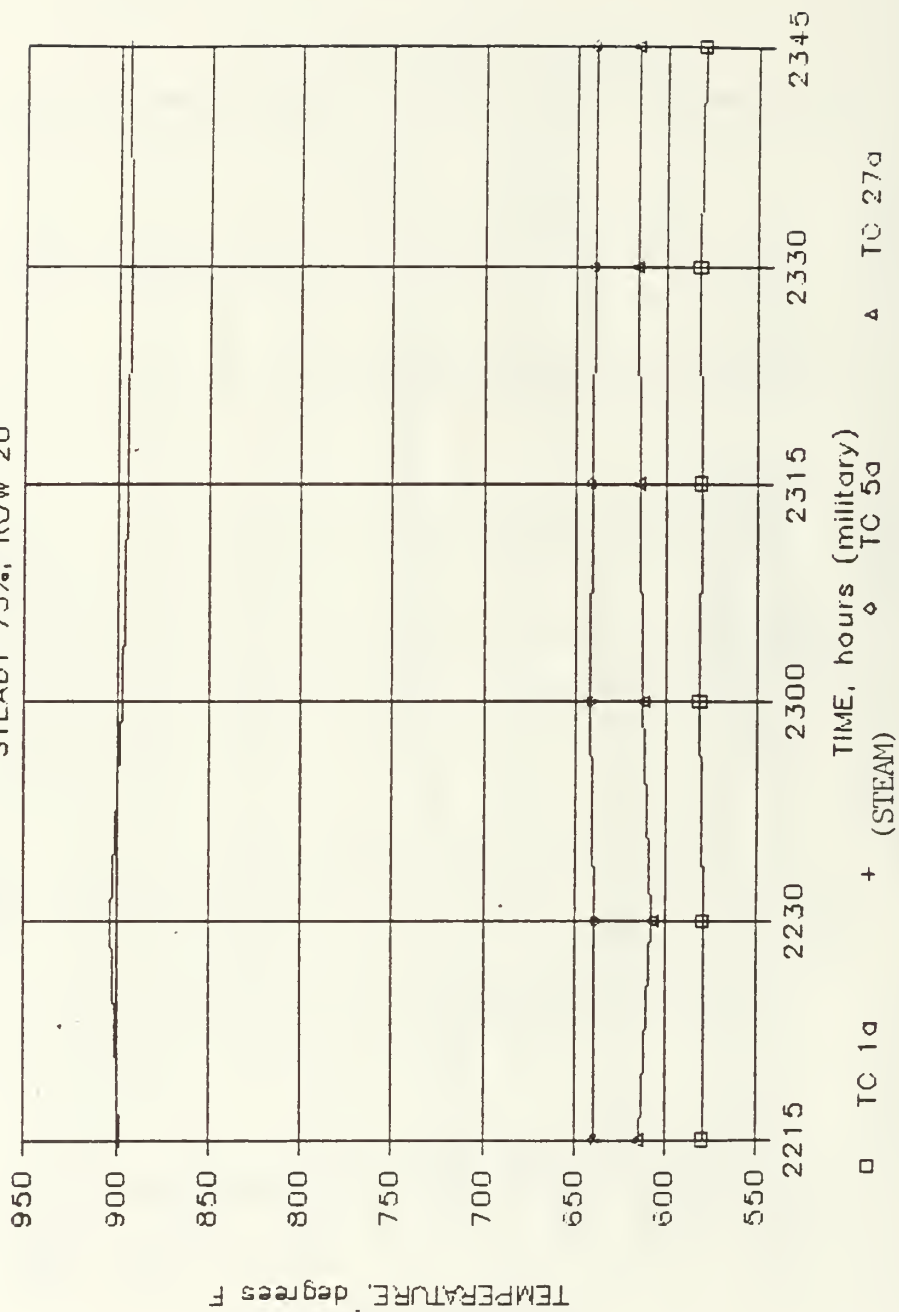
LHA-3 THERMAL DATA

STEADY 50%, ROW 54



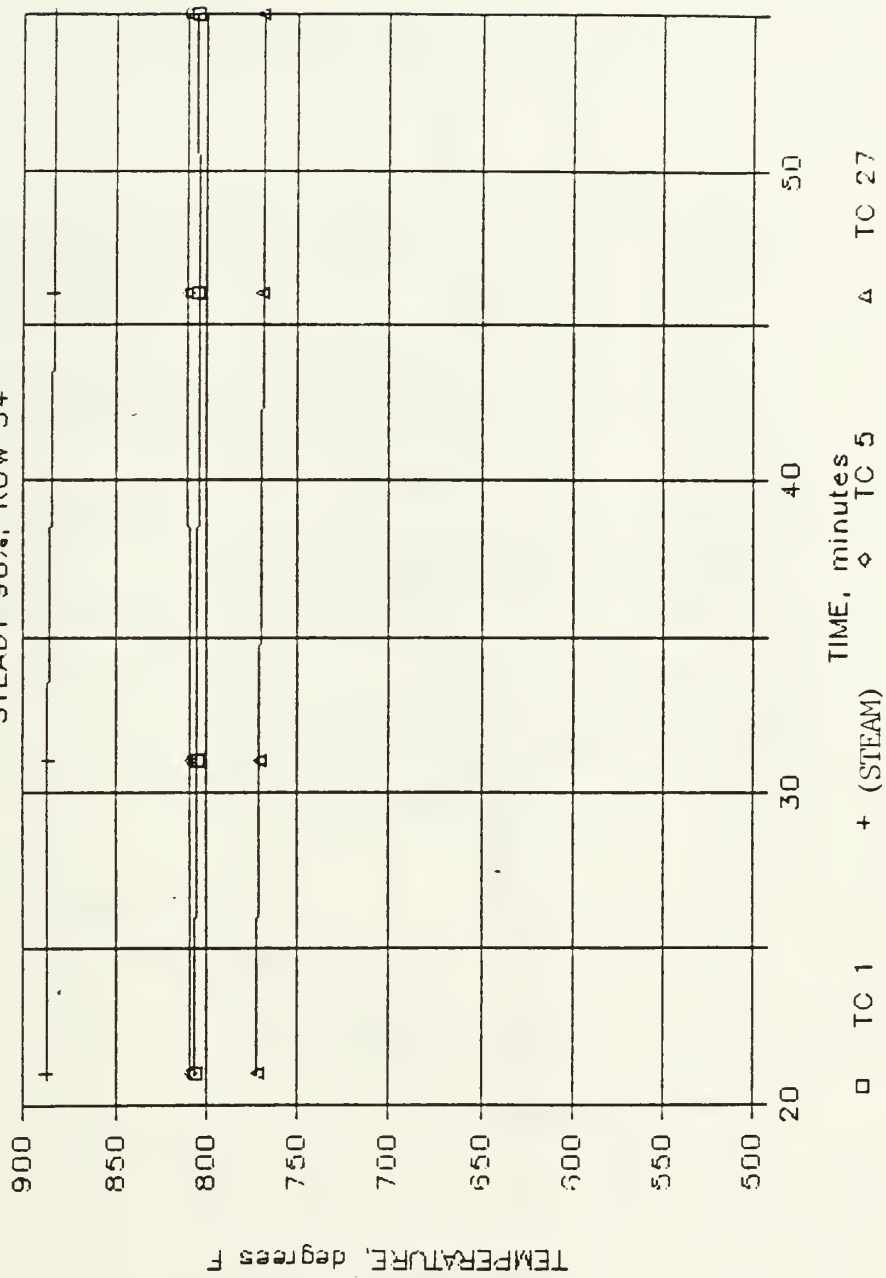
LHA-3 THERMAL DATA

STEADY 75%, ROW 20



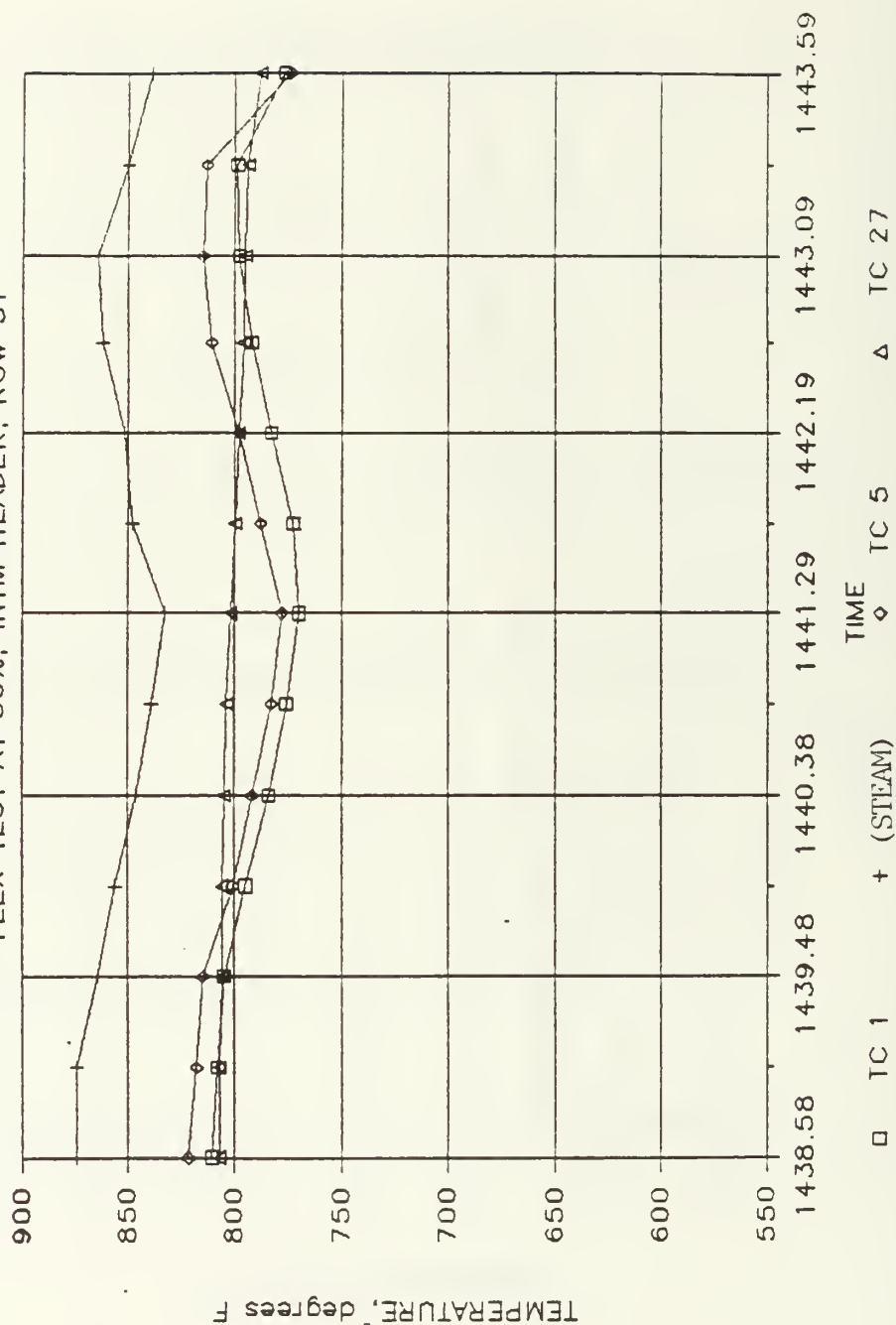
LHA-3 THERMAL DATA

STEADY 90%, ROW 54



LHA-3 THERMAL DATA

FLEX TEST AT 50%, INTM HEADER, ROW 54



USS BELLEAU WOOD - LHA 3
FORWARD BOILER
PLAN OF SUPERHEATER HEADERS

DATE: 3/3

TIME: 11/0/0

POWER: 50%

INLET-OUTLET
HEADER

TC(36) 503 °F

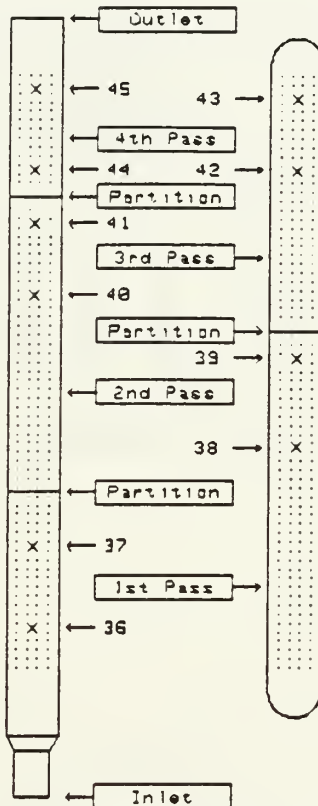
TC(37) 503 °F

TC(40) 686 °F

TC(41) 691 °F

TC(44) 887 °F

~~TC(45) 500 °F~~



INTERMEDIATE
HEADER

TC(38) 587 °F

TC(39) 592 °F

TC(42) 808 °F

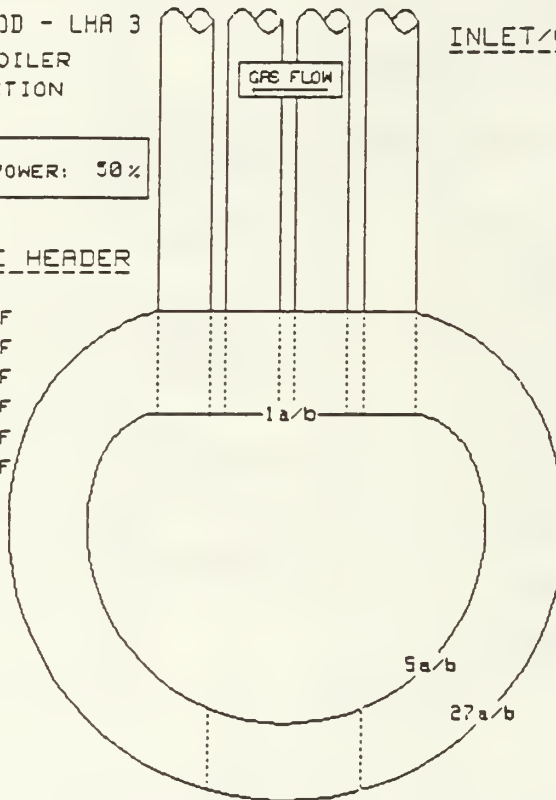
TC(43) 800 °F

USS BELLEAU WOOD - LHA 3
FORWARD BOILER
CROSS-SECTION

DATE: 3/3
TIME: 11/0/53 POWER: 50%

INTERMEDIATE HEADER

ROW 20 (1a) 569°F
(1b) 569°F
(5a) 624°F
(5b) 626°F
(27a) 605°F
(27b) 598°F



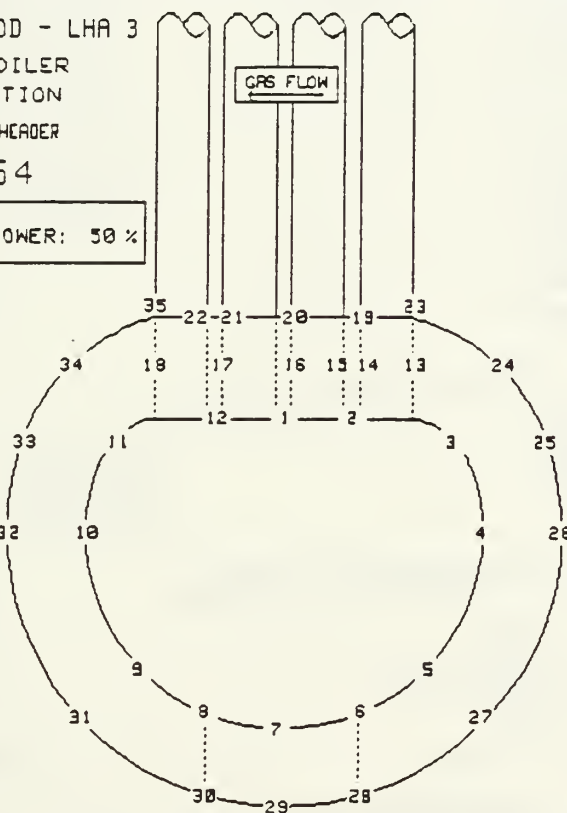
INLET/OUTLET HEADER

ROW 2 (1a) 688°F
(1b) 503°F
(5a) 503°F
(5b) 502°F
(27a) 494°F
(27b) 499°F
ROW 22 (1a) 639°F
~~(1b) 524°F~~
(5a) 588°F
(5b) 599°F
(27a) 569°F
(27b) 560°F
ROW 53 ~~(1a) 509°F~~
(1b) 689°F
(5a) 683°F
~~(5b) 732°F~~
(27a) 682°F
(27b) 676°F
ROW 67 ~~(1a) 892°F~~
(1b) 893°F
(5a) 878°F
(5b) 876°F
(27a) 766°F
(27b) 750°F

USS BELLEAU WOOD - LHA 3
FORWARD BOILER
CROSS-SECTION
INTERMEDIATE HEADER
ROW 54

DATE: 3/3
TIME: 11/0/19 POWER: 50 %

TC(1) = 798°F
TC(2) = 809°F
TC(3) = 817°F
TC(4) = 823°F
TC(5) = 829°F
TC(6) = 819°F
TC(7) = 800°F
TC(8) = 794°F
TC(9) = 787°F
TC(10) = 784°F
TC(11) = 776°F
TC(12) = 776°F
TC(13) = 814°F
TC(14) = 777°F
TC(15) = 803°F
TC(16) = 780°F
TC(17) = 814°F



TC(18) = 798°F
~~TC(18) = 798°F~~
~~TC(19) = 817°F~~
~~TC(20) = 823°F~~
~~TC(21) = 829°F~~
TC(22) = 775°F
TC(23) = 786°F
TC(24) = 755°F
TC(25) = 744°F
TC(26) = 780°F
TC(27) = 786°F
TC(28) = 783°F
TC(29) = 755°F
TC(30) = 769°F
TC(31) = 755°F
TC(32) = 742°F
TC(33) = 757°F
TC(34) = 756°F
TC(35) = 770°F

```

*****
*
*               USS BELLEAU WOOD - LHA 3
*             FORWARD BOILER
*
*   DATE: 3/3                TIME: 11/1/53                POWER 50 %
*
*****

```

PHASE 2 - INTERMEDIATE HEADER / ROW 54

TC(1)=797°F	TC(21)=774°F
TC(2)=808°F	TC(22)=774°F
TC(3)=816°F	TC(23)=794°F
TC(4)=822°F	TC(24)=754°F
TC(5)=827°F	TC(25)=745°F
TC(6)=817°F	TC(26)=780°F
TC(7)=800°F	TC(27)=787°F
TC(8)=793°F	TC(28)=783°F
TC(9)=786°F	TC(29)=755°F
TC(10)=783°F	TC(30)=770°F
TC(11)=774°F	TC(31)=756°F
TC(12)=774°F	TC(32)=743°F
TC(13)=813°F	TC(33)=756°F
TC(14)=775°F	TC(34)=756°F
TC(15)=802°F	TC(35)=769°F
TC(16)=779°F	
TC(17)=813°F	
TC(18)=796°F	
TC(19)=755°F	
TC(20)=756°F	

PHASE 1 - SUPERHEATER HEADER TEMPERATURES

TC(36)=503°F	TC(41)=690°F
TC(37)=503°F	TC(42)=806°F
TC(38)=585°F	TC(43)=798°F
TC(39)=590°F	TC(44)=883°F
TC(40)=684°F	TC(45)=814°F

PHASE 3- INTERMEDIATE HEADER TEMPERATURES

ROW 20 (1a) =568°F
 ROW 20 (1b) =568°F
 ROW 20 (5a) =623°F
 ROW 20 (5b) =624°F
 ROW 20 (27a)=606°F
 ROW 20 (27b)=599°F

PHASE 3- INLET-OUTLET HEADER TEMPERATURE

ROW 2 (1a) =687°F	ROW 53 (1a) =682°F
ROW 2 (1b) =502°F	ROW 53 (1b) =687°F
ROW 2 (5a) =503°F	ROW 53 (5a) =682°F
ROW 2 (5b) =502°F	ROW 53 (5b) =521°F
ROW 2 (27a)=494°F	ROW 53 (27a)=682°F
ROW 2 (27b)=489°F	ROW 53 (27b)=676°F
ROW 22 (1a) =638°F	ROW 67 (1a) =521°F
ROW 22 (1b) =521°F	ROW 67 (1b) =891°F
ROW 22 (5a) =592°F	ROW 67 (5a) =876°F
ROW 22 (5b) =601°F	ROW 67 (5b) =874°F
ROW 22 (27a)=569°F	ROW 67 (27a)=765°F
ROW 22 (27b)=559°F	ROW 67 (27b)=749°F

APPENDIX B

MATERIAL PROPERTY TEST DATA

Chemical Composition and Mechanical Properties of ASTM A 387, Grade 22 Steel

Chemical Composition

<u>Element</u>	<u>Specification</u>	<u>Analysis</u> ¹
C	0.15 max	0.12
Mn,	0.30 - 0.60	0.42
P	0.03	<0.02
S	0.030	0.03
Si	0.50 max	0.22
Cr	2.00 - 2.50	1.98
Mo	0.90 - 1.20	0.89

Tensile Properties

	<u>Specification</u>	<u>Measured</u>
Yield Strength (0.2%), ksi	30 min	35.3, 33.4
Tensile Strength, ksi	60 - 85	67.2, 69.1
Elongation, %	18 min	38, 37
Reduction of Area, %	—	65, 67

¹Analysis from Philadelphia Naval Shipyard, M3-194

APPENDIX C

HEADERT INPUT FILE

HEADERT

PAGE # 1

```

C*****
C
C                                HEADERT
C                                BY LT JON W. MAUFMANN MAY, 1987
C*****
C
C      SOLUTION OF THE HEAT CONDUCTION PROBLEM FOR THE LHA-1 CLASS HEADER
C
C*****
C
C      THE OUTPUT OF THIS PROGRAM IS THE STEADY STATE TEMPERATURES AT EACH OF
C      THE 1001 NODE POINTS OF THE MODEL
C
C*****
C
C      THE OUTPUT FROM THIS PROGRAM IS READ INTO THE "POTENTIAL" BLOCK
C      OF THE HEADER PROGRAM PRIOR TO EXECUTION
C
C*****NUMBER OF NODE POINTS AND LOAD CONDITIONS*****
C
SYSTEM
N=1001 L=1
:
C*****DEFINITION OF ACTIVE DEGREES OF FREEDOM*****
C
RESTRAINTS
1,1001,1      R=1,1,0,1,1,1
C*****ELEMENT TYPE FOR THE ANALYSIS*****
C
ASOLID
M=1 MAX=1 ATYPE=0
1 T=1
C*****MATERIAL PROPERTIES*****
C
T=0 E=1      U=0.00      G=1
C*****ELEMENT DEFINITIONS (CONNECTIVITIES)*****
C
1 S= 1,4,2      G= 6,1 M=1
7 S= 879,880,894 G= 7,1
14 S= 43,46,44   G= 7,1
21 S=88,101,89   G= 6,6
57 S=257,272,258 G= 12,7
141 S= 632,633,645 G= 6,6
177 S= 963,964,976 G= 6,1
183 S= 924,925,937 G= 6,1
189 S= 840,841,853 G= 6,1
195 S= 801,802,814 G= 6,1
:
C*****CONSTRAINT OF COINCIDENT NODE POINTS*****
C
CONSTRAINTS
3,36,3      C= 0.88,88,0,0,0      I= 0,13,13,0,0,0
37          C= 0.879,879,0,0,0
38          C= 0.894,894,0,0,0
39          C= 0.617,617,0,0,0
40          C= 0.886,886,0,0,0
41          C= 0.901,901,0,0,0
42          C= 0.916,916,0,0,0

```

43	C= 0.893,893,0,0,0	
44	C= 0.908,908,0,0,0	
45	C= 0.632,632,0,0,0	
48,81,3	C= 0.633,633,0,0,0	I= 0,1,1,0,0,0
100,256,13	C= 0.257,257,0,0,0	I= 0,15,15,0,0,0
255	C= 0.452,452,0,0,0	
254	C= 0.467,467,0,0,0	
253	C= 0.482,482,0,0,0	
252	C= 0.497,497,0,0,0	
251	C= 0.512,512,0,0,0	
250	C= 0.527,527,0,0,0	
249	C= 0.542,542,0,0,0	
248	C= 0.557,557,0,0,0	
247	C= 0.572,572,0,0,0	
246	C= 0.587,587,0,0,0	
245	C= 0.602,602,0,0,0	
451	C= 0.924,924,0,0,0	
788	C= 0.924,924,0,0,0	
975	C= 0.924,924,0,0,0	
1001	C= 0.801,801,0,0,0	
950	C= 0.801,801,0,0,0	
852	C= 0.801,801,0,0,0	
988	C= 0.937,937,0,0,0	
865	C= 0.814,814,0,0,0	
631	C= 0.632,632,0,0,0	
909	C= 0.617,617,0,0,0	
244	C= 0.617,617,0,0,0	
271	C= 0.963,963,0,0,0	
286	C= 0.964,964,0,0,0	
301	C= 0.965,965,0,0,0	
316	C= 0.966,966,0,0,0	
331	C= 0.967,967,0,0,0	
346	C= 0.968,968,0,0,0	
361	C= 0.969,969,0,0,0	
376	C= 0.970,970,0,0,0	
391	C= 0.971,971,0,0,0	
406	C= 0.972,972,0,0,0	
421	C= 0.973,973,0,0,0	
436	C= 0.974,974,0,0,0	
466	C= 0.775,775,0,0,0	
481	C= 0.762,762,0,0,0	
496	C= 0.749,749,0,0,0	
511	C= 0.736,736,0,0,0	
526	C= 0.723,723,0,0,0	
541	C= 0.710,710,0,0,0	
556	C= 0.697,697,0,0,0	
571	C= 0.684,684,0,0,0	
586	C= 0.671,671,0,0,0	
601	C= 0.658,658,0,0,0	
616	C= 0.645,645,0,0,0	
989,1000,1	C= 0.840,840,0,0,0	I= 0,1,1,0,0,0
618,630,1	C= 0.910,910,0,0,0	I= 0,1,1,0,0,0
789,800,1	C= 0.925,925,0,0,0	I= 0,1,1,0,0,0
951,962,1	C= 0.802,802,0,0,0	I= 0,1,1,0,0,0
927	C= 0.878,878,0,0,0	

*****INPUT AND GENERATION OF NODE POINTS*****

JOINTS

1	Y= .630	Z= 3.000	
2	Y= .661	Z= 3.000	
3	Y= .693	Z= 3.000	
4	Y= .630	Z= 2.987	
6	Y= .698	Z= 2.987	
7	Y= .630	Z= 2.974	
9	Y= .702	Z= 2.974	
10	Y= .630	Z= 2.961	
12	Y= .707	Z= 2.961	
13	Y= .630	Z= 2.948	
15	Y= .712	Z= 2.948	
16	Y= .630	Z= 2.935	
18	Y= .716	Z= 2.935	
19	Y= .630	Z= 2.922	
21	Y= .721	Z= 2.922	
22	Y= .630	Z= 2.909	
24	Y= .726	Z= 2.909	
25	Y= .630	Z= 2.896	
27	Y= .731	Z= 2.896	
28	Y= .630	Z= 2.883	
30	Y= .736	Z= 2.883	
31	Y= .630	Z= 2.870	
33	Y= .740	Z= 2.870	
34	Y= .630	Z= 2.857	
36	Y= .745	Z= 2.857	
37	Y= .630	Z= 2.844	
38	Y= .690	Z= 2.844	
39	Y= .750	Z= 2.844	L= 1,2,12
79	Y= .630	Z= 1.000	G= 37,79,3
80	Y= .690	Z= 1.000	G= 38,80,3
81	Y= .750	Z= 1.000	G= 39,81,3
85	Y= .630	Z= 0.000	G= 79,85,3
86	Y= .690	Z= 0.000	G= 80,86,3
87	Y= .750	Z= 0.000	G= 81,87,3
88	Y= .693	Z= 3.000	
89	Y= .714	Z= 3.010	
90	Y= .735	Z= 3.017	
91	Y= .755	Z= 3.023	
92	Y= .776	Z= 3.026	
93	Y= .797	Z= 3.029	
94	Y= .817	Z= 3.030	
95	Y= .838	Z= 3.029	
96	Y= .858	Z= 3.026	
97	Y= .879	Z= 3.022	
98	Y= .900	Z= 3.016	
99	Y= .921	Z= 3.009	
100	Y= .938	Z= 3.000	
113	Y= .938	Z= 2.995	
126	Y= .938	Z= 2.989	
139	Y= .938	Z= 2.984	
152	Y= .938	Z= 2.975	
165	Y= .938	Z= 2.970	
178	Y= .938	Z= 2.960	
191	Y= .937	Z= 2.952	
204	Y= .933	Z= 2.936	
217	Y= .928	Z= 2.921	
230	Y= .921	Z= 2.906	

243	Y= .912	Z= 2.892	
256	Y= .901	Z= 2.880	
255	Y= .889	Z= 2.869	
254	Y= .875	Z= 2.860	
253	Y= .860	Z= 2.854	
252	Y= .845	Z= 2.848	
251	Y= .830	Z= 2.845	
250	Y= .813	Z= 2.844	
249	Y= .799	Z= 2.844	
248	Y= .788	Z= 2.844	
247	Y= .778	Z= 2.844	
246	Y= .768	Z= 2.844	
245	Y= .757	Z= 2.844	
244	Y= .750	Z= 2.843	
231	Y= .745	Z= 2.857	
218	Y= .740	Z= 2.870	
205	Y= .736	Z= 2.883	
192	Y= .731	Z= 2.896	
179	Y= .726	Z= 2.909	
166	Y= .721	Z= 2.922	
153	Y= .716	Z= 2.935	
140	Y= .712	Z= 2.948	
127	Y= .707	Z= 2.961	
114	Y= .702	Z= 2.974	
101	Y= .698	Z= 2.987	L= 88,12,12
257	Y= .938	Z= 3.000	
271	Y= 1.200	Z= 3.000	G= 257,271,1
451	Y= 1.200	Z= 2.581	G= 271,451,15
631	Y= .750	Z= 2.581	G= 451,631,15
617	Y= .750	Z= 2.843	
630	Y= .750	Z= 2.601	G= 617,630,1
602	Y= .757	Z= 2.844	
587	Y= .768	Z= 2.844	
572	Y= .778	Z= 2.844	
557	Y= .788	Z= 2.844	
542	Y= .799	Z= 2.844	
527	Y= .813	Z= 2.844	
512	Y= .830	Z= 2.845	
497	Y= .845	Z= 2.848	
482	Y= .860	Z= 2.854	
467	Y= .875	Z= 2.860	
452	Y= .889	Z= 2.869	
437	Y= .901	Z= 2.880	
422	Y= .912	Z= 2.892	
407	Y= .921	Z= 2.906	
392	Y= .928	Z= 2.921	
377	Y= .933	Z= 2.936	
362	Y= .937	Z= 2.952	
347	Y= .938	Z= 2.960	
332	Y= .938	Z= 2.970	
317	Y= .938	Z= 2.975	
302	Y= .938	Z= 2.984	
287	Y= .938	Z= 2.989	
272	Y= .938	Z= 2.995	L= 257,14,24
632	Y= .750	Z= 2.581	
644	Y= .750	Z= 1.000	G= 632,644,1
788	Y= 1.200	Z= 2.581	G= 632,788,13
800	Y= 1.200	Z= 1.000	G= 788,800,1

801 Y= 1.470 Z= 2.581 G= 644,800,13 L= 632,12,12
 813 Y= 1.470 Z= 1.000
 827 Y= 2.000 Z= 2.581
 839 Y= 2.000 Z= 1.000 Q= 801,827,813,839,13,1
 840 Y= 1.470 Z= 3.000
 852 Y= 1.470 Z= 2.581
 866 Y= 2.000 Z= 3.000
 878 Y= 2.000 Z= 2.581 Q= 840,866,852,878,13,1
 879 Y= .630 Z= 2.844
 893 Y= .630 Z= 2.581
 909 Y= .750 Z= 2.844
 923 Y= .750 Z= 2.581 Q= 879,909,893,923,13,1
 924 Y= 1.200 Z= 2.581
 950 Y= 1.470 Z= 2.581
 936 Y= 1.200 Z= 1.000
 962 Y= 1.470 Z= 1.000 Q= 924,950,936,962,13,1
 963 Y= 1.200 Z= 3.000
 989 Y= 1.470 Z= 3.000
 975 Y= 1.200 Z= 2.581
 1001 Y= 1.470 Z= 2.581 Q= 963,989,975,1001,13,1

:

C*****

C

INPUT OF BOUNDARY CONDITION TEMPERATURES

C

(IN PLACE OF Z DISPLACEMENTS)

C

DISPLACEMENTS

1,85,3 U= 0,0,350
 2 U= 0,0,350
 3 U= 0,0,350
 89,100,1 U= 0,0,350
 258,271,1 U= 0,0,350
 976 U= 0,0,350
 989 U= 0,0,350
 853 U= 0,0,350
 866 U= 0,0,350
 867 U= 0,0,346
 868 U= 0,0,342
 869 U= 0,0,338
 870 U= 0,0,334
 871 U= 0,0,330
 872 U= 0,0,326
 873 U= 0,0,322
 874 U= 0,0,318
 875 U= 0,0,314
 876 U= 0,0,310
 877 U= 0,0,306
 878 U= 0,0,302
 828 U= 0,0,298
 829 U= 0,0,294
 830 U= 0,0,290
 831 U= 0,0,286
 832 U= 0,0,282
 833 U= 0,0,278
 834 U= 0,0,274
 835 U= 0,0,270
 836 U= 0,0,266
 837 U= 0,0,262
 838 U= 0,0,258
 839 U= 0,0,254

:

APPENDIX D

HEADER INPUT FILE

```

C                                     HEADER                                     PAGE # 1
C
C*****
C
C                                     HEADER
C                                     BY LT JON W. KAUFMANN MAY, 1987
C*****
C      STRESS ANALYSIS OF THE LHA-1 CLASS HEADER/TUBE ATTACHMENT WELD JOINT
C
C*****
C      THIS PROGRAM STUDIES THE EFFECTS OF TEMPERATURE AND A LONGITUDINAL
C      TUBE LOAD ON THE SUPERHEATER HEADER ATTACHMENT WELD JOINT
C
C*****
C*****NUMBER OF NODE POINTS AND LOAD CONDITIONS*****
C
SYSTEM
N=1001 L= 3
:
C*****DEFINING THE ACTIVE DEGREES OF FREEDOM*****
C
RESTRAINTS
1,1001,1      R=1,0,0,1,1,1
827,839,1     R=1,1,1,1,1,1
866,878,1     R=1,1,1,1,1,1
:
C*****ELEMENT TYPE FOR THE ANALYSIS*****
C
ASOLID
M=1 MAX=1 ATYPE=0 P=1. T= 0,1.
1 T=1
C*****MATERIAL PROPERTIES*****
C
T=0 E=29600 U=.30 A=.0000065
C*****ELEMENT DEFINITIONS (CONNECTIVITIES)*****

1 S= 1,4,2      G= 6,1 M=1 TZ= 300.0
7 S= 879,880,894 G= 7,1
14 S= 43,46,44  G= 7,1
21 S=88,101,89  G= 6,6
57 S=257,272,258 G= 12,7
141 S= 632,633,645 G= 6,6
177 S= 963,964,976 G= 6,1
183 S= 924,925,937 G= 6,1
189 S= 840,841,853 G= 6,1
195 S= 801,802,814 G= 6,1
:
C*****CONSTRAINING OF COINCIDENT NODE POINTS*****
C
CONSTRAINTS
3,36,3      C= 0,88,88,0,0,0      I= 0,13,13,0,0,0
37          C= 0,879,879,0,0,0
38          C= 0,894,894,0,0,0
39          C= 0,617,617,0,0,0
40          C= 0,886,886,0,0,0
41          C= 0,901,901,0,0,0
42          C= 0,916,916,0,0,0

```


C

HEADER

PAGE # 2

43	C= 0,893,893,0,0,0	
44	C= 0,908,908,0,0,0	
45	C= 0,632,632,0,0,0	
48,81,3	C= 0,633,0,0,0,0	I= 0,1,0,0,0,0
100,256,13	C= 0,257,257,0,0,0	I= 0,15,15,0,0,0
255	C= 0,452,452,0,0,0	
254	C= 0,467,467,0,0,0	
253	C= 0,482,482,0,0,0	
252	C= 0,497,497,0,0,0	
251	C= 0,512,512,0,0,0	
250	C= 0,527,527,0,0,0	
249	C= 0,542,542,0,0,0	
248	C= 0,557,557,0,0,0	
247	C= 0,572,572,0,0,0	
246	C= 0,587,587,0,0,0	
245	C= 0,602,602,0,0,0	
451	C= 0,924,924,0,0,0	
788	C= 0,924,924,0,0,0	
975	C= 0,924,924,0,0,0	
1001	C= 0,801,801,0,0,0	
950	C= 0,801,801,0,0,0	
852	C= 0,801,801,0,0,0	
988	C= 0,937,937,0,0,0	
865	C= 0,814,814,0,0,0	
631	C= 0,632,632,0,0,0	
909	C= 0,617,617,0,0,0	
244	C= 0,617,617,0,0,0	
271	C= 0,963,963,0,0,0	
286	C= 0,964,964,0,0,0	
301	C= 0,965,965,0,0,0	
316	C= 0,966,966,0,0,0	
331	C= 0,967,967,0,0,0	
346	C= 0,968,968,0,0,0	
361	C= 0,969,969,0,0,0	
376	C= 0,970,970,0,0,0	
391	C= 0,971,971,0,0,0	
406	C= 0,972,972,0,0,0	
421	C= 0,973,973,0,0,0	
436	C= 0,974,974,0,0,0	
466	C= 0,775,775,0,0,0	
481	C= 0,762,762,0,0,0	
496	C= 0,749,749,0,0,0	
511	C= 0,736,736,0,0,0	
526	C= 0,723,723,0,0,0	
541	C= 0,710,710,0,0,0	
556	C= 0,697,697,0,0,0	
571	C= 0,684,684,0,0,0	
586	C= 0,671,671,0,0,0	
601	C= 0,658,658,0,0,0	
616	C= 0,645,645,0,0,0	
989,1000,1	C= 0,840,840,0,0,0	I= 0,1,1,0,0,0
618,630,1	C= 0,910,910,0,0,0	I= 0,1,1,0,0,0
789,800,1	C= 0,925,925,0,0,0	I= 0,1,1,0,0,0
951,962,1	C= 0,802,802,0,0,0	I= 0,1,1,0,0,0

C*****POTENTIAL DATA BLOCK*****

C

C THE RESULTS FROM EXECUTION OF HEADERT ARE INSERTED IN THIS BLOCK

C

HEADER

PAGE # 3

C

C*****

C

C*****PRESSURE LOAD CONDITION*****

C

POTENTIAL

1,85.3 P=.700,.700

1,3.1 P=.700,.700

89,100,1 P=.700,.700

258,271,1 P=.700,.700

:

C*****DEFINITION OF LOAD COMBINATIONS*****

C

COMBO

1 C= 1,1,1

2 C= 0,1,0

3 C= 0,0,1

4 C= 1,0,0

5 C= 1,1,0

6 C= 0,1,1

:

C*****LONGITUDINAL TUBE LOAD*****

C

C

C

LOADS

85 L= 3 F= 0,0,-0.0253

86 L= 3 F= 0,0,-0.1013

87 L= 3 F= 0,0,-0.0253

:

C*****INPUT AND GENERATION OF NODE POINTS*****

C

JOINTS

1 Y= .630 Z= 3.000

2 Y= .661 Z= 3.000

3 Y= .693 Z= 3.000

4 Y= .630 Z= 2.987

6 Y= .698 Z= 2.987

7 Y= .630 Z= 2.974

9 Y= .702 Z= 2.974

10 Y= .630 Z= 2.961

12 Y= .707 Z= 2.961

13 Y= .630 Z= 2.948

15 Y= .712 Z= 2.948

16 Y= .630 Z= 2.935

18 Y= .716 Z= 2.935

19 Y= .630 Z= 2.922

21 Y= .721 Z= 2.922

22 Y= .630 Z= 2.909

24 Y= .726 Z= 2.909

25 Y= .630 Z= 2.896

27 Y= .731 Z= 2.896

28 Y= .630 Z= 2.883

30 Y= .736 Z= 2.883

31 Y= .630 Z= 2.870

33 Y= .740 Z= 2.870

34 Y= .630 Z= 2.857

36 Y= .745 Z= 2.857

37	Y= .630	Z= 2.844	
38	Y= .690	Z= 2.844	
39	Y= .750	Z= 2.844	L= 1,2,12
79	Y= .630	Z= 1.000	G= 37,79,3
80	Y= .690	Z= 1.000	G= 38,80,3
81	Y= .750	Z= 1.000	G= 39,81,3
85	Y= .630	Z= 0.000	G= 79,85,3
86	Y= .690	Z= 0.000	G= 80,86,3
87	Y= .750	Z= 0.000	G= 81,87,3
88	Y= .693	Z= 3.000	
89	Y= .714	Z= 3.010	
90	Y= .735	Z= 3.017	
91	Y= .755	Z= 3.023	
92	Y= .776	Z= 3.026	
93	Y= .797	Z= 3.029	
94	Y= .817	Z= 3.030	
95	Y= .838	Z= 3.029	
96	Y= .858	Z= 3.026	
97	Y= .879	Z= 3.022	
98	Y= .900	Z= 3.016	
99	Y= .921	Z= 3.009	
100	Y= .938	Z= 3.000	
113	Y= .938	Z= 2.995	
126	Y= .938	Z= 2.989	
139	Y= .938	Z= 2.984	
152	Y= .938	Z= 2.975	
165	Y= .938	Z= 2.970	
178	Y= .938	Z= 2.960	
191	Y= .937	Z= 2.952	
204	Y= .933	Z= 2.936	
217	Y= .928	Z= 2.921	
230	Y= .921	Z= 2.906	
243	Y= .912	Z= 2.892	
256	Y= .901	Z= 2.880	
255	Y= .889	Z= 2.869	
254	Y= .875	Z= 2.860	
253	Y= .860	Z= 2.854	
252	Y= .845	Z= 2.848	
251	Y= .830	Z= 2.845	
250	Y= .813	Z= 2.844	
249	Y= .799	Z= 2.844	
248	Y= .788	Z= 2.844	
247	Y= .778	Z= 2.844	
246	Y= .768	Z= 2.844	
245	Y= .757	Z= 2.844	
244	Y= .750	Z= 2.843	
231	Y= .745	Z= 2.857	
218	Y= .740	Z= 2.870	
205	Y= .736	Z= 2.883	
192	Y= .731	Z= 2.896	
179	Y= .726	Z= 2.909	
166	Y= .721	Z= 2.922	
153	Y= .716	Z= 2.935	
140	Y= .712	Z= 2.948	
127	Y= .707	Z= 2.961	
114	Y= .702	Z= 2.974	
101	Y= .698	Z= 2.987	L= 88,12,12
257	Y= .938	Z= 3.000	

271 Y= 1.200	Z= 3.000	G= 257,271,1
451 Y= 1.200	Z= 2.581	G= 271,451,15
631 Y= .750	Z= 2.581	G= 451,631,15
617 Y= .750	Z= 2.843	
630 Y= .750	Z= 2.601	G= 617,630,1
602 Y= .757	Z= 2.844	
587 Y= .768	Z= 2.844	
572 Y= .778	Z= 2.844	
557 Y= .788	Z= 2.844	
542 Y= .799	Z= 2.844	
527 Y= .813	Z= 2.844	
512 Y= .830	Z= 2.845	
497 Y= .845	Z= 2.848	
482 Y= .860	Z= 2.854	
467 Y= .875	Z= 2.860	
452 Y= .889	Z= 2.869	
437 Y= .901	Z= 2.880	
422 Y= .912	Z= 2.892	
407 Y= .921	Z= 2.906	
392 Y= .928	Z= 2.921	
377 Y= .933	Z= 2.936	
362 Y= .937	Z= 2.952	
347 Y= .938	Z= 2.960	
332 Y= .938	Z= 2.970	
317 Y= .938	Z= 2.975	
302 Y= .938	Z= 2.984	
287 Y= .938	Z= 2.989	
272 Y= .938	Z= 2.995	L= 257,14,24
632 Y= .750	Z= 2.581	
644 Y= .750	Z= 1.000	G= 632,644,1
788 Y= 1.200	Z= 2.581	G= 632,788,13
800 Y= 1.200	Z= 1.000	G= 788,800,1
801 Y= 1.470	Z= 2.581	G= 644,800,13 L= 632,12,12
813 Y= 1.470	Z= 1.000	
827 Y= 2.000	Z= 2.581	
839 Y= 2.000	Z= 1.000	Q= 801,827,813,839,13,1
840 Y= 1.470	Z= 3.000	
852 Y= 1.470	Z= 2.581	
866 Y= 2.000	Z= 3.000	
878 Y= 2.000	Z= 2.581	Q= 840,866,852,878,13,1
879 Y= .630	Z= 2.844	
893 Y= .630	Z= 2.581	
909 Y= .750	Z= 2.844	
923 Y= .750	Z= 2.581	Q= 879,909,893,923,15,1
924 Y= 1.200	Z= 2.581	
950 Y= 1.470	Z= 2.581	
936 Y= 1.200	Z= 1.000	
962 Y= 1.470	Z= 1.000	Q= 924,950,936,962,13,1
963 Y= 1.200	Z= 3.000	
989 Y= 1.470	Z= 3.000	
975 Y= 1.200	Z= 2.581	
1001 Y= 1.470	Z= 2.581	Q= 963,989,975,1001,13,1

:

APPENDIX E

EXCERPT FROM ASME BOILER CODE

Table PG-23.1

SECTION I — POWER BOILERS

1986 Edition

TABLE PG-23.1 (CONT'D)
MAXIMUM ALLOWABLE STRESS VALUES FOR FERROUS MATERIALS, ksi
(Multiply by 1000 to Obtain psi)

Nominal Composition	Product Form	Spec. Number	Grade or Class	Notes	Specified Minimum Tensile	For Metal Temperatures Not Exceeding °F							
						- 20 to 100	200	300	400	- 20 to 400	500	600	650
Low Alloy Steels (Cont'd)													
1½Cr-½Mo-Si	Forg.	SA-182	F11	...	70.0	17.5	17.5	17.5	17.5
1½Cr-½Mo-Si	Plate	SA-387	11Cl.2	(4)	75.0	18.8	18.8	18.8	18.8
1½Cr-½Mo	Cast.	SA-217	WC6	(4)(5)	70.0	17.5	17.5	17.5	17.5
2Cr-½Mo	Smis. Tb.	SA-213	T3b	...	60.0	15.0	15.0	14.7	14.4
2Cr-½Mo	Smis. Pp.	SA-369	FP3b	...									
2½Cr-1Mo	Plate	SA-387	22Cl.1	...	60.0	15.0	15.0	15.0	15.0
2½Cr-1Mo	Smis. Tb.	SA-213	T22	...									
2½Cr-1Mo	Smis. Pp.	SA-335	P22	...									
2½Cr-1Mo	Forg.	SA-336	F22a	...									
2½Cr-1Mo	Smis. Pp.	SA-369	FP22	...									
2½Cr-1Mo	Forg.	SA-182	F22a	...									
2½Cr-1Mo	Fittings	SA-234	WP22	(20)									
2½Cr-1Mo	Cast.	SA-217	WC9	(4)(5)	70.0	17.5	17.5	17.3	16.9	...	16.8	16.8	16.7
2½Cr-1Mo	Forg.	SA-182	F22	...	75.0	18.8	18.8	18.3	18.0	...	17.9	17.8	17.7
2½Cr-1Mo	Plate	SA-387	22Cl.2	(4)									
2½Cr-1Mo	Forg.	SA-336	F22	...									
3Cr-1Mo	Plate	SA-387	21Cl.1	...	60.0	15.0	15.0	15.0	15.0
3Cr-1Mo	Smis. Tb.	SA-213	T21	...									
3Cr-1Mo	Smis. Pp.	SA-335	P21	...									
3Cr-1Mo	Forg.	SA-336	F21a	...									
3Cr-1Mo	Smis. Pp.	SA-369	FP21	...									
3Cr-1Mo	Forg.	SA-182	F21	...	75.0	18.8	18.8	18.3	18.0	...	17.9	17.8	17.7
3Cr-1Mo	Plate	SA-387	21Cl.2	(4)									
3Cr-1Mo	Forg.	SA-336	F21	...									
5Cr-½Mo	Fittings	SA-234	WP5	(20)	60.0	15.0	15.0	14.5	14.4	...	14.4	14.1	13.9
5Cr-½Mo	Plate	SA-387	5	...									
5Cr-½Mo	Smis. Tb.	SA-213	T5	...									
5Cr-½Mo	Smis. Pp.	SA-335	P5	...									
5Cr-½Mo	Smis. Pp.	SA-369	FP5	...									
5Cr-½Mo	Forg.	SA-336	F5	...									
5Cr-½Mo-Si	Smis. Tb.	SA-213	T5b	...									
5Cr-½Mo-Si	Smis. Pp.	SA-335	P5b	...									
5Cr-½Mo-Ti	Smis. Tb.	SA-213	T5c	...									
5Cr-½Mo-Ti	Smis. Pp.	SA-335	P5c	...									
5Cr-½Mo	Forg.	SA-182	F5	...	70.0	17.5	17.5	17.0	16.8	...	16.8	16.5	16.3
5Cr-½Mo	Forg.	SA-336	F5a	...	80.0	20.0	20.0	19.4	19.2	...	19.2	18.7	18.6
5Cr-½Mo	Forg.	SA-182	F5a	...	90.0	22.5	22.4	21.8	21.6	...	21.6	21.3	20.9
5Cr-½Mo	Cast.	SA-217	C5	(4)(5)	90.0	22.5	22.4	21.8	21.6	...	21.6	21.3	20.9

TABLE PG-23.1 (CONT'D)
 MAXIMUM ALLOWABLE STRESS VALUES FOR FERROUS MATERIALS, ksi
 (Multiply by 1000 to Obtain psi)

For Metal Temperatures Not Exceeding °F																	Spec. Number	Grade or Class
700	750	800	850	900	950	1000	1050	1100	1150	1200	1250	1300	1350	1400	1450	1500		
Low Alloy Steels (Cont'd)																		
17.5	17.5	17.5	17.1	15.9	11.0	6.9	4.6	2.8	(2.1)	(1.2)	SA-182	F11
18.8	18.8	18.8	18.3	15.9	11.0	6.9	4.6	2.8	(2.1)	(1.2)	SA-387	11Cl.2
17.5	17.5	17.5	17.1	15.9	11.0	6.9	4.6	2.8	SA-217	WC6
14.2	13.9	13.5	13.1	12.5	10.0	6.2	4.2	2.6	(1.4)	(1.0)	SA-213 SA-369	T3b FP3b
15.0	15.0	15.0	14.4	13.1	11.0	7.8	5.8	4.2	(3.0)	(1.6)	SA-387 SA-213 SA-335 SA-336 SA-369 SA-182 SA-234	22Cl.1 T22 P22 F22a FP22 F22a WP22
16.6	16.1	15.7	15.0	14.2	11.0	7.6	5.8	4.4	(2.5)	(1.3)	SA-217	WC9
17.5	17.2	16.9	16.4	15.8	11.0	7.6	5.8	4.4	(2.5)	(1.3)	SA-182 SA-387 SA-336	F22 22Cl.2 F22
14.8	14.5	13.9	13.2	12.0	9.0	7.0	5.5	4.0	(2.7)	(1.5)	SA-387 SA-213 SA-335 SA-336 SA-369	21Cl.1 T21 P21 F21a FP21
17.5	17.2	16.9	16.4	13.1	9.5	6.8	4.9	3.2	(2.4)	(1.3)	SA-182 SA-387 SA-336	F21 21Cl.2 F21
13.7	13.2	12.8	12.1	10.9	8.0	5.8	4.2	2.9	2.0	1.3	SA-234 SA-387 SA-213 SA-335 SA-369 SA-336 SA-213 SA-213 SA-335	WP5 5 T5 P5 FP5 F5 T5b P5b T5c P5c
16.0	15.4	14.9	14.1	10.8	8.0	5.8	4.2	2.9	2.0	1.3	SA-182	F5
18.2	17.6	17.0	14.3	10.8	8.0	5.8	4.2	2.9	2.0	1.3	SA-336	F5a
20.5	19.8	19.1	14.8	10.8	8.0	5.8	4.2	2.9	2.0	1.3	SA-182	F5a
20.5	19.8	19.1	14.3	10.9	8.0	5.8	4.2	2.9	2.0	1.3	SA-217	C5

APPENDIX F PROJECTED BOILER OPERATING CYCLE (CV-60 CLASS)

<u>No. of cycles</u>	<u>Type of pressure/temperature cycle</u>
1	150% design pressure hydro
3	125% max. operating pressure hydro
60	100% max. operating pressure hydro
150	cold (0 psi) to operating pressure and temperature
150	steam blanket (150 psi) to operating pressure and temperature
225	cold (0 psi) to steam blanket (150 psi)
300	125 psi variation at operating pressure and temperature

LIST OF REFERENCES

1. NAVSEA Technical Manual S9221-A3-MMO-020/LHA-1 CL Volume 2, *Description, Operation and Maintenance Instructions Type V2M Boiler*, Naval Sea Systems Command, Washington, D.C., 1979.
2. Bathe, K.E., and Wilson, E.L., *Numerical Methods in Finite Element Analysis*, Prentice Hall, Inc., Englewood Cliffs, New Jersey, 1976.
3. Hollings, J.P. and Wilson, E.L., "3-9 Node Isoparametric Planar or Axisymmetric Finite Element", Report UC SESM 78-3, Department of Civil Engineering, University of California, Berkeley, 1977.
4. Boyer, H.E., and Gall, T.L., *Metals Handbook Desk Edition*, American Society For Metals, Metals Park, Ohio, 1985.
5. Gere, J.M. and Timoshenko, S.P., *Mechanics of Materials*, PWS Publishers, Boston, Massachusetts, 1984.
6. Bathe, K.J., *Finite Element Procedures In Engineering Analysis*, Prentice Hall, Inc., New Jersey, 1982.

INITIAL DISTRIBUTION LIST

	No. Copies
1. Defense Technical Information Center Cameron Station Alexandria, VA 22304-6145	2
2. Library, Code 0142 Naval Postgraduate School Monterey, CA 93943-5002	2
3. Chairman, Code 69Hy Department of Mechanical Engineering Naval Postgraduate School Monterey, CA 93943-5004	1
4. Professor Gilles Cantin, Code 69Ci Department of Mechanical Engineering Naval Postgraduate School Monterey, CA 93943-5004	4
5. Professor Edward L. Wilson Structural Engineering Division Department of Civil Engineering University of California, Berkeley Berkeley, CA 94720	3
6. Professor Ramesh Kolar, Code 67 Department of Aeronautics Naval Postgraduate School Monterey, CA 93943-5004	1
7. Professor K.J. Bathe Department of Mechanical Engineering Massachusetts Institute of Technology 77 Massachusetts Avenue Cambridge, MA 02139	1
8. Dr. Jean Louis Batoz U.T.C. Universite de Technologie 60206 Compiègne Cedex, FRANCE	1
9. Professor Thomas Hughes Division of Applied Mechanics Room 283 Durand Stanford, CA 94305	1

10. Dr. Rem Jones, Code 172 1
David W. Taylor Naval Ship
Research and Development Center
Bethesda, MD 20084
11. Mr. Craig Fraser, Code 2814 1
David W. Taylor Naval Ship
Research and Development Center
Annapolis Laboratory
Annapolis, MD 21402-5067
12. CDR Lael Easterling, USN, Code 56X6 1
Navsea Boiler Engineering Division
NAVSEA Headquarters
Washington, DC 20362-5101
13. Dr. Alan Kushner, Code 4325 1
Office Of Naval Research
800 North Quincy Street
Arlington, VA 22217
14. Mr. Joseph Carrado, Code 1702 1
David W. Taylor Naval Ship
Research and Development Center
Bethesda, MD 20034
15. R.A. Langworthy 1
Applied Technology Laboratories
U.S. Army Research and Technology Laboratory
Fort Eustis, VA 23604
16. LT Jon W. Kaufmann, USN 5
10 Sycamore Drive
Roslyn, NY 11576

DUDLEY KNOX LIBRARY
NAVAL POSTGRADUATE SCHOOL
MONTEREY, CALIFORNIA 93943-6002

Thesis
K1486 Kaufmann
c.1 Stress analysis of the
LHA-1 class superheater
header by finite element
method.

4 OCT 88

14193

Thesis
K1486 Kaufmann
c.1 Stress analysis of the
LHA-1 class superheater
header by finite element
method.

thesK1486

Stress analysis of the LHA-1 class super



3 2768 000 73416 4

DUDLEY KNOX LIBRARY